Journal Pre-proof

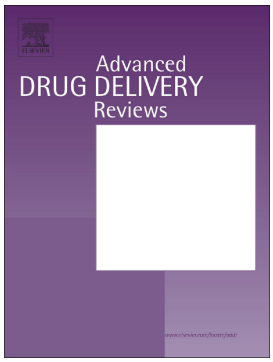

Therapeutic potential of polypeptide-based conjugates: Rational design and analytical tools that can boost clinical translation

Tetiana Melnyk, Snežana Đorđević, Inmaculada Conejos-Sánchez, María J. Vicent

PII: S0169-409X(20)30144-7

DOI: https://doi.org/10.1016/j.addr.2020.10.007

Reference: ADR 13657

To appear in: *Advanced Drug Delivery Reviews*

Received date: 18 July 2020

Revised date: 9 October 2020

Accepted date: 14 October 2020

Please cite this article as: T. Melnyk, S. Đorđević, I. Conejos-Sánchez, et al., Therapeutic potential of polypeptide-based conjugates: Rational design and analytical tools that can boost clinical translation, *Advanced Drug Delivery Reviews* (2020), https://doi.org/10.1016/j.addr.2020.10.007

This is a PDF file of an article that has undergone enhancements after acceptance, such as the addition of a cover page and metadata, and formatting for readability, but it is not yet the definitive version of record. This version will undergo additional copyediting, typesetting and review before it is published in its final form, but we are providing this version to give early visibility of the article. Please note that, during the production process, errors may be discovered which could affect the content, and all legal disclaimers that apply to the journal pertain.

© 2020 Published by Elsevier.

Journal Pre-proof

Therapeutic Potential of Polypeptide-Based Conjugates: Rational Design and Analytical Tools That Can Boost Clinical Translation

[#] Tetiana Melnyk

Centro de Investigación Príncipe Felipe, Polymer Therapeutics Lab., Av. Eduardo Primo Yúfera 3, E-46012 Valencia (Spain)

E-mail: tmelnyk@cipf.es

[#] Snežana Đorđević

Centro de Investigación Príncipe Felipe, Polymer Therapeutics Lab., Av. Eduardo Primo Yúfera 3, E-46012 Valencia (Spain)

E-mail: sdordevic@cipf.es

[*] Dr. Inmaculada Conejos-Sánchez

Centro de Investigación Príncipe Felipe, Polymer Therapeutics Lab., Av. Eduardo Primo Yúfera 3, E-46012 Valencia (Spain)

Tel.: +34 963289681 (Ext 1308); Fax: +34 963289701

E-mail: iconejos@cipf.es

[*] Dr. María J. Vicent

Centro de Investigación Príncipe Felipe, Polymer Therapeutics Lab., Av. Eduardo Primo Yúfera 3, E-46012 Valencia (Spain)

Tel.: +34 963289681 (Ext 2307); Fax: +34 963289701

E-mail: mjvicent@cipf.es

Co-Corresponding authors [*] Authors with an equal contribution [#]

Table of Contents

Journal Pre-proof

Journal Pre-proof

Abstr

Journal Pre-proof

Journal Pre-proof

Abstract

The clinical success of polypeptides as polymeric drugs, covered by the umbrella term “polymer therapeutics,” combined with related scientific and technological breakthroughs, explain their exponential growth in the development of polypeptide-drug conjugates as therapeutic agents. A deeper understanding of the biology at relevant pathological sites and the critical biological barriers faced, combined with advances regarding controlled polymerization techniques, material bioresponsiveness, analytical methods, and scale up-manufacture processes, have fostered the development of these nature-mimicking entities. Now, engineered polypeptides have the potential to combat current challenges in the advanced drug delivery field. In this review, we will discuss examples of polypeptide-drug conjugates as single or combination therapies in both preclinical and clinical studies as therapeutics and molecular imaging tools. Importantly, we will critically discuss relevant examples to highlight those parameters relevant to their rational design, such as linking chemistry, the analytical strategies employed, and their physicochemical and biological characterization, that will foster their rapid clinical translation.

Keywords: Polypeptide, Polymer Therapeutics, Polypeptide-Drug conjugates, Analytical Tools, Controlled Drug Delivery, Bioresponsiveness, Physico-chemical characterization

Graphical Abstract

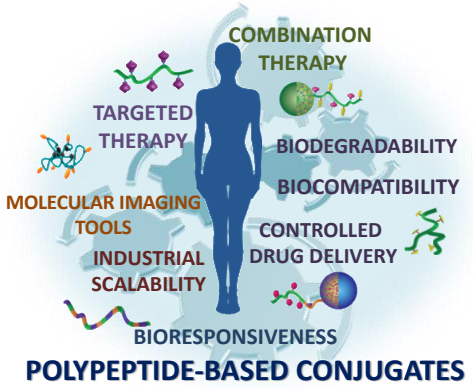

Abbreviations

3D6-Fab	3D6 antibody fragments
Ab	Antibody
AAS	Atomic absorption spectroscopy
AF4	Asymmetric flow field flow fractionation
AFM	Atomic force microscopy
AGM	Aminoglutethimide
AGT	Alanine:glyoxylate aminotransferase
AKI	Acute kidney injury
Ala	Alanine
antiTF1849	Anti-Tissue factor Ab (clone 1849)
APN	Aminopeptidase N
Apo	Apolipoprotein
Arg	Arginine
Asp	Aspartic acid

Journal Pre-proof

BDMC	Bisdemethoxycurcumin
BNCT	Boron-neutron capture therapy
BSA	Bovine serum albumin
BSH	^{10}B- sodium borocaptate
CA4	Combretastatin-A4
CD	Circular dichroism
CDDP	Cisplatin (cis-diamminedichloridoplatinum(II))
CFTR	Cystic fibrosis transmembrane regulator gene
Cit	Citrulline
-CL-	Crosslinked
CPLGLAGG	Glycine-Proline-Leucine-Glycine-Leucine-Alanine-Glycine-Glycine
CPT	Camptothecin
CS	Chitosan
cRGD	Cyclic Arg-Gly-Asp
CSF	Cerebrospinal fluid
Cys	Cysteine
DACH-Pt	Diaminocyclohexane platinum
DDBA	4,4'-dithiodibutyric acid
DDPA	3,3'-dithiodipropionic acid
DDS	Drug delivery systems
DIP	N-(N',N'-diisopropylaminoethyl)
DLS	Dynamic light scattering

Journal Pre-proof

Journal Pre-proof

DNA	
DNAA	Naphthalene disulfonic acid
DOC	Docetaxel
DOCA	Deoxycholate
DoE	Design of experiments
DOTA	1,4,7,10-tetraazacyclododecane-1,4,7,10-tetraacetic acid
Dox	Doxorubicin
DSF	Disulfiram
DTPA	Diethylenetriaminepentacetate
DTT	Dithiothreitol
DTX	Docetaxel
EMA	European Medicines Agency
EPI	Epirubicin
EPR	Enhanced permeability and retention
ESI	Electrospray ionization
FA	Folic acid
Fabs	3D6 monoclonal anti-Aβ antibody fragment
FAS	Fasudil
FCS	Fluorescence correlation spectroscopy
FDA	Food and Drug Administration Agency
FFF	Field flow fractionation
FLD	Fluorescence detector
FLUO	Fluocinolone acetonide

Journal Pre-proof

Journal Pre-proof

FRET	
FU	5-fluorouracil
-g-	Grafted
G-CSF	Granulocyte-colony-stimulating factor
Gd	Gadolinium
GEM	Gemcitabine
GFLG	Glycine- Phenylalanine-Leucine-Glycine
GI	Gastrointestinal tract
Glu	Glutamic acid
Glut-1	Glucose transporter
Gly	Glycine
Gly-Gly-Pro-Nle	Glycine-Glycine-Proline-Norleucine
GPC	Gel permeation chromatography
GPLGIAGQ	Glycine-Proline-Leucine-Glycine-Isoleucine-Alanine-Glycine-Glutamine
GSH	Glutathione
HA	Hyaluronic acid
HA-CP	Hyaluronic acid- poly-L-glutamate- cross-polymer
hGH	Human growth hormone
HIFU	High-intensity focused ultrasound
His	Histidine
HIV	Human immunodeficiency viruses
HPLC	High-performance liquid chromatography
HPMA	poly(N-(2-hydroxypropyl)methacrylamide)

Journal Pre-proof

HPV	
HSA	Human serum albumin
i.v.	Intravenous
ICP-MS	Inductively coupled plasma – mass spectrometer
iNPG	Injectable nanoparticle generator
i.p.	Intraperitoneal
IR	Infrared detector
LC-MS	Liquid chromatography-mass spectrometry
Lys	Lysine
MALDI-TOF MS	Matrix-assisted-laser-desorption time-of-flight mass spectrometer
MALS	Multi-angle light scattering
MAPK	Mitogen-activated protein kinase
mDBF	Modified dabrafenib
MDR	Multidrug-resistant
MDS	Molecular dynamics simulation
MgFFF	Magnetic FFF
MMAE	Monomethyl auristatin E
MMP	Metalloproteinase
MNP	Magnetic nanoparticles (Fe)
PEG	Poly(ethylene glycol)
MRI	Magnetic resonance imaging
MS	Mass spectrometry
MSD	Mean square displacement

Journal Pre-proof

Journal Pre-proof

MSI	
Mw	Molecular weight
NCA-ROP	N-carboxyanhydride ring-opening polymerization
NIPPAM	N-isopropylacrylamide
NMR	Nuclear magnetic resonance
OEI	Oligoethylemine
OES	Optical emission spectroscopy
OFAT	One factor at a time approach
P-18	Peptide probe, cleavable by matrix metalloproteinase 13 (MMP-13)
PAA	Polyaspartamide
PArg	Polyarginine
PAsp	Polyaspartic acid
pBAL	β-actin driven luciferase
PBLG	Poly(γ-benzyl-L-glutamate)
PBMC	peripheral blood mononuclear cell
PDCs	Polypeptide-drug conjugates
PDI	Polydispersity index
PDMAPMA	N,N-dimethylaminopropyl methacrylamide
PDT	Photodynamic therapy
PEG	Poly(ethylene glycol)
pEGFP	Cytomegalovirus driven enhanced green fluorescent protein
PEI	Polyethylenimine
PET	Positron emission tomography

Journal Pre-proof

PGA	
PI3Kγ	Phosphoinositide 3-kinase gamma isoform
PK	Pharmacokinetics
PLF	Plerixafor
PLO	Polyornithine
PPhe	Polyphenylalanine
PPT	Podophyllotoxin
Pro	Proline
PSar	Polysarcosine
Pt	Platinating agents
PTX	Paclitaxel
PVGLIG	Proline-Valine-Glycine-Leucine-Isoleucine-Glycine
R	Recovery
RBC	Red blood cell
Rg	Geometric radius
RI	Refractive index
RNA	Ribonucleic acid
S/N	Signal-to-noise
SALS	Small-angle light scattering
SANS	Small-angle neutron scattering
Sar	Sarcosine
SAS	Small-angle scattering
SAXS	Small-angle X-ray scattering

Journal Pre-proof

Journal Pre-proof

SdFF	
SEC	Size exclusion chromatography
SEM	Scanning electron microscopy
Ser	Serine
siPLK1	Selectively silence Polo-like kinase 1
siRNA	Small interfering ribonucleic acid
SLM	Selumetinib
SN38	Active metabolite of irinotecan
ssDNA	single-stranded Deoxyribonucleic acid
STIs	Sexually transmitted infections
TAA	Tumor-associated antigens
TCO	Trans-cyclooctene
TEM	Transmission electron microscopy
TF	Anti-tissue factor
Tf	Transferrin
TF	Anti-tissue factor
TFA	Trifluoroacetic acid
TMAPA	Trimethylaminopropylamide
TME	Tumor microenvironment
TNBC	Triple negative breast cancer
TREN	Tris(2-aminoethyl)amine
Tyr	Tyrosine
UHPLC	Ultra-performance HPLC

Journal Pre-proof

Journal Pre-proof

UV-V	
Val	Valine
ZnPc	Zinc (II) phthalocyanine

1. Introduction

There currently exist over 25 examples of polymer therapeutics in clinical use today. Two such nanomedicines became top-selling drugs in the USA in the last decade, including Copaxone®, a polypeptide-based polymeric drug for the treatment of multiple sclerosis [1–3]. Polymer-drug conjugates are a subtype within the polymer therapeutics family; while the first generation mainly addressed cancer treatment, their therapeutic application now extends to multiple other conditions [4–6]. Ringsdorf first described the four main features relevant to the design of polymer-drug conjugates [7], and although we now consider them in a more versatile manner, their general basis remains: (i) a hydrophilic polymeric carrier, ideally biodegradable and multivalent with a high loading capacity; (ii) adequate drug(s) selection with appropriate potency and structural functionality that allows conjugation; (iii) bioresponsive polymer-drug(s) linkers that allow controlled drug(s) release at the site of action under selected endogenous or exogenous triggers; and (iv) the possibility of implementing targeting moieties to enhance accumulation at the pathological site [8]. With these four features in mind, rationally-designed polymer-drug conjugates have gained attention due, in part, to their ability for the accurate and controlled release of bioactive agents under specific biological scenarios

Journal Pre-proof

[2]. [illegible] cated approaches.

1.1. Polypeptides as Polymeric Carriers for Polymer-Drug Conjugates

The use of polypeptides as the polymeric component provides advantages regarding their clinical translation given their similarities to native proteins, which include safety, low immunogenicity, biocompatibility, and biodegradability. Said parameters allow for prolonged treatment schedules in chronic or infectious diseases, neurological disorders, or tissue regeneration [9]. As polypeptides become degraded in the presence of specific proteases to yield small non-toxic metabolites that are excreted from the body, they suit repeated parenteral administration; however, for immunomodulatory purposes, they can be easily engineered by selecting immunogenic amino acid sequences within the polypeptide structure [10]. Furthermore, the use of high molecular weight (Mw) polypeptide carriers allows for the optimization of pharmacokinetics (PK) and the administration of high drug doses with a minimal polymeric component [9]. The versatility of the synthetic chemistry associated with polypeptide conjugates, in comparison with other types of nanomedicine, has also widened their applicability [11].

Recent advances in polymerization techniques have enabled the controlled and reproducible synthesis of well-defined polypeptides with unique architectures that can be translated to the industrial scale [12–15]. In comparison with the resource-heavy and time-consuming manufacturing processes associated with natural polymeric materials, synthetic polypeptides can be generated from a wide range of precursor materials and offer a range of post-modification possibilities. The introduction of bioresponsive moieties into polypeptidic materials allows for stimuli-sensitive drug release, while the design of

Journal Pre-proof

comp es to improve properties such as cellular uptake, drug release, or clearance [16].

While polymer-drug conjugates have already reached clinical approval with Movantik® [17], and further examples are currently under evaluation in clinical/preclinical studies [2], reports with polypeptide analogs remain scarce. However, the application of synthetic polypeptides as carriers is currently in exponential growth for a variety of therapeutic [18–20] or diagnostic indications [21–23].

Inherent difficulties still exist regarding the precise design, synthesis, and development of advanced polypeptide-drug conjugates (PDCs) with a defined biological output, although the numerous advantages deriving from their biodegradability and multivalency may act to compensate (**Figure 1.**). Such difficulties likely arise from the intricate conformational changes of these polymeric carriers, the linking chemistry employed, and the nature of the selected drug(s) [24]. Moving forward, we must fully understand the critical design features of PDCs to diminish the impact of these challenges and enhance the number of translated examples. Critical design features include, (i) the selection of structural elements before synthesis (e.g., amino acid nature, architecture, linker design, and responsiveness), (ii) the optimization of the physico-chemical properties of the resulting conjugate (e.g., size, charge, conformation, geometry, and topology), (iii) the correlation of these properties with the biological output obtained in preclinically relevant models, and, (iv) fine-tuning through reiterative design cycles. The identification of structural predictors and functional biomarkers [4] derived from the implementation of iterative bio- and physico-chemical characterization protocols will significantly contribute to their advanced development [1,24].

Figure 1

Journal Pre-proof

synthetic strategies, physicochemical characterization steps, and the bioanalysis implemented. We will also explore strategies used in related polypeptide-based systems from which PDC design may benefit and highlight how these insights can contribute to the clinical translation of PDCs.

2. Rational Design and Key Requirements Towards the Development of Polypeptide-Drug Conjugates

PDCs are a subfamily of polymer-drug conjugates that use synthetic polyamino acids as the polymeric carrier component [11,25]. The evaluation of eleven PDCs in advanced clinical trials supports the clinical benefit of polypeptide-based materials, with two polymeric drugs reaching market approval: *Vivagel*®, a topically administered polylysine (PLL)-dendrimer employed as an antibacterial and antiviral (HIV-1 and HSV-2) agent [26,27], and *Copaxone*®, a random copolymer of L-Glutamic (Glu), L-Alanine (Ala), L –Lysine (Lys), and L-Tyrosine (Tyr) used in the treatment of multiple sclerosis [28–30].

The potential of synthetic polypeptides was first recognized in 1959 by Kenny et al. in a study of poly-L-glutamic acid (PGA) as a plasma expander [31]; moving to the present day, PGA has now found applications in a range of drug delivery systems (DDS) that have reached clinical stages [32]. The versatility of the synthetic chemistry involved and the ability to incorporate bioresponsive linking moieties and other biomimetic features greatly enhance the scope of PDCs in comparison with other types of nanomedicine [11]; however, said nanomedicines must meet defined and exact prerequisites for successful translation to the clinical setting.

The rational design of a PDC begins with a complete understanding of the ***biological barriers*** that each conjugate must bypass to reach the selected cellular/molecular target. This “journey” starts with the selected administration route [24,33]. Intravenous (i.v.) administration represents the preferred

Journal Pre-proof

route eting through the enhanced permeability and retention (EPR) effect (in the absence of active targeting moieties) [34–36], and improved therapeutic outcomes [2]. Alternative routes include oral [37], intranasal [38,39], subcutaneous [40], intraperitoneal (i.p.) [41–43], pulmonary [44,45], vaginal [27], topical [46], intrathecal [19], and ocular [47] administration, with each route requiring the optimization of the final therapeutic formulation with regards to the parameters that affect interactions with biological interfaces. The nature of the polymer/active agent, bioresponsive moieties, and physico-chemical parameters such as size, charge, geometry, or solution conformation govern the *in vivo* behavior of a PDC [24,33,48] and establish the requirements for their rational design.

The main requirement for the development of PDCs is the feasibility and simplicity of ***polymer chain modification*** that allows the desired ***bioresponsive conjugation*** of a therapeutic agent, targeting moiety and/or fluorescent probe. While more than 500 amino acids exist (around 240 encountered in nature and the rest as intermediates in metabolism) [49], only seven of those that appear in the human genetic code possess characteristics that have fostered their implementation as building blocks for PDC – the positively charged amino acids arginine (Arg) and Lys, the uncharged polar amino acid serine (Ser), the uncharged hydrophobic amino acid Tyr, and finally, the negatively charged amino acids Glu and aspartic acid (Asp). In practice, Glu, Asp, and Lys represent the most exploited amino acids in the synthesis of PDCs due to their side-chain functionalities, as will be discussed in forthcoming sections of this review. Other amino acids are incorporated to achieve shielding (i.e., sarcosine (Sar, N-methyl Gly)) [50], active mitochondrial targeting (i.e., proline (Pro)) [51], bioresponsiveness within a peptidic sequence, acting as protease substrate (i.e., for Cathepsin B: GFLG, biotin-avidin systems [52,53] or for matrix metalloproteinases (MMPs): GPLGIAGQ, PVGLIG [53], CPLGLAGG [54] and others [55]), or 3D conformational change when part of hydrophobic domains [56], among other examples.

Journal Pre-proof this

effect observed in the clinics with Vivagel® and Copaxone™ used as polypeptidic drugs [1,2,27]. Under a rational design-based approach, we can take advantage of the inherent biological activity of polypeptides to construct multimodal PDCs. As an example, poly(Arg-Gly-Asp) inhibits lung metastasis and the migration of B16-BL6 melanoma cells in mice [57,58]. The incorporation of a zwitterionic sequence within a disordered polypeptidic carrier (ZIPPs) increases plasma residence time by imparting "stealth" behavior. Using this strategy, Banskota et al. demonstrated that a combination of Lys and Glu in the ZIPP conferred superior PK to conjugated glucagon-like peptide-1 (GLP1) in a mouse model of type-2 diabetes [59]. Other polypeptides, such as polyornithine (PLO) and polyarginine (PArg), have been widely explored in gene delivery due to their cationic nature (a topic out with the scope of this review [60]). However, there exist examples of these polymers as components of PDCs, such as liver-targeted PLO-small interfering RNA (siRNA) conjugates [61].

The ***robustness and scalability of PDC synthesis*** and, more importantly, the final ***manufacturing process*** represent essential considerations regarding clinical translation. As various synthetic strategies can generate polypeptides, the properties of the final product will differ. Peptide synthesis commonly employs peptide bond formation via condensation, a sequential process of coupling two amino acids with N- and C-terminus protecting groups in solution or on a solid phase [62]; however, this procedure is generally inapplicable to large scale polypeptide synthesis due to economic considerations. Similarly, recombinant techniques involving the expression of an amino acid sequence by, for example, *E. coli* (commonly used for elastin-like polypeptides synthesis [63]), also suffer from poor process scalability. Overall, these constraints prompted the implementation of polymeric carriers such as poly(ethylene glycol) (PEG) or poly(N-(2-hydroxypropyl)methacrylamide) (HPMA) instead of polypeptides due to their associated relatively rapid and facile manufacturing processes [25].

Journal Pre-proof

d the controlled, reproducible, and cost-effective synthesis of poly-amino acids (even at large Mw) at the kilogram scale [12–15,64]. This polymerization process requires the use of specific amino acid derivatives (NCA with protected or modified side-chain functional groups) to generate a final product that contains modified side chains or that can be post-synthetically modified [65]. The choice of ***(macro)initiator*** is critically important to NCA-ROP, as this determines the living character of the polymerization process, the low polydispersity (PDI) of the resultant polypeptides [66], and the final topology, allowing for the generation of linear, branched, and dendrimeric architectures following the use of multifunctional moieties [67,68]. Dendrimeric materials structurally differ from linear analogs, with advantages including monodisperse distribution and a rigid structure that impedes viscosity at high concentrations. Chain growth control and steric hindrance for large Mw dendrimers remain as significant problems related to the attainment of symmetrical structures, where the NCA-ROP polymerization resulting in narrow size distribution keep the leading positions [12–15], and, similar to dendrimers, also allows the generation of star-like or highly-ordered branched polypeptides [67–70]. Examples in the literature include linear, branched, or dendrimeric forms of PLL (**Table 1**), with any associated activity dependent on the structure. For example, dendrimeric and linear polyanions differ in their antiviral activity, which is highly dependent on the branching degree [71]. A general trend supports increasing potency upon increased generation, with the fourth generation displaying higher activity than lower generations [71].

The inclusion of PEG as a macroinitiator confers amphiphilicity to the resulting polypeptidic chain and provides the basis of well-known polymeric micelles. Many examples have been described by Kataoka et al., with several now under evaluation at advanced clinical stages as anticancer agents (**Table 1-3**) [72]. Many studies employ PEGylation to tailor the PK of nanosized DDS, not only by increasing circulation time due to an increase in size [73], but also by impeding recognition by the immune system (known as opsonization), phagocytosis, and elimination [74]. However, evidence of intracellular vacuolation and

Journal Pre-proof

clinic lergo biological processes that result in the production of toxic carboxylic metabolites related to the development of hypercalcemia and acidosis [77]. Studies have also shown that PEG (irrespectively of Mw) can alter the P-glycoprotein transporter directly or indirectly and affect its function [78]. Within the polypeptide armory, polysarcosine (PSar) [79] has emerged as an alternative to PEG, as PSar can grant water-solubility, flexibility, immune evasion, and low immunogenicity without associated adverse effects [50]. Furthermore, studies of several PSar-polypeptide micelles data as non-viral vectors or in targeted drug delivery, among other applications, have already provided promising preclinical data [79].

The ***overall size*** of a given nanosized DDS, including PDCs, represents an essential parameter that governs resistance to elimination by the reticuloendothelial, hepatic, or renal systems, the modulation of blood circulation time, and hence the preferential accumulation in the tumor or inflamed sites due to the EPR effect. Sizes of > 100 nm favor accumulation in well vascularized pathological sites [34,36]; however, efficient therapeutic outcomes following PDC treatment also require adequate tissue diffusion and penetration. Importantly, Cabral et al. established that treatment with PDCs of <100 nm in size led to optimal penetration in poorly permeable cancers, such as that achieved with a 30 nm size PEG-PGA-1,2-diaminocyclohexane-platinum(II) micelle [80]. There exist a range of strategies that can enhance accumulation and permeation, although this topic lies outside of the scope of this review [80,81].

Polypeptide chain functionality and the selected therapeutic agents define the synthetic strategy used for conjugation. Furthermore, the connection between the bioactive agent(s) and the polymeric carrier via ***specific linking moieties*** provides for the tight control of drug release [82]. The first PDCs employed simple amide or ester one-step bond formation to generate linking moieties, due to the straightforward linking chemistry of Glu, Asp, and Lys terminal carboxylic/amine functional groups, that supported the slow release of conjugated elements [24]. More structurally advanced linkers now provide stimuli-responsiveness and site-specific drug conjugation, which represents another requirement for PDCs in particular, as well as DDS in general. We will

Journal Pre-proof

exter trate examples displaying sensitivity to physiological gradients (e.g., pH, hypoxia, temperature, redox potential, presence of specific enzymes) or external stimuli (e.g., photoirradiation, magnetic fields, electric fields, ultrasound, temperature) [83].

Another means to achieve ***stimuli-responsive*** PDCs takes advantage of the ***intrinsic polyelectrolyte properties*** of the polypeptidic carrier itself. Optimal design in this respect can promote, for example, pH-triggered conformational changes based on the shielding/exposure of side-chain charges after the differential protonation stage [56]. The introduction of specific moieties between polymeric fragments/blocks or orthogonal crosslinking agents within three-dimensional architectures allows for the development of multiresponsive polypeptidic systems [84,85]. For example, a disulfide motif (-SS-) introduced between PEG and PAsp polymeric blocks conferred redox-responsiveness to a PEG-SS-PAsp-Doxorubicin (Dox) conjugate, while a hydrazone linker employed between Dox and PAsp conferred pH-responsiveness [86].

Polypeptidic carriers also tend to ***self-assemble*** due to their intrinsic properties; therefore, the stability of self-assembled polypeptide-based DDS under physiological conditions is another requirement, which depends on forces including hydrophobic/hydrophilic balance, π-π stacking, and dipole interactions [24]. The stabilization of self-assembled architectures permits the use of these systems as efficient drug carriers; in this context, the complexation of platinating agents (Pt) to negatively charged PGA and PAsp polypeptides allows for efficient drug incorporation and cross-linking derived from the chelation of Pt(II). Recent examples confirm the generation of particles with suitable hydrodynamic radii (80-100 nm) [41,87] and stability in serum [88]. Furthermore, size can be precisely controlled by varying the loading of the Pt drug [80].

drug amount also affects the size. Furthermore, ***crosslinking*** of polypeptidic chains with biodegradable or non-biodegradable linkers can allow for the generation of stabilized and flexible structures, controlled drug release, and tunable size. “Click” reactions represent the most widely used strategy for crosslinked polypeptidic materials [95] due to high reaction efficiency under mild conditions and high selectivity. Cu(I) catalyzed azide-alkyne cycloaddition [96] and copper-free click chemistry [97,98], amide [99], thiol-ene, and Diels-Alder reactions [100,101] are among the commonly used technique for the generation of non-degradable crosslinkers. Other types of crosslinkers have also been successfully applied for polypeptidic materials, and include genipin [102,103], bioresponsive disulfides [104–107], boronic acid [108,109], and aldehyde/amine derivatives [110]. The advantages of the crosslinked system have been demonstrated for PGA [96,111] and PLL [107] with significant increases in blood circulation observed *in vivo*.

Another physical parameter to consider is the ***net charge*** of a given PDC***.*** Charge has a significant effect on *in vivo* fate, with toxicity observed in those examples with a positive surface charge [112]. As an example, the positive charge associated with PLL or PArg limits their systemic applications; however, these polypeptides have found use as topical virucides, such is the case of Vivagel® [27]. However, after adequate charge shielding approaches, PLL, PLO, or PArg could represent suitable materials for the development of PDCs or non-viral vectors for systemic delivery [20,40,43,113,114]. Chemical alterations, such as amidation of amino side groups, can compensate for unwanted charge. As an example, Han et al. modified a Lys into a pH-sensitive β-carboxylic amide to create smart negatively-charged micelles based on amidated PLL-poly(L-leucine) diblock copolymers that regain a positive charge upon hydrolysis to assist in internalization at the site of action [115]. Charge can also be diminished by adequate PEG-mediated shielding [44,116], as is the case of DEP® technology and dendrimeric PEG-PLL in Phase I-II clinical trials [117,118] (see detailed information in section 3.1.1) (***Table 1***).

Journal Pre-proof

renal excretion in the case of negatively charged systems [96,119]). Slightly negative or neutral charges reduce non-specific cellular uptake and opsonization [24]. Qi et al. designed a multilayer system based on PEG-PLL-poly-aspartamide with the toxin monomethyl auristatin E (MMAE) and employed layer-by-layer assembly with PEG-PGA to quench the positive surface charge and minimize non-specific biological adhesion and prevent premature opsonization [42]. Their nanosized DDS dissociated at the low pH typical of the tumor microenvironment (TME), leading to improved cell internalization through the exposure of the positive charges of the amine. The design employed in this study also supported increased drug loading on a per-vehicle basis when compared to antibody-drug conjugates. More importantly, evaluation in an ovarian cancer model demonstrated tumor growth inhibition and extended animal survival when compared to free MMAE treatment, which induced severe weight loss. In a patient-derived xenograft-platinum-resistant model, MMAE conjugates also exhibited enhanced antitumor efficacy and doubled animal survival when compared to cisplatin (CDDP) therapy [42].

The last but not least important prerequisite that can increase success in clinical translation is the ***active targeting*** of a given PDC via surface modification with receptor-ligands, which include a multitude of molecules that facilitate cellular uptake via receptor-mediated endocytosis [120]. Previously reported targeted polypeptide-based nanosystems have employed folic acid (FA, folate receptor target) [41,106,121–124], hyaluronic acid (HA, CD44 target) [125], glucose (Glut-1 target) [107], biotin (avidin target) [126], aptamers (ssDNA/RNA fragment), antibody whole/fragment [99,127], proteins (transferrin) [128] or peptides (cyclic Arg-Gly-Asp (cRGD) peptide) [129] and leptin [130]. Although not all given examples are conjugates, these targeting moieties, as well as others reported in different DDS, could be implemented in PDCs. Of note, despite the enormous potential for site-specific delivery and promising *in vivo* results of targeted systems, the associated increase in complexity raises challenges for large-scale manufacturing that complicates their clinical translation. Furthermore, conflicting results in the literature have raised a debate with regards to whether ligand-targeting significantly enhances accumulation when

Journal Pre-proof

comp and recognition moieties should be adequately selected for efficient active targeting [132,133].

3. Advancing Polypeptide-drug Conjugates Towards the Clinics

As already mentioned, Glu, Asp, and Lys are the most widely employed amino acids in PDCs. Therefore, we will review the reported literature on related PDCs, but we will also include other amino acid-based-PDCs that exhibit interesting properties. Forthcoming sections will address their implementation in combination therapies, the linking chemistry strategies employed, and recent progress in this area, with critical insight into the required analytical techniques for their characterization. This latter point represents a critical feature that could lay the foundations for the development of the next generation of PDCs that reach clinical application.

3.1. Preclinical and Clinical Examples of Polypeptide-based Conjugates

3.1.1 Polylysine (PLL)-based Conjugates

The approval of Vivagel® [26] and the phase I/II clinical studies with DEP® technology [118] both support the use of PLL in PDCs (***Table 1***). PLL-derivatives are also currently being preclinically evaluated as anticancer therapies through the conjugation of drugs via bioresponsive linkers (***Table 1***), immunotherapeutics (mainly with mRNA-based vaccines) [134], and microbiocides [135]. PLL has found use as a non-viral vector [60], whose description falls outside the scope of this review; however, we will discuss outcomes of related studies that have relevance to PDC development where appropriate.

Table 1

I/II), and the Bcl2/xL inhibitor AZD4320 (AZD0466, phase I) are being evaluated in clinical trials in solid tumors [118] and hematological tumors in the case of AZD0466 (alone and in combination with rituximab) [136]. For the three conjugates bearing chemotherapeutic agents, clinical results have provided evidence for disease stabilization and a reduction in side effects (neutropenia and bone marrow toxicity) [117,118]. In all cases, drug loading and PLL-drug linker design represented critical features - for example, in the case of the PEG-PLL dendrimer-AZD4320 conjugate (AZD0466), mathematical modeling determined the optimal drug release rate to achieve maximal therapeutic index (preclinical antitumor efficacy vs. cardiovascular tolerability) and secure clinical progression [137].

Dendrimeric and linear PEG-PLL carriers are also under preclinical evaluation with a wide variety of chemotherapeutics and molecularly-targeted drugs. As stated previously, drug loading and linker design represent key design parameters. The use of the cathepsin B-cleavable GFLG linker (which has demonstrated utility in targeted drug release) in PEG-PLL dendrimer conjugates of gemcitabine (GEM) [113] and Dox [138] prompted similar two-fold higher inhibition of tumor growth, higher apoptosis compared to the free drug, and a lack of tissue damage.

A comparison between two redox-sensitive linkers (3,3'-dithiodipropionic acid [DDPA] and 4,4'-dithiodibutyric acid [DDBA]) employed for the conjugation of curcumin to a PEG-b-PLL linear block copolymer revealed that, in similar conditions of drug loading and size, the thermodynamic parameters of cycle formation of each self-immolative system had significant influence [139]. The longer length of the DDBA linker prompted more stable 1,5 ring formation, faster drug release, and consequently higher cytotoxicity in three different cancer cell lines and a xenograft tumor-bearing mouse model. Conjugation of ^{10}B-sodium borocaptate (BSH) to PEG-b-PLL through a redox-responsive linker yielded multifunctional polymeric micelles (of approx. 50 nm in diameter) that allowed for endosomal escape and the enhanced delivery of BSH to cancer cells required as part of a boron-neutron capture therapy (BNCT)

Journal Pre-proof

appr serve toxicity without irradiation.

Recently, Toshiyama et al. conjugated ubenimex (Ube, also known as bestatin), a protease inhibitor clinically used for patients with acute myeloid leukemia and lymphedema, to a PEG-b-PLL block copolymer through a peptidic linker and achieved high loading (up to 40 mol%) [43]. The conjugates demonstrated comparable/or higher activity than free Ube thanks to the strengthening of the molecule-to-cell interactions via selective targeting towards aminopeptidase N (APN)/CD13^{+} hepatocellular carcinoma cancer stem cells. Exposure to the PEG-b-PLL-Ube conjugate alone or in combination with chemotherapeutic drugs (fluorouracil, CDDP, or Dox) prompted a clear increase in intracellular reactive oxygen species levels by inhibiting APN activity. This effect triggered a potent antitumor effect *in vivo* in a HuH7 hepatocarcinoma xenograft model with no apparent adverse effects upon i.p. administration.

Zhou et al. developed actively tumor-targeted (using FA), redox-responsive, and high drug-loaded micelles composed of PEG-b-PLL conjugated to CPT through disulfide bonds as an enhanced cancer therapeutic [94]. The ability of FA-PEG-b-PLL-CPT to self-assemble into micelles of around 100 nm in diameter also allowed the exploration of combination therapy via the encapsulation of hydrophobic chemotherapeutic drugs such as Dox [94].

As mentioned in previous sections, the administration route employed can alter the therapeutic success of a given PDC. The intratracheal instillation of a dendrimeric PEG-PLL-Dox conjugate as a lung metastasis treatment reduced tumor burden by more than 95% in comparison with i.v. administration, which triggered only a 30% reduction [44]. The authors highlighted the potential of PEGylated dendrimers as inhalable DDSs to promote the prolonged exposure of lung-resident cancers to chemotherapeutic drugs and to improve anti-cancer activity. Studies on the clearance of this PDC concluded that the majority of the dose (around 60%) dissipated from the lungs after 24 h via absorption across the pulmonary epithelium and clearance into the intestine,

Journal Pre-proof

presu fe of approximately six days, suggesting that the conjugate promoted the controlled and prolonged exposure of Dox to the lungs. The authors also suggested urine secretion of degraded fragments and drainage into pulmonary lymphatics as other clearance mechanisms. Related studies conducted in humans that employed a cysteine-PLL-PEG polymer for DNA delivery as a cystic fibrosis treatment provide support for the suitability for nasal delivery and safety of this dendrimeric system [38].

PLL has also been explored for diagnostic purposes as a component of magnetic resonance imaging (MRI) contrast agent probes. Dendrimeric PLL conjugated to diethylenetriaminepentacetate acid (DTPA) via an amide bond for gadolinium (Gd) complexation [141] offered higher longitudinal relaxivity values. The administration of this conjugated complex resulted in enhanced tumor accumulation and its maintained presence for up to 24 h post-injection in comparison with the unconjugated DTPA-Gd complex.

Finally, due to a possible implementation in newly designed targeted PDCs, we highlight a recent study by Xie et al. that described a bioresponsive crosslinked PEG-PLL nanomicellar complex that penetrated the blood-brain barrier and successfully delivered active 3D6 antibody fragments (3D6-Fab) to inhibit beta-amyloid aggregation as part of a potential Alzheimer's disease treatment approach [107]. The nanomicelles displayed stability in blood and disassembled in a stepwise-manner within the acidic and reductive environment of the endosome and brain parenchyma, respectively, due to the loss of ionic interactions and disulfide link breakage, which prompted the release of large amounts of bioactive antibodies. Functionalization with glucose (to target the glucose transporter (Glut)-1 protein) conferred brain targeting under specific glycemic controlled condition and promoted a 41-fold enhancement of 3D6-Fab brain accumulation when compared to free Fab. Finally, the study confirmed *in vivo* therapeutic efficacy through the inhibition of Aβ1−42 aggregation in Alzheimer's disease mice.

PGA is a biocompatible polymer that undergoes intracellular degradation by cathepsin B, a protease that becomes highly upregulated in malignant cells [142]. Initially, PGA-drug conjugates focused on improving the solubility of conventional first-line cancer therapeutics such as paclitaxel (PTX) or CPT, and reducing systemic exposure and adverse side effects for highly toxic drugs such as Dox and CDDP (**Table 2**). PGA-paclitaxel (PGA-PTX, also known as CT-2103, PPX, or Opaxio^{TM}) represents one of the few conjugates that has reached phase III clinical trials [143]. In comparison with other polymer-PTX conjugates, Opaxio^{TM}, which uses an ester bond for drug conjugation, exhibited high drug loading capacity (37 wt% vs. 5 wt% for the discontinued HPMA-PTX conjugate [144]) and presented enhanced stability in blood. PGA conjugation of PTX also allowed for more rapid patient administration (10-20 min infusion compare to 3-24 h for free drug) and did not require premedication with corticosteroids and antihistamines due to the lower associated toxic side-effects [145]. Moreover, PGA-PTX prompted enhanced outcomes when combined with radiotherapy, demonstrated comparable efficacy to the free drug, and prompted favorable progression-free and overall survival rates [146]. Unfortunately, the development of PGA-PTX was halted in 2016 due to a lack of significant improvement compared to the current standard of care [147]. PGA-CPT, known as CT-2106, also reached the clinics and employed an ester linking moiety with a glycine spacer that stabilized the active lactone form of CPT and enhanced aqueous solubility [148]. Phase I/II studies with CT-2106 in patients with refractory solid tumors provided evidence of lower toxicity when compared to free CPT; however, economic concerns led to the discontinuation of this conjugate [143,149].

Table 2

Journal Pre-proof

Journal Pre-proof

more efficient PGA-drug conjugates. These include the requirement for patient stratification in clinical trials (discriminating by patient estrogen levels that correlate with cathepsin B endogenous level [150]), a more profound understanding of the mechanisms of action, the optimized design of clinical trials, and the need of effective academic-industry partnerships during drug development [147]. Furthermore, additional chemical modifications to the PGA main chain can support further improvements in the biological output of PGA-drug conjugates. The introduction of carbocysteine moieties significantly improved the solubility of PGA-PTX conjugates [151], while PTX conjugation via β-thiopropionate esters prompted more rapid hydrolysis, thereby providing a more efficient release rate when compared an ester bond. Of note, the presence of targeting moieties such as cRGD enhanced *in vivo* targeting and antitumor activity in an orthotopic triple negative breast cancer (TNBC) model when compared with non-targeted PGA-PTX [152]; therefore, the further exploration of active-targeting strategies may provide for enhanced therapeutic outcomes.

NK012 (**Table 2**), a PEG-PGA-conjugate of SN-38 (the active metabolite of irinotecan) using an ester bond that self-assembles into a polymeric micelle, is currently being evaluated in refractory solid tumors (phase I), metastatic and recurrent colorectal cancer (phase II), relapsed non-small-cell lung carcinoma (phase II), and advanced metastatic TNBC (phase II) [143,149,153]. Trials evaluating NK012 in combination with carboplatin in TNBC (phase I) and with 5-fluorouracil (FU) and leucovorin in colorectal cancer (phase I) are also ongoing (NCT01238939). In another example using PEG-PGA as a carrier, the inherent polypeptide-metal complexation ability provided by the -COOH groups of PGA has been extensively studied by Kataoka et al. and several examples are also under evaluation in clinical trials (**Table 2**). These include a diaminocyclohexane platinum (DACH-Pt/) micelle (NC-4016) for advanced solid tumors and lymphoma (phase I), and a cisplatin micelle (NC-6004) for pancreatic cancer (phase III) [154], which underwent testing alone and in combination with pembrolizumab, 5-FU, cetuximab, and gemcitabine [143].

Journal Pre-proof rm of

the conjugate [155]. *In vivo* studies confirmed that PEG-PGA-BSH conjugates became retained in the tumor to a greater degree and induced a significantly greater antitumor effect when compared to both PGA-BSH and free BSH, which induced negligible tumor growth suppression. The authors attributed these effects to lower tumor penetration and intratumoral retention of the PGA-BSH, which instead became distributed around the blood vessels [155].

As an alternative to the block-copolymer formation, many have explored the relevance of grafted forms of PEG-PGA (PGA-g-PEG). The implementation of PGA-g-PEG can save both labor and monetary costs deriving from the need to prepare and purify PEG-NH_2 (the initiator for NCA-ROP polymerization), such as is described in a study by Yu et al. that employed PEG-OH for PGA-g-PEG construction [156]. A PGA-g-PEG-CDDP conjugate displayed comparable antitumor efficacy at an equal dose to the free drug in a human MCF-7 breast adenocarcinoma model and significantly lower body weight loss at higher concentrations, suggesting lower systemic toxicity upon an increased therapeutic dose. Additional research has explored the covalent conjugation of other anticancer agents to this PGA-g-PEG platform. Conjugation of podophyllotoxin via an ester bond resulted in 82.5% tumor suppression in a multiple drug-resistant breast cancer model when compared to a reduction of 37% for the free form of the toxin [157]. Conjugation of the vascular disrupting agent combretastatin-A4 (CA4) via an ester bond provided significantly higher tumor suppression when compared to the free drug in a murine C26 colon tumor model [158]. PGA-g-PEG-CA4 demonstrated preferential accumulation around tumor vessels, sustained drug release, and 74% tumor suppression in comparison to a 24% reduction for an equal dose of the free drug [158]. Encouragingly, repeated treatments led to almost complete tumor regression, suggesting that the selected dose regime could represent a highly effective treatment option. Further studies demonstrated an improvement in tumor inhibition following the administration of PGA-g-PEG-CA4 in combination with plerixafor, an immunostimulant used to mobilize hematopoietic stem cells into the bloodstream, and the inhibition of lung metastasis [159].

iated macrophages in the 4T1 orthotopic breast cancer-bearing mouse model [160]. However, treatment with a selective inhibitor of the phosphoinositide 3-kinase gamma isoform (PI3Kγ) attenuated this immunosuppressive effect and prompted a synergistic anti-tumor effect, which significantly extended the mean survival time from 52 days in PGA-g-PEG-CA4 -treated mice to 61.8 days. Additionally, the combination of PGA-g-PEG-CA4 with the PI3Kγ inhibitor improved the tumor therapeutic effect of NLG919, an inhibitor of immune checkpoint molecule indoleamine 2,3-dioxygenase. These findings highlight the therapeutic potential of the combination of CA4 as a vascular disrupting agent with an immune modifier to induce tumor inhibition.

The application of PGA as a photosensitizing agent in photodynamic therapy (PDT) may provide a means to circumvent the low absorptivity of photosensitizers in an aqueous environment [161,162]. The conjugation of a zinc (II) phthalocyanine (ZnPc)-derivative to PGA permitted high absorptivity in the near-infrared (NIR) region at its λmax of 675 nm in an aqueous environment, elevated singlet oxygen generation efficiency, increased uptake by 4T1 breast cancer cells, enhanced photocytotoxic efficacy, and a high light-dark toxicity ratio (> 1.5-fold than ZnPc) at higher concentrations. Further studies revealed that the conjugate accumulated well in 4T1 mouse mammary tumors, and, as part of an antitumor PDT approach, induced a more significant tumor volume reduction (91%) when compared to ZnPc alone (50%). Furthermore, this study reported a suitable cardiovascular safety profile and a lack of lung metastasis.

Apart from cancer, PGA has been explored in tissue regeneration approaches or as modulators of cell death, in inflammatory- [163], ischemia- [164,165], or amyloid-related pathologies. As an example, Córdoba-David et al. recently described a nanosized soft-assembled star-shaped PGA conjugate of bisdemethoxycurcumin (St-PGA-CL-BDMC) as an effective treatment for acute kidney injury [111]. A previous study reported the biodegradability, biocompatibility, enhanced in vitro cell internalization rate, and significantly higher half-life *in vivo* for this novel stabilized carrier type when compared to

Journal Pre-proof

linea more favorable PK profile. Moreover, the rational design of the conjugate took advantage of the natural kidney tropism of PGA [111] and the use of a pH-responsive ester linker to allow BDMC release in acidic environments, which include inflamed tissues (such as damaged kidney tissue) or the endocytic-lysosomal pathway in native tubular cells.

PGA has also shown potential in the topical delivery of drugs - as an example, Dolz-Pérez et al. reported the development of a PGA-fluocinolone acetonide (FLUO) conjugate for the advanced topical treatment of psoriasis [46]. When applied within a HA-PGA cross-polymer, PGA-FLUO effectively reduced disease-associated phenotypes and proinflammatory cytokine levels in tissue and serum in an *in vivo* mouse model of human psoriasis. Due to the observed improvements in skin permeability and bioavailability, this study highlighted the potential use of polypeptidic formulations for localized dermal drug delivery.

Several studies have also underscored the ability of PGA conjugation to protect the native structure of proteins [166,167]. An intracellular deficit in the alanine:glyoxylate aminotransferase (AGT) liver peroxidase induces the rare disorder primary hyperoxaluria Type I; however, treatment with a PEG-PGA-AGT conjugate using a disulfide linker permitted the cytosolic release of AGT and the restoration of glyoxylate-detoxification in CHO-GO eukaryotic cell lines [166]. In a similar study, Maso et al. conjugated granulocyte colony-stimulating factor (G-CSF) and human growth hormone (hGH) to a PEG-b-PGA to enhance the induction of granulopoiesis [167]. Apart from achieving superior responses than PEG-protein analogs, *in vivo* analysis revealed the induction of granulopoiesis in parallel with comparable or better bioavailability and bioactivity than the commercial golden standard Pegfilgrastim, a PEGylated form of the recombinant human G-CSF analog filgrastim.

Journal Pre-proof

related to long-term toxicity with non-biodegradable probes. As an example, Zhang et al. explored a PGA-DTPA conjugate modified with an aliphatic chain as an MRI contrast agent after Gd^{3+} complexation in a rat glioma model [170]. This PDC demonstrated high signal enhancement regarding the detection of the tumor rim with tracer activity up to 2 hrs when compared to 20 min when using the commercially available Magnevist (non-polymeric formulation), and rapid clearance (within 24 hrs) from the body. Finally, a sophisticated approach to the early detection and monitoring of osteoarthritic progression employed a PGA-modified protease specific probe [21]. In this study, Duro-Castano et al. conjugated a fluorescent resonance energy transfer-based peptide probe cleavable by MMP-13 (a protease that degrades type II collagen in cartilage) to PGA and demonstrated its in vivo specificity.

Finally, recent tumor theranostic approaches that employed polypeptide-graft-polypeptoid copolymers based on PGA–PSar moieties functionalized with trans-cyclooctene (TCO) for later ^{111}In-tetrazine ligation [171] have provided promising data regarding their implementation as theranostic agents. The interaction of tetrazines with TCO represents one of the fastest bioorthogonal reactions known and is therefore increasingly used for in vivo click chemistry to offer new opportunities for polypeptide development [172]. The authors employed this polymer-based targeting agent for pre-targeted imaging and separated tumor accumulation from the imaging step. Results demonstrated adequate image contrast for 2 hrs after administration of the radiolabeled tetrazine compound, demonstrating the beneficial logistics and thus lower radiation dose received by patients. Finally, another related tumor theranostic approach employed poly(L-γ-glutamyl-glutamine)-paclitaxel (PGG-PTX) to chemically conjugate DTPA-Gd for MRI (PGG-PTX-DTPA-Gd). The capacity for *in vivo* fluorescence imaging monitoring in a lung cancer model demonstrated not only tumor accumulation by the EPR effect, with a significantly enhanced and prolonged signal intensity in tumor tissue, but also effective antitumor inhibition [173].

Polyaspartic acid (PAsp) differs from PGA by one side chain -CH_2 group, increased structural rigidity, and a different cell internalization pathway [174]; however, PAsp retains protease biodegradability [175].

There exist preclinical examples of PAsp as a homopolymer - for example, Di Meo et al. introduced a long ethylene glycol-bis(succinic acid) linker (ester and amide functionality) when conjugating PAsp to Dox to obtain a conjugate that acted as an intra-tumor reservoir for gradual drug release [176]. This PAsp-Dox conjugate provided for enhanced antitumor activity and prolonged survival when compared to free Dox treatment in a breast cancer model [176]. However, as in the case of PLL and PGA, PEG-block copolymers of PAsp remain the most advanced examples within the clinics (**Table 3**).

Table 3

Matsumura et al. engineered a PEG-PAsp-Dox conjugate (NK-911, the first polymeric micelle evaluated in human clinical studies) using an amide linker that could be loaded with Dox via physical entrapment through π–π stacking [177]. NK-911 has been evaluated in a phase II clinical trial for metastatic pancreatic cancer, although results have yet to be reported [178]. Similarly, a polymeric micelle compose of a PEG-PAsp conjugate of the chemotherapeutic drug epirubicin using an acid-labile hydrazone bond (NC-6300) is currently under evaluation in phase I/II clinical trials for solid tumors and soft tissue and metastatic sarcoma [179]. NC-6300 exhibited an improved safety profile with lower toxicity and allowed administration of epirubicin at a higher individual and cumulative dose in phase I studies. Maeda et al. also evaluated NC-6300 as part of a combination therapy with high-intensity focused ultrasound (HIFU), where it demonstrated significant tumor growth inhibition in PaCa-2 human pancreatic cancer cells in vitro and a murine model of colon cancer [180] (**Figure *2***).

Journal Pre-proof

An exploration of NC-6300 targeted with an anti-tissue factor antibody (clone 1849) provided evidence of enhanced antitumor activity in pancreatic and gastric cancer mice models (high tissue factor expression) and equivalent antitumor activity in a pancreatic cancer model (low tissue factor expression) when compared to a non-targeted analog [181]. Unfortunately, the selected antibody prompted blood coagulation, requiring the selection of a replacement (Ab 1859); however, the authors observed similarly enhanced anti-tumor efficacy with this alternative antibody [127].

The bioresponsiveness of PAsp-associated conjugates can derive from both the polypeptide-drug linker and the polypeptide matrix itself [182,183]. For example, the introduction of a disulfide linking moiety between the polymeric blocks of PEG-PAsp conferred redox-responsiveness, while a hydrazone linking moiety between the polymeric blocks and Dox provided pH-responsiveness [86]. This advanced dual-responsive PEG-PAsp-Dox conjugate also permitted the encapsulation of Dox via hydrophobic interactions and π-π stacking. *In vitro* evaluation of this conjugate confirmed low Dox release at pH 7.4, higher release at pH 5, and even higher release in the presence of 10 mM glutathione (GSH). However, the *in vivo* effectiveness of this conjugate remains undescribed.

Polypeptide conjugation of water-soluble therapeutic agents can improve their safety profiles by hindering rapid penetration into healthy tissue and excretion. GEM conjugation to a modified PEG-PAsp polymer via an acid-labile cyclic acetal linker provided for prolonged blood residence time and enhanced tumor accumulation [184]. Results demonstrated comparable tumor growth suppression for the conjugate at a much lower dose compared to the free drug and a better safety profile.

Journal Pre-proof

Journal Pre-proof

h via 1,4,7,10-tetraazacyclododecane-1,4,7,10-tetraacetic acid (DOTA) conjugation for Gd complexation [185]. Higher accumulation and sustained radioactivity in the femur 60 min after injection when compared to a low-Mw positron emission tomography (PET) probe demonstrated the potential of this conjugate in the detection of bone metastases. Jiang et al. explored an FA-targeted PEG-PAsp-DTPA/Gd system as an MRI probe, with results demonstrating enhanced tumor signal intensity over a longer time window [123]. Similarly, the conjugation of the BODIPY-Br2 photosensitizer (which possess high singlet oxygen generation efficiency and NIR fluorescence) to a pH-sensitive amphiphilic PAsp polypeptide generated a macro-photosensitizer for an NIR imaging-guided PDT approach for cancer treatment [186]. Of note, the lack of cytotoxicity and biocompatibility of PAsp-based systems make them an attractive approach to the design of theranostics.

With the design of the next generation of PDCs in mind, the inherent properties of PAsp as microbicide has the potential to synergize with a conjugated antibiotic. Yavvari et al. explored this approach, where the fine-balance of charge and hydrophobicity guides activity against microbacteria [187]. The non-hemolytic and non-toxic nature of PAsp derivatives in mammalian cells provide significant advantages over existing antimicrobial agents.

Journal Pre-proof

3.1.4 Expansion to Hybrid Materials

Hybrids have recently emerged as a promising class of exciting materials for biomedical applications. This term usually refers to complex systems that encompass two or more elements that differ by nature and/or function elements and display complementary properties [188]. The development of hybrid polypeptide-containing materials aims to generate carriers with fully optimized parameters to permit efficient pathological site tropism and extravasation,

Journal Pre-proof

cellu[illegible] and further detailed below.

Table 4

Xu et al. reported the loading of PGA-Dox conjugated via a pH-sensitive hydrazone linker into porous discoidal silicon carriers 2.5 μm in diameter and 700 nm in thickness (iNPG-PGA-Dox) to target liver and lung metastasis thanks to their optimized size and geometry and dimensions (**Figure 3**) [189]. This approach prompted elevated levels of tumor cell internalization and endosomal escape, which bypassed mechanisms of drug resistance and enhanced Dox release in the perinuclear region. Both PGA-Dox and iNPG-PGA-Dox failed to induce cardiac damage when compared to free Dox, while the increased size of iNPG-PGA-Dox inhibited renal clearance and lung accumulation. This hybrid material improved median survival, with 50% half of the animals achieving long-term survival (**Figure 3**).

Figure 3

While oral delivery may represent the most convenient administration route for PDCs, the acidic stomach environment, the need to penetrate through the intestinal mucosa, and problematic drug release represent significant barriers. A hybrid system based on a PGA-g-PEG-Dox conjugate employing a pH-responsive linker coated with chitosan via electrostatic interaction displayed low Dox release in an acidic pH, suggesting the ability of this hybrid conjugate to survive in the gastrointestinal tract [190]. The chitosan layer acts as a mucoadhesive agent and facilitates the opening of tight junctions and mucus permeability in the small intestine [191]. The pH level (7.4) in the terminal ileum favors chitosan layer detachment due to deprotonation and releases

Journal Pre-proof

PGA- omal escape provided evidence for the overall efficacy in an Ehrlich ascites carcinoma model [190].

The introduction of stimuli-responsive crosslinkers into hybrid materials, as explained before for purely polypeptidic approaches, can help to trigger intracellular drug release. Tai et al. developed a bioreducible carrier based on a disulfide-crosslinked hybrid carrier utilizing an Arg-His-Cys polypeptide with grafted stearyl moieties for siRNA delivery [192]. Arg moieties induce nucleotide complexation, Cys moieties are used for disulfide crosslinking and cytoplasm-sensitive dissociation, His moieties act as a proton sponge that raises the pH within the endosome to allow endosomal escape, and the stearyl moieties allow enhanced cellular uptake and endosomal escape. The results confirmed the essential nature of the His and stearyl moieties to successful transfection, while the assessment of *in vivo* gene silencing in a Luc-HeLa xenograft model provided evidence for a 2.5-fold more significant reduction in luciferase expression for cationic crosslinked stearyl-polypeptide complexed with siRNA compared to naked siRNA. Yao et al. employed the same carrier for a combination therapy approach employing miR-34a (a miRNA activated by p53 that regulates apoptosis and cellular senescence) and Dox in a DU145 prostate carcinoma xenograft model [193]. This hybrid material-based anti-tumor approach prompted preferential accumulation in the tumor, higher necrosis, and a more significant anti-tumor effect when compared to microRNA micelles, free Dox, and Dox micelles [193]. The same approach could be applied to the design of advanced PDCs, as the presence of an adequately bioresponsive linker for Dox (i.e., hydrazone [179,194]) could significantly improve the *in vivo* results as an additional layer of PK control for Dox sustained release would be present.

Journal Pre-proof

The failure of many single therapeutic-based approaches often derives from the sheer molecular complexity of most diseases; however, the development of combination-based therapies that simultaneously target different molecular pathways may improve outcomes [195,196]. Additionally, targeting multiple aspects of the same pathway can lead to synergistic therapeutic outcomes [197,198]. In the case of cancer, combination therapies are widely used in the clinic where they exhibit demonstrated anti-tumor efficacy; however, achieving the required drug ratio in a tumor cell is made difficult by the differing absorption, distribution, and metabolism rates of the different single therapeutic agents employed. Therefore, nanoformulations that allow simultaneous delivery [199], including those with simultaneous conjugation of drug combinations to the same polypeptidic carrier, represent attractive and feasible options. Polypeptidic carriers provide multivalency for the conjugation of several drugs, targeting moieties, and/or monitoring probes, while precisely chosen linking chemistries can allow for the controlled release of the desired drug ratio in a specific organ/tissue [24].

Polypeptide-based combination therapies encompasses various possible strategies; these include the conjugation of two drugs in a single polypeptide chain ("Type III"), a PDC with a second polymer-encapsulated drug, the combination of a physical mixture of two PDCs, or a PDC with a free drug/other therapies administered in parallel [200–204]. Type III combination approaches assure the simultaneous co-delivery of active agents, that, together with the presence of adequate bioresponsive linkers, allow the fine-tuning of the release kinetics profiles to enhance drug synergism in a personalized manner [201]. The paucity of reported studies (summarized in **Table 5**) reflects the relative difficulty in generating a single polypeptide containing more than one drug in a single chain; however, options such as bioresponsive crosslinked and/or self-assembled systems represent unexplored alternatives to the above-mentioned strategies that could provide for the development of novel architectures bearing synergistic drug combinations [96,205].

After the establishment of the concept of a combination therapy based in the conjugation of two drugs to a single polymer [206], some notable examples employing polypeptides have emerged. PGA derivatives tend to be the most numerous; Markovsky et al. demonstrated that a PGA-based combination conjugate possessing hydrazone-linked Dox and ester-linked PTX displayed therapeutic synergy following administration to a mammary adenocarcinoma model [207]. PGA-Dox-PTX effectively inhibited tumor growth when compared to a combination of free drugs or single polypeptide conjugates and displayed an improved safety profile. In a related study [89], Li et al. established that linear PGA and a PEG-polyglycerol dendrimer bearing Dox and PTX displayed increased tumor accumulation and higher antitumor activity when compared to single agents.

Combinations of mitogen-activated protein (MAP) kinases pathway inhibitors can decrease acquired resistance in advanced melanoma, and clinical trials have demonstrated objective tumor responses in approximately half of the patients treated in this manner [208]. With this in mind, Pisarevsky et al. reported that a PGA-based combination conjugate of selumetinib and modified dabrafenib (both MAPK inhibitors) exhibited enhanced tumor growth inhibition and prolonged survival rate in a melanoma mouse model when compared to the combination of free drugs and the United States Food and Drug Administration (FDA)-approved combination of dabrafenib and trametinib (another MAPK inhibitor) [82].

Interestingly, the rational selection of the linker can significantly influence the overall potential of a given combination, as reported in two studies of PGA-based combination conjugates of Dox and the aromatase inhibitor aminoglutethimide (AGM) [91,194]. The choice of a protease-labile AGM linking moiety revealed a link between linker hydrophobicity and enzyme accessibility to allow cleavage that directly influenced drug release kinetics [91] and the inhibition of metastasis in an orthotopic breast cancer model. Furthermore, the influence of drug loading on conjugate conformation and release kinetics

Journal Pre-proof

indic with AGM, resulted in an enhanced combination conjugate that prompted significantly greater tumor growth inhibition when compared to the free drugs [194] (**Figure 4**).

Figure 4

Examples of drug conjugation plus encapsulation using the same polypeptidic carrier are also common; this approach is particularly useful when one of the drugs lacks adequate the chemical functionalities required for conjugation or in case of cross-reactivity issues with the other conjugated drug. Examples include CPT linked via an ester bond to PGA-g-PEG, which allowed the physical entrapment of Dox and significantly higher tumor accumulation post-administration, thereby improving tumor inhibition when compared to the combination of free drugs [93].

Studies combining drug conjugation and metal complexation for combination therapy also abound [72]. Recently, Li et al. reported the use of a disulfide self-immolative linker instead of an ester bond in a PEG-PGA-CPT conjugate in an orthotopic breast cancer 4T1 model [88]. The authors observed that further cross-linking of the particles with CDDP significantly improved antitumor efficacy. CPT became efficiently released in a reducing environment (exposure to 10 mM dithiothreitol - DTT), and CDDP provided additional stability to the polypeptidic micelles that extended blood circulation times. These improvements resulted in a higher remaining dose, more efficient tumor accumulation, and thus enhanced tumor suppression when compared to the combination of free drugs [88]. Song et al. explored a PEG-PGA-PPhe triblock copolymer with PTX entrapped in the hydrophobic core and CDDP attached to the PGA central core via polymer-metal complexation [87]. Evaluation in an aggressive xenograft A549 human lung model provided evidence for enhanced tumor growth inhibition and safety (no evident liver and lung toxicity) when compared to a combination of free drugs, which induced severe side effects and body weight loss. A

Journal Pre-proof

subse the prolongation of median survival when compared to both a non-targeted formulation and free drug treatment [41].

Combination therapies comprising the physical mixtures of PDCs also deserve consideration, as, if adequately engineered, they can intrinsically assemble in one unique combination micelle that can be stabilized by crosslinking. For example, single PLL-PTX and HA-GEM conjugates formed using via ester bonds yielded stable micelles upon electrostatic interactions and displayed efficient antitumor activity when compared to the combination of free drugs [209].

Finally, therapeutic approaches such as siRNA can also benefit from inclusion in polypeptide-based combination therapies, as already demonstrated with encapsulation approaches such as that reported by Sun et al. in an article that provided evidence for the synergistic effect of anti-Bcl-2 siRNA and Dox encapsulation within a PEG-PLL-PAsp copolymer in a HepG2/ADM multidrug-resistant hepatoblastoma model [210]. This combination therapy provided enhanced tumor suppression with no obvious cardiotoxicity and body weight loss when compared to free Dox treatment. In another example, Zhou et al. co-delivered docetaxel and MMP-9 siRNA using a diblock polyglycerol-C18-PLL carrier, finding significantly higher tumor inhibition when compared to single-drug formulations and better blood compatibility compared to polyethyleneimine (PEI) [211].

Journal Pre-proof

3.3 Selection and Optimization of Polypeptide-drug Linking Chemistry

The selection of the linking moiety relies on the available functional groups on the polypeptide carrier and selected cargo, the required administration route and associated microenvironmental conditions, and the biological barriers faced on the “journey” to the targeted tissue/cellular compartment. Optimal linking moieties allow for prolonged plasma stability followed by efficient and controlled release kinetics under the desired conditions. The first generation of

Journal Pre-proof

PDCs stinct types of advanced linkers and spacers that modulate drug release/accessibility/exposure can significantly improve therapeutic outcomes.

Post-polymerization modifications that introduce additional functionalities, targeting moieties, or fluorescence probes mainly employ non-biodegradable linkers [213]; however, targeting specific intracellular sites or transcytosis processes may require bioresponsive linkers, as cleaving the targeting ligand from the conjugate could secure cargo release without cell recycling [120,132,133]. Of note, self-immolative linkers require several synthetic steps, an approach that involves increased costs and scalability limitations, and, additionally, metabolites must be studied to avoid undesired effects. We will discuss the various linking strategies related to PDCs and analyze challenges and future opportunities in the following sections (**Figure 5**).

Figure 5

3.3.1 pH-responsive Linkers

pH-sensitive linkers represent the most broadly used linking moieties and take advantage of the lower pH of inflammatory sites, the TME (due to the Warburg effect [214]), and the intracellular organelles and vesicles that play important roles in the uptake of DDSs [53]. Acid pH-cleavable linkers employed for drug conjugation or the creation of acid-degradable polymers include orthoester, acetal/ketal, imine, hydrazone, and cis-aconityl bonds (**Figure 5**) [215,216].

Imine and hydrazone linkers represent the most commonly employed moieties, due to the straightforward reaction between the carbonyl group (aldehyde or ketone) and amine or hydrazide groups, respectively, under mildly acidic conditions. Additionally, linker stability can be modified via the inclusion of an electron-donating/withdrawing group through resonance or steric effects. As they exhibit higher stability than imine binds due to the

Journal Pre-proof

deloc ...on in general. The introduction of a positive charge on the nitrogen (trimethylhydrazonium ion) increases resistance to hydrolysis, even at low pH, due to the resistance to protonation [217]. The introduction of an aromatic component into a carbonyl compound group represents another strategy to increase linker stability [218]. The stabilization of the hydrazone bond can be summarized in the following relation: Ar-CH=N-N-CO-Ar ~ Ar-CH=N-N-CO-Alk ~ Alk-CH=N-$N^{+}R_3$ >> Alk-CH=N-N-CO-Ar > Alk-CH=N-N-CO-Alk and can be explained by the overlap of the p-orbitals from the double bond and the structure stabilization by the aromatic ring that does not favor protonation. The Dox reactive carbonyl group has been widely employed for hydrazone linkage, leading to relative stability in blood circulation and improved drug release kinetics in the TME [44,86].

Acetals or ketals exhibit stability under basic conditions but hydrolyze rapidly in acidic microenvironments [219]. While instability under aqueous acidic conditions has limited their use as linking moieties, cyclic acetals display higher stability. Examples in drug delivery include PAsp-GEM, which displays stability and low drug release at physiological pH, but significantly higher levels of GEM release in response to acidic conditions [184]. These characteristics prompted comparable tumor growth inhibition in vivo when using a four-times lower dose of PAsp-GEM when compared to the free drug.

Ester bonds undergo cleavage under acidic conditions and through the activity of hydrolytic proteins such as esterases [220]. Ester linkers form part of those PDCs that have yielded promising data in clinical trials (examples include the previously detailed NK012, Opaxio, and CT-2106), with many others under preclinical evaluation (**Table 1-5**). Ester bond stability can be modulated by the addition of strong electron-withdrawing groups to increase the rate of hydrolysis; however, the presence of a substituted acyl or alkoxy groups results in steric hindrance and generates the opposing effect [218].

Journal Pre-proof

with a partial positive charge on the ester carbonyl carbon that readily undergoes hydrolysis under mildly acidic conditions. Examples using β-thiopropionate esters include a study of PGA-PTX conjugates [151] and another that compared ester and β-thiopropionate linkers in PEG-PLL-dexamethasone conjugates [221]. While both linkers displayed stability at physiological pH and triggered drug release at acidic pH, the β-thiopropionate linker permitted a four-fold higher drug release, most probably due to the pH and redox-sensitive release of dexamethasone (a corticosteroid) that triggered a marked neutralization of tumor-promoting inflammation in colorectal cancer therapy [221].

Of note, pH-responsive PDCs do suffer from important limitations. pH differences between tumor and normal tissue may not be sufficient to permit targeted drug release, and the required pH level can often lie a significant distance away from the blood vessels, which limits responses in perivascular regions [53].

Journal Pre-proof

3.3.2 Protease-responsive Linkers

A wealth of knowledge has established that proteolytic enzymes (proteases) play key roles in early and progressive stages of diseases such as cancer and degenerative conditions [222,223]. Proteases specifically cleave biologically important molecules with a high turnover rate and affect disease progression by modulating the cellular microenvironment. Increased protease expression in lesions associated with cancer/degeneration provides a means to guide the development of PDCs and inform on linker choice [224–226].

As a prime example, the lysosomal cysteine proteases papain (that can digest/cleave substrates such as Gly-Gly-Leu [227]) or Cathepsin B are overexpressed in the TME of certain cancers, where they can regulate the innate and adaptive arms of the immune system [228], as well as in ischemic sites

with Cathepsin B-cleavable linkers include a PEG-PLL dendrimer conjugated to GEM via an amide bond using a GFLG linker that demonstrated strict enzyme-dependent drug release kinetics [113]. Cathepsin B-cleavable linkers can also be combined with self-immolative linkers to improve drug release, as demonstrated with various forms of dendrimeric PEG-PLL-Dox conjugates [230]. The authors observed optimal drug release for a Val-Cit linker with a self-immolative diglycolic acid motif when compared to a non-self-immolative glutaric acid-GLFG linker.

Cathepsin K, a related cysteine protease that cleaves the Gly-Gly-Pro-Nle peptidic sequence, has been explored in polymer-drug conjugates [231]; however, this has not yet extended to descriptions in PDCs. Cathepsin K overexpression in bone tissue resorption sites suggests a potential utility in therapeutics for breast or prostate cancer bone metastases, osteoporosis, and other bone-related pathologies [231–233].

MMPs are another class of proteases overexpressed in many cancer types that have roles in tumor invasion, metastasis, and angiogenesis [234], and various other pathologies [222]. MMP family members cleave a wide variety of short peptides [53], with examples in PDCs including PEG-PLL conjugated to Dox via a CPLGLAGG peptide, a specific substrate for MMP-2 [54].

Importantly, protease-specific cleavable agents that non-invasively image protease activities *in vivo* will offer unique opportunities for disease state monitoring. Several protease-sensitive activatable ligands have been developed based on a polymeric carrier using fluorescent reporter [235–237]. While such probes have been used to demonstrate proof-of-principle for *in vivo* imaging approaches in various disease models, they suffer from several disadvantages such as low specificity and limited PK properties. The conjugation of protease-specific probes to polypeptidic carriers can overcome these limitations. This strategy was recently demonstrated with an *in vivo* optical imaging probe comprised of a PGA-conjugated Förster resonance energy transfer

Journal Pre-proof

(FRET) and provide a real-time readout on the therapeutic efficacy of MMP13 inhibitors [21].

3.3.3 Redox-responsive Linkers

Disulfide linkers provide redox sensitivity to PDCs, allowing stability in plasma where GSH levels are approximately 5 μM, and cleavage in the cytosol of tumor cells, where GSH levels rise to 1–10 mM [238]. Indeed, GSH levels in tumor cells can be up to four times that observed in normal cells, thereby providing a suitable trigger that guides linker choice in the design of efficient anti-tumorigenic PDCs [239]. Disulfide linker stability can be enhanced by introducing electron-donating groups (e.g., methyl groups) next to the disulfide bond, while the introduction of aromatic groups favors bond dissociation [240]. As an example, two different studies reported the attachment of the thiol group of BSH to PEG-PGA [155] and PEG-PLL [140] via a small spacer to enhance stability under physiological conditions and allow rapid release in a reducing environment.

The incorporation of redox-responsive functionalities can be carried out even in the absence of thiol groups via the use of various synthetic strategies. This includes the implementation of self-immolative linkers that undergo degradation in response to the reductive environment and result in intact drug release. The sequentially triggered chemical rearrangements implicated involve two main mechanisms: quinone methide elimination or intramolecular cyclization. Introducing electron-donating groups that increase electron density in the aromatic ring can accelerate electron transfer and thus degradation for quinone methide elimination, while electron-withdrawing groups can have the opposite effect [218]. The detailed mechanisms and crucial factors affecting the degradation have been previously reported [241]. The electrophilicity of the carbonyl group determines the cyclization rate for the second type of self-immolative linkers; thus, carbonates faster undergo degradation than carbamates. The type of cycle is also important - lower ring chains are energetically

Journal Pre-proof

prefe[illegible] 1,4-membered cycle providing for slower drug release kinetics [139]. Examples with CPT [88] and monomethyl auristatin E [42] confirmed improved drug release in the presence of reducing agents. The utility of redox-sensitive self-immolative approaches has also been demonstrated in the field of regenerative medicine, where the intrathecal administration of a PGA-SS-fasudil conjugate in acute and chronic models of spinal cord injury led to enhanced neuroprotection-neuroregeneration, with a clear advantage over and free fasudil (a potent Rho-kinase inhibitor) *in vivo* [19].

Of note, sensitive diselenide linkers display similarities to disulfide linkers and can provide redox-responsiveness [242]; however, they have yet to be explored in the development of PDCs.

3.3.4 Strong Non-covalent Interactions - Metal Complexation

Strong ionic bonding between metals and carboxylic group-bearing polymeric chains has been widely employed in the design of nanomedicines. As mentioned above, metal complexation represents the most straightforward method to obtain Pt-based drugs with examples of such PDCs already in the clinic [154]. PGA and PAsp polypeptides possess substantially stronger innate complexation capabilities when compared to traditional encapsulation, and they display a higher degree of responsiveness at lower pH due to the protonation of carboxylic groups involved in Pt-based drug release.

Examples at the preclinical stage include Pt-based drugs in combination conjugates. PEG-PGA-Phe-PTX-CDDP micelles released significantly higher levels of CDDP at acidic pH when compared to physiological pH [87]. PEG-PGA-CPT-CDDP conjugates, in which CPT was first linked to the polypeptidic carrier through a disulfide bond and then self-assembled into micelles, showed remarkably prolonged blood circulation, controlled CPT release, and high antitumor efficacy. In these cases, micelles were stabilized using CDDP as a crosslinker after complexation with the -COOH moieties of PGA [88].

Journal Pre-proof

M ,169]

and as potent anticancer therapeutics, as demonstrated with an apoptosis-inducing PLL-based conjugate [243]. This example simultaneously acted as an intracellular Ca2+ homeostasis perturbing agent that induced synergetic apoptosis and suppressed cell migration and invasion [243]. Furthermore, metal complexation using PDCs have also been employed as protectants for acute radiation syndrome, as is the case of RadProtect® (in phase I clinical evaluation, also known as CC-AMI, developed by Original BioMedicals), a PEG-b-PGA micelle linked by ferrous ion that chelates the -COOH of the PGA chain and -SPO_3H of amifostine for controlled release of the cytoprotective drug into the bloodstream [244,245].

4. Analytical Strategies for Characterization of Polypeptide-drug Conjugates

Due to the (poly)ionic and proteinic nature of PDCs, their translation from the bench to the bedside can be an arduous and expensive undertaking, as this transition requires reproducible and scalable polymerization techniques, exhaustive characterization, the implementation of sophisticated analytical tools, and the collection of safety and efficacy data. The rapid detection of the most promising candidates will reduce costs and time, and the implementation of clinically-relevant characterization techniques can hasten PDC development [1]. As PDCs are complex, heterogeneous, and multi-component ionic systems, they represent a significant analytical challenge; moreover, combination therapies that employ two (or more) active agents within the same polymer main chain add further complexity. A multidisciplinary approach that integrates “know-how” from the fields of polyelectrolyte characterization [246,247], pharmaceutics [248,249], and analysis of antibody-drug and other drug-conjugates [250–252], may provide broad insight into adequate characterization strategies for PDCs.

Journal Pre-proof

A olves measurements of “clean” sample solutions during the synthesis and manufacturing process, and in bioanalysis, which itself includes biological sample analysis through in vitro, in vivo and clinical studies. [253]. In the following sections, we will discuss the utility of recently reported analytical techniques for the assessment of PDC quality, physicochemical and biological characterization techniques, and the obstacles that we currently face. For a more detailed review of the techniques used in the characterization of DDSs, we direct the reader to the following references[24,254].

4.1. Insight into the Physicochemical Characterization of PDCs

The multistep synthesis of PDCs involves diverse chemical reactions that require purification from residual reagents and chemical identification after each step. A combination of techniques is generally required for adequate characterization before progression to biological evaluation. Physicochemical properties must be optimized to successfully generate effective PDCs and exploit their unique PK features. These properties will impact clinical safety and efficacy and can vary depending on polypeptide nature, route of administration, and desired application. The most important features for all conjugates are size, Mw, charge, drug loading, free drug content, solution conformation, drug release, and the presence of aggregates (high Mw impurities) [25,255]. While the covalent attachment of drugs to a polypeptide backbone usually represents a random process that influences heterogeneity [256], the accurate determination of drug loading represents, alongside free drug content, a parameter of immense importance. A free drug content of less than 2wt% of total drug loading is mandatory for progression to biological characterization [206].

Each characterization step requires a set of well-defined analytical methods/protocols to ensure product quality. The routine methods employed for the physicochemical characterization of PDCs have been described before [254] and fall outside the scope of this review. Instead, we will discuss those

Journal Pre-proof

consi ne to rapidly and efficiently foster translation.

Nuclear magnetic resonance (NMR) represents the most routinely employed technique thanks to its non-invasive nature, the minimal sample preparation required, and its suitability for the attainment of information under physiological conditions [257]. NMR can unravel chemical composition and structure, estimate drug loading, and identify impurities (side products of reaction). Also, information regarding conformation, polymer chain dynamics, and interactions with biological components can be gleaned from NMR analyses. Unfortunately, NMR analysis becomes impossible following the crosslinking of polymers during the polymerization process or as a post-polymerization chemical treatment due to signal broadening; however, crosslinked polymers are amenable to analysis by NMR spectroscopy using techniques such as solid-state NMR [258]. Despite these qualities and versatility, NMR has one main drawback – low sensitivity – that derives from low interaction energies; however, the implementation of various strategies can increase NMR sensitivity [259]:

i. **Higher sample concentration** allows signal detection of low abundancy drug in a conjugate; however, this approach can lead to broad peaks, poor resolution, and complicated data analysis, and requires a balance between high selectivity and resolution.

ii. **Optimization of NMR pulse sequences** - An NMR experiment is divided into two parts: a short pulse sequence, measuring the relevant spin signal, and a more extended period of spin relaxation [260]. The addition of relaxation agents (such as paramagnetic [Cr(acetylacetonate)$_3$] or lanthanide complexes) reduces recovery times of excited nuclei and substantially increases sensitivity [261,262]. Lanthanide complexes interact with the solvent to allow proton exchange with water to then enhance the relaxation of the targeted biomolecule [263]. The reduction of spin relaxation times that

have been implemented in 3D or 4D experiments of biomolecules [264,265].

iii. **Increasing magnetic field strength** by employing superconducting NMR magnets and hybrid NMR magnets at 1 and 1.2 GHz, respectively. NMR signals increase quadratically with an increase in magnetic field strength, thanks to an increased relaxation rate [266].

iv. **Spin-alignment transfer strategies**, which include dynamic nuclear polarization and *para*-hydrogen-induced polarization in liquid and solid-state NMR. Signal averaging represents the most commonly employed method under conditions of low signal-to-noise (S/N) ratio; however, introducing the hyperpolarization of nuclear spins through the above-mentioned techniques can significantly increase the S/N ratio. The potential of these techniques has been shown demonstrated in numerous studies, including those exploring polypeptide folding, macromolecular interactions, structural characterization of biomolecules in an endogenous cellular context, or rapid real-time detection of metabolism both in vitro and in vivo [267–271].

v. **Optimization of NMR probes and coils** – reducing the coil size and NMR probe temperature can increase the S/N ratio [272,273].

Techniques such as dynamic light scattering (DLS), size exclusion chromatography (SEC), gel permeation chromatography (GPC), small-angle neutron (SANS), X-ray (SAXS) and light (SALS) scattering, matrix-assisted-laser-desorption time-of-flight mass spectrometer (MALDI-TOF MS), analytical ultracentrifugation, scanning/transmission electron microscopy (SEM/TEM and cryo-TEM), or atomic force microscopy (AFM) provide information regarding size, average Mw, or conformation (**Figure 6**). These features determine the biodistribution, clearance route, cellular uptake, and biological performance of PDCs [91,96,274,275]. The size range for successful targeting and adequate half-life time differs depending on the administration route; however, we understand less about the influence of conformation, although it does modulate final output [96]

Journal Pre-proof

While ***dynamic light scattering (DLS)*** represents a straightforward and rapid technique to implement, results must be supported by findings from complementary methods due to problems related to the absorption of light, the presence of large aggregates, mathematical calculations, and the available amount of the sample. In general, DLS is employed for stability studies in biological fluids or phosphate buffer saline by following size and the appearances of aggregates [276–278]; nevertheless, a better indicator of PDC stability is free drug content, which is usually assessed by HPLC coupled with different detectors [279]. Unfortunately, there exists a general lack of data regarding stability during storage, stability in solution or biological fluids, and stability following freeze and thaw cycles. The relevancy/ necessity of such data has been demonstrated with other DDSs in the clinics [280] and should be considered in early development stages for PDCs. We note the term stability not only associates with polypeptide mainchain and polypeptide-drug linker but also with the polypeptide-targeting ligand bond. Thus, additional studies should be performed for every PDC decorated with a targeting moiety.

Electron microscopy, and, in particular, transmission electron microscopy (TEM), can directly image and characterize polypeptide-based nanosystems of varied sizes and shapes. This includes rod-like PGAs [281], vesicular PEG-b-PGA-Dox conjugates [121], polypeptide polyplexes [282], St-PGAs, or crosslinked, self-assembled St-PGAs [96]. However, depending on the potency of the instrument, size can still represent a limitation, while the low contrast of polypeptides can make TEM a tricky technique to implement. One of the main drawbacks of microscopic techniques is the need for sample preparation procedures requiring the addition of conducting agents for the imaging of non-conductive materials and drying, diluting, and/or freezing, which can affect sample morphology [283].

Journal Pre-proof

Journal Pre-proof

based nanosystems in solutions that mimic physiological media. The possibility of sample analysis without prior sample preparation, as for microscopic analysis, is of major importance since such systems given their intended biomedical use. Moreover, specific surface interactions in microscopic analysis can lead to surface-induced morphological changes, as exemplified by Miller et al. [284]. The authors demonstrated fiber formation in TEM analysis of an octapeptide, although SAS failed to provide evidence of self-assembly in solution [285]. SAS is particularly well suited to the study of protein and polypeptide self-assembly, as it allows the investigation of objects and features in the 10 to 500 nm scale. For example, Zagorodko et al. established the presence of nanorod-shaped supramolecular species formed by St-PGAs with benzene-tri carboxamide-based cores of different hydrophobicity by SAXS and SANS [281]. The obtained profiles demonstrated that St-PGAs with hydrophobic cores behaved as typical polyelectrolytes at low concentration, but assembled into one dimensional-nanorods upon an increase in concentration due to supramolecular interactions in the center of the molecule. SAXS has also been successfully employed in the analysis of the self-assembly of PLL into micelles, in a study that investigated the influence of the degree of ε-PLL modification (a natural L-lysine polymer produced by biotechnological processes) with octenyl succinic anhydride. Results suggested that the increased degree of substitution promoted micelle aggregation to form the larger particles previously seen by DLS [285].

SAS can also provide information regarding how drug/linker conjugation influences PDC structure in solution. Conejos-Sánchez et al. employed SANS to explore the formation of PGA-doxycycline conjugates with varying drug loadings [279]. SANS revealed that differences in drug loading did not significantly influence conjugate solution conformation, with all conjugates exhibiting similar *in vitro* activities; however, drug conjugation itself significantly changed PGA conformation. Arroyo-Crespo et al. employed scattering data to investigate the structures of PGA based combination-drug conjugates with fixed Dox content and varying AGM content when conjugated through a glycine linker [91]. While low AGM loading permitted sufficient flexibility to retain a helical

Journal Pre-proof

confo umor efficacy.

While sophisticated SAS techniques can provide valuable information regarding PDCs, they are costly and generally inaccessible for routine analysis and usually employed for selected candidates only. Alternatively, techniques such as circular dichroism [286–289], SEC, or ***field flow fractionation (FFF)*** coupled with light scattering detectors provide easier and more accessible options to study secondary structures and could be a valuable alternative that is easy to implement at the industrial scale. Alongside MALDI-TOF [138,290,291], SEC and GPC have been used for decades to estimate Mw, PDI, size, and purity of polymers produced by cells or living organisms or chemical synthesis [292] and are the method of choice for the characterization of polypeptides and hybrid polypeptide materials [87,91,92,167,293–295]. However, FFF has emerged as a complementary characterization technique given numerous advantages over SEC, which include, i) enhanced separation of high Mw molecules, ii) a lack of shear degradation and interaction with columns, iii) that lack of requirement for calibrations curve obtained from standard materials that do not match the analyte, iv) "tailor-made" separation by cross-flow adjustment, v) the adjustment of separation according to the special requirements of a given sample (a gradient of any shape can be implemented), and vi) the ability to analyze gels and complex nanosystems [296]. To the best of our knowledge, examples of FFF-based characterization of PDCs have yet to be reported; however, entities such as the US National Cancer Institute Nanotechnology Characterization Laboratory (NCI-NCL) and, the European Nanomedicine Characterization Laboratory (EUNCL) have included asymmetric FFF (AF4) analysis as part of the first-line characterization tools required for the analysis of complex nanosystems and, therefore, the implementation of an associated technique for PDC analysis is a must [297]. An example of the general utility of AF4 when compared to SEC in the characterization of PDC adjacent conjugates, is described by Rebolj et al., who demonstrated the need for two SEC columns to obtain comparable data to AF4 analysis for a 19 kDa PEG-G-CSF conjugate [298].

Journal Pre-proof

arrier liquid is pumped from inlet to outlet, establishing a parabolic flow. An additional force is applied perpendicularly to the direction of primary flow, forcing the sample to accumulate towards the channel back wall, thereby inducing separation. The mechanism of separation depends on the force applied; accordingly, FFF can be divided into flow, electrical, centrifugal/sedimentation, gravitational, and thermal FFF techniques that separate components by hydrodynamic diffusion, behavior in an electric field, chemical composition, mass, and thermal diffusion, respectively. Sedimentation (SdFFF) and magnetic (MgFFF) FFF have also been described in the characterization of ligand-decorated DDS. MgFFF represents an important means to optimize magnetic DDSs [299–302], while SdFFF has been implemented in the separation of poly(d,l-lactic-co-glycolic acid) microspheres of different sizes [303] and stability studies after lyophilization and storage [304].

FFF can be coupled with a range of detectors, such as UV VIS, refraction, fluorescence, DLS, and multi-angle light scattering (MALS) detectors, viscometers, or inductively coupled plasma-mass spectrometers (ICP-MS). Separation is generally performed under mild conditions and applies to delicate samples of biological origin, such as proteins, protein complexes, and nucleic acids [305]. A single measurement and the analysis of FFF obtained chromatogram – fractogram, yield the size and concentration of each component in a mixture at high resolution without the problem of discriminating smaller particles observed in batch DLS [306].

FFF is also suited to the analysis of neutral and charged particles, a clear advantage for the analysis of polyelectrolytic PDCs. The relationship between the geometric radius (R_g) and Mw obtained from FFF-MALS can provide information regarding shape, where the slope of the logarithmic dependency indicates a sphere, random coil, or rod-like shape [307]. Of note, developing a suitable fractionation method can represent a time-consuming experience; however, the implementation of experimental design (or Design of Experiments or “DoE” approach) (see section 5.3) can make FFF more accessible through a

Journal Pre-proof

comb[illegible]le an evaluation of drug loading, as the extinction coefficient needs to be adapted to the environment. Fractions can be collected and further characterized, allowing the detection of chain degradation metabolites, the visualization of particles and aggregates in separate solutions, and the determination of total drug loading and release kinetics after separation. Levels of any “free” unconjugated drug/moiety can be determined following the addition of a UV-VIS or fluorescence detectors coupled to a cross-flow waste-line [311]. Nevertheless, free drug concentration may lie under the limit of detection, and membrane adsorption must be considered. FFF also displays significant advantages when coupled with ICP-MS regarding the analysis of metal ionic components of DDSs, impurities, or metallic nanoparticle toxicity in physiological fluids [312].

FFF also lends itself well to the analysis of pharmaceutics and polymeric compounds as a quality control technique. Engel et al. reported one of the few validated AF4-MALS methods in drug delivery in determining poly(D,L-lactide-coglycolide) content in solid dosage forms and the quantitative analysis of particles during the release in a dissolution test [313].

FFF represents one of the most important biophysical tools available for the study polyelectrolytes, with any existing limitations mainly deriving from the detector employed. For example, the analysis of nanoparticles with sizes smaller than 10 nm with FFF may not be optimal, as the MALS detector possesses a limit of detection from 5 to 10 nm (depending on the manufacturer). In this case, analytical ultracentrifugation (AUC), an absorbance-based and label-free tool, may represent a better method for the characterization of nanoparticles with sizes of 1-10 nm [314]. AUC is especially suitable in simultaneously determining the free drug content and total drug loading within a single run, given the negligible sedimentation speed of the free drug when compared to the polypeptide/polymer-conjugated drug, due to the difference in Mw [315]. The implementation of AUC as a characterization tool has recently been discussed by Gioria et al. [316], however, this study focuses on the characterization of liposomes and encapsulated drugs, as no examples relating to PDCs currently exist in the literature. Future comparative studies to elucidate whether SdFFF can

Journal Pre-proof

simul ...tation of PDCs.

Even though examples of the implementation of FFF in the characterization of PDCs remain scarce, this technique represents an exciting alternative to SEC methodology, and the number of relevant studies will likely continue to grow.

4.2 Bioanalysis

The adequate design of bioanalytical studies can allow the efficient evaluation of the ability of PDC to safely cross biological barriers and reach its intended target tissue/cell. Bioanalyses tackle cell viability, stability in biological fluids, cell specificity, immunogenicity, hemocompatibility, *in vivo* efficacy, and can provide an understanding of the molecular pathways responsible for the pharmacological output. The results of these studies will contribute to an improved design of polypeptide-drug conjugates.

Concerning the ***interaction with biological components*** in circulation, the ionic and proteinic nature of PDCs implies the study of immunogenicity (mainly monitored using peripheral blood mononuclear cells [317,318], ***and hematocompatibility*** (mainly studied through red blood cell assays [319]). Furthermore, non-specific protein adsorption, which affects PDC uptake and targeting efficiency, must also be characterized [115,320]. A common way to control protein corona composition is to exploit hydrophilic polymers such as PSar (as an example of a polypeptide) that reduces nonspecific interactions and increases biocompatibility [321–323]. Analysis of other DDSs has proven the enrichment of the protein corona with disease-specific proteins that remained undetectable by conventional proteomics. The detection of these proteins may foster the discovery of novel diagnostic biomarkers, as demonstrated in studies that tested the ability of proteins to bind to amphotericin B-containing liposomes (AmBisome®), clinically used to treat fungal infections, and

Journal Pre-proof

disco om a substantial number of inert plasma proteins that bind to PDCs, functional proteins can be adsorbed to the PDC surface to provide targeting functionalities. Said proteins include apolipoproteins (such as ApoA, C, and E) that direct the transport through lymphatic and circulatory systems [326,327] or those (ApoE, ApoJ, and ApoA1) that direct brain targeting [328–330].

PDC ***stability in biological fluid*** relies on the nature of the polypeptide carrier and the drug linker employed. The stability of conjugates in plasma and drug release under the conditions located at the site of action [331] are fundamental parameters. Besides free drug content, the key aspects for later PK studies include the quantification of drug release and total drug loading amount. Simple sample preparation for drug release studies and high-throughput, sensitive, and accurate analytical techniques are fundamental for the performance of related studies. Said studies analyze drug release within complex scenarios running from a simple mixture of enzymes, cell medium, or pH buffers (150 mM Cl^- and pH 7.4 to mimic blood and the tumor microenvironment; 20 mM Cl^- and pH 6.9 to mimic intracellular medium like early endosomes; 70 mM Cl^- and pH 5.5 to mimic late endosomes and lysosomes [332]), to biological fluids such as plasma [333], cerebrospinal fluid (CSF) [19], or urine. However, these analyses are also helpful in the monitoring of metabolites of polypeptide chain degradation during ***in vivo studies*** to determine dose schedules and administration route choice, essential elements that need to be considered for efficient delivery to the site of action [333,334]. PK aspects like adsorption, distribution, metabolism, excretion, immunogenicity, and hematocompatibility must be evaluated to predict safety and efficacy [335].

We now hope to discuss recent advances regarding emerging techniques and versatile bioanalytical methods that will provide valuable future insight during the biological characterization of PDCs.

Journal Pre-proof

The ***interaction of plasma proteins*** with PDCs is influenced by charge and favored by a positively-charged system [336,337]. Characterization is usually performed by incubating the sample with bovine serum albumin (BSA) under physiological conditions. The concentration of adsorbed BSA can then be analyzed after precipitation and centrifugation, while free BSA can be determined in the supernatant by bicinchoninic acid protein assay kits. While such protein precipitation methods are straightforward, they do suffer from problems such as the interrupted stability of the protein corona and the loss of "real" information regarding adsorbed proteins. Experimental characterization remains a challenging task due to the complexity of the systems and weak interactions between PDCs and plasma proteins. FFF may represent the best option for the analysis of these complexes in plasma without prior sample preparation since the DDS-protein complex remains intact in the FFF channel. A study of the affinity of three core-crosslinked polymeric nanoparticles with long circulation times (HPMA, PSar, and PEG) to proteins by AF4 has been previously reported [338]. Subsequent MALS and proteomics analysis by mass spectrometry (MS) then established the absence of complexation of the polymeric nanoparticles with proteins, as their size and PDI remained unchanged after plasma incubation.

Fluorescence correlation spectroscopy represents another method that facilitates size monitoring in complex biological matrices like plasma or serum and can be used to evaluate the impact on serum protein adsorption by determination of hydrodynamic size [69]. Nevertheless, the molecules require labeling with a fluorophore for this technique.

Interestingly, the binding of plasma proteins to polypeptides has been implemented to prolong the survival times in human serum without increasing Mw. The binding of human serum albumin (HSA) to a set of polypeptides of varying charge, size, and hydrophobicity, covalently linked to 3,5-

Journal Pre-proof

bis[[b was evaluated by surface plasmon resonance with HSA covalently immobilized on a sensor chip, according to observed uptake and off-rates on sensograms. The results indicated that Zn^{2+} ion chelating agents might provide a general route to increased survival times of peptides in serum in therapeutic and diagnostic applications [339].

Molecular dynamics simulation (MDS), a supplementary *in silico* method, has also emerged as a means to assess the interaction of hydrophilic polymers with the surface of albumin. MDS is based on the classical approximations of the underlying interactions between the atoms [340], where atom velocities and their position in the simulated system derive from Newton's equations of motion [341] and an empirical force field [342]. MDS represents a valuable tool for the design and optimization of drug candidates and polymeric structures and has been employed, for instance, to evaluate the impact of surface modifications of mannosamine-conjugated multifunctional PGA-dendrimers as nanocarriers of the MART-1, gp100:44, and gp100:209 tumor-associated antigens and their dynamic interactions with target receptors [343]. Additionally, MDS was implemented in the study of the adsorption dynamics and the effect of protein adsorption on the conformation of PEG [344] and polypeptides such as PSar and poly-alanine [345]. PEG and PSar developed a similar interaction pattern with the protein surface, in terms of the affinity and intensity of the interaction. PAla and a polymer isomer of PSar known to self-aggregate and induce protein aggregation displayed a higher affinity for the protein surface than PEG and PSar, which they attributed to how the polymer interacts with water, and, in particular, to the tendency of the polymer to reduce the surface exposed to water either by self-aggregating or by adsorbing to the protein surface [345]. These examples demonstrate the ability of MDS to predict both the protein corona composition and how it influences polymer targeting and efficacy. This model may also allow for the prediction of targeting ligand binding to its receptor, akin to other techniques based on surface plasmon resonance (SPR).

[346] have also been evaluated [347]. For example, the Pt-S bonds formed upon the reaction of free CDDP with GSH increase absorption at 260 nm, thereby making UV spectroscopy an easy and effective technique to monitor time-dependent absorption and reaction degree [348]. He et al. revealed that a PGA-CDDP conjugate reacted with GSH to a lesser extent when compared to free CDDP, possibly since the conjugation of CDDP to PGA makes the substitution kinetics of the Pt-S complex slow. Additionally, the authors stated that the spherical structure of the PGA-CDDP conjugate acted as a shield for CDDP against the detoxification of GSH.

4.2.2. Pharmacokinetics

The physicochemical and biological characteristics of any DDS directly influence their PK, as recently reviewed by Hashida [349]. Herein, we will focus on those described considerations regarding PK for PDCs and the methods used in PK studies.

The PK profiles of a range of PEGylated polypeptides conjugated to G-CSF [167] or Dox [44] have been studied. After i.v. administration of PEG-PGA conjugates, the authors quantified G-CSF concentration in serum using a Human G-CSF ELISA Kit; the derived PK data established that the bioavailability and bioactivity of two PGA-PEG20G-CSF conjugates (with different PGA block length) were comparable or better to those established for Pegfilgrastim. The study also demonstrated that the presence of a negatively charged PGA blocks prolonged G-CSF half-life, as expected. In another related study, Kaminskas et al. employed HPLC and SEC for the PK evaluation of Dox or a dendrimeric PEG-PLL-Dox administered to the lungs via liquid instillation [44]. HPLC determined total Dox concentration in plasma, bronchoalveolar lavage fluid, and lung tissue by fluorescence detection, while degradation studies using SEC detected dendrimer scaffolds and low Mw breakdown products in plasma and urine. These studies revealed a two-fold quicker clearance of PEG-PLL dendrimer-Dox

Journal Pre-proof

conju najor part of the dendrimer was excreted by urine and comprised low Mw breakdown products; however, a small amount was detected in 6- and 7-day plasma samples and in lung tissue homogenate supernatant.

The determination of metabolite levels of both the bioactive agent and carrier represents an essential part of PK that can be performed during release kinetics studies; however, the detection of the bioactive moiety and polypeptide as a single entity remains a challenging task. Thus, levels of free/released bioactive moiety are often determined in bodily fluids instead. The ability of MALDI-TOF to detect polypeptides can be exploited in metabolomics-based analysis and the detection of degradation products and has already been applied to the quantification of drug metabolites in PGA-PTX and HPMA-PTX conjugate drug release studies [350]. While matrix effects from amino acids present in biological fluids must be considered during the analysis of polypeptides metabolites, information on this type of analysis is generally lacking. Therefore, this knowledge gap may provide opportunities for new analytical methods and data analysis to eliminate the naturally present amino acids that may interfere.

NMR in metabolomics has become a relevant tool for the understanding of the molecular mechanisms involved in responses to anticancer polymer-drug conjugates; however, no examples are currently available for PDCs. During the *in vitro* and *in vivo* studies of Dox/HPMA-Dox, Armiñán et al. employed NMR-based metabolic profiling to evaluate the biochemical pathways involved [351]. Experiments in MCF7 breast cancer cells revealed metabolic changes in response to the altered cellular trafficking of both free Dox (diffusion) and the HPMA-Dox (lysosomotropic drug release and endocytosis). NMR metabolomics in combination with other qualitative techniques (such as MALDI/TOF imaging, MS with separation techniques such as liquid chromatography (LC), and gas chromatography (GC), supercritical fluid chromatography, and capillary electrophoresis [352]) could represent the first step forwards a rapid, effective, and non-destructive means to characterize the efficacy and toxicity of PDCs.

guides design optimization, therapeutic dose, and administration regimen [353]. Non-invasive imaging techniques require the conjugation of an additional moiety for monitoring purposes in tissues/cell compartments. Li et al. synthesized a macromolecular fluorophore (PF) by conjugating a small molecule NIR-II (the second NIR, at 1000−1700 nm) fluorophore (Flav7) to an amphiphilic polypeptide (poly[oligo(ethylene glycol) methyl ether methacrylate]-block-poly[2-amino-N_4-(2-diisopropylamino-ethyl)-l-aspartic acid] or $P(OEGMA)_{21}$-$P(Asp)_{16}$-iPr) that enabled visualization of tumor features by NIR-II fluorescence imaging [354]. Additionally, NIR-II fluorescence imaging monitored photothermal ablation with PF on tumors with a low dose of NIR-II fluorophore and light irradiation. In a related study, Cheah et al. employed fluorescence in the *ex vivo* imaging of a zinc (II) phthalocyanine (ZnPc) derivative (Pc 1) conjugated to PGA (1-PG) in biodistribution studies [162]. The intensity of emitted fluorescence was semi-quantitatively analyzed at different time points and established that a large quantity of administered 1-PG and Pc 1 accumulated within the tumor, liver, and lungs. Additionally, fluorescence imaging studies identified the time point associated with the highest tumor accumulation of Pc 1 and 1-PG to initiate PDT.

Confocal immunofluorescence techniques have been widely employed for the analysis of intracellular uptake of conjugates [111], and a novel methodology based on fluorescence correlation spectroscopy (FCS) was recently described [355]. By NIR dye labeling, FCS allowed the direct determination of stability and half-life of PSar-based core-crosslinked micelles in flowing blood [355]. This technique does not require the separation of solid (cells) and liquid (plasma) components of the blood, thereby maintaining the properties and integrity of the DDS under review. Furthermore, FCS can estimate the concentration of the fluorescent species in blood and distinguish between free drugs and those contained within DDSs due to their difference in size.

Mass spectrometry imaging (MSI) has emerged as a label-free technology for bioimaging and the determination of the spatial distribution of biomolecules, drugs, and other xenobiotics in tissue sections, organs, and even whole animal body sections [356]. MSI is a non-destructive method that

Journal Pre-proof

simu , MSI and by MS/MS to identify and quantify analytes directly [353]. Nevertheless, sample preparation and complex data analysis make MSI handling more difficult. MSI has found application in the analysis of drug and metabolite distribution studies in tumor tissues [357,358] and 3D cell cultures [359] and tumor vascularization [360], antibody imaging in 3D colon-cancer cell cultures [361], the determination of treatment schedule and the optimization of combination therapy approaches [362,363], metabolomics and biomarker discovery [364,365], and 3D imaging of tumors [366] among other notable applications.

In vivo distribution studies of a polypeptidic micelle (NK105 - PEG-PAsp-PTX) in a pancreatic cancer xenograft model demonstrated that NK105 delivered more PTX to the tumor and less to neural tissues when compared to the free drug, thereby supporting greater anti-tumor efficacy and less neurotoxicity [367]. In a related study of PLA-PEG nanoparticles encapsulating AZD2811, an aurora kinase inhibitor, and AZD1152, a water-soluble prodrug of AZD2811, Ashton et al. demonstrated that MSI permitted the monitoring of the free drug, the polymeric carrier, and the prodrug throughout the adenocarcinoma tumor tissue during *in vivo* studies with nude rats bearing human colon adenocarcinoma (SW620) xenografts [368]. The nude rats were treated with a single dose of AZD2811 (25 mg/kg), AZD1152 (25 mg/kg) or AZD2811 nanoparticles (25 mg/kg) on days one and three, and by implementing MSI, the free drug released from AZD2811 nanoparticles could be detected for up to six days after the last administration, indicating sustained drug delivery. For comparison, the active moiety (AZD2811) was detected in the tumor at 2 and 6 hours after dosing but was undetectable at 24 hours after the treatment with AZD1152 prodrug and AZD2811. Additionally, these studies demonstrated that AZD2811 nanoparticles accumulated in colon adenocarcinoma with minimal impact on bone marrow pathology and provide improved efficacy and tolerability in preclinical models with less frequent dosing [368].

These examples highlight the potential uses of MSI in the bioanalysis of DDS - we anticipate that MSI will revolutionize the characterization of PDCs biodistribution and PK data collection.

Journal Pre-proof

The analytical protocols for PDC characterization involve numerous steps from method development, sample preparation, sample analysis, and method validation to data analysis [369]. Most often, scientists choose the most straightforward approach for the method development – autotuning or "one factor at a time" (OFAT). Autotuning, implemented by using software provided by the manufacturer, can be useful when high sensitivity is not required, while the OFAT approach can be used in analysis when the method parameters do not influence each other. Nevertheless, neither autotuning nor OFAT suffice for appropriate method development, as OFAT provides local knowledge (knowledge only about the performed experiment) and does not take into account the interactions between variables [370]. The most advisable way to evaluate and optimize method variables is to use a DoE approach to identify those factors that influence the results; this minimizes uncontrolled effects and uses statistical analysis to evaluate their impact [371]. Although the field is generally unaware of the advantages of DoE, literature resources implementing OFAT-based approaches to the optimization of related procedures are available and even increasing [370], especially in LC-MS [372]. Kurve et al. optimized their LC-MS methodology and minimized matrix effects by implementing DoE to achieve high sensitivity, low detection limits, and acceptable accuracy in the analysis of three pesticides thiabendazole, aldicarb, and imazalil [373]. Adjustment of electrospray ionization source and MS parameters reduced (but did not eliminate) matrix effects, while factorial design provided a means to define optimal conditions for the lowest matrix effects [373]. As an example of the implementation of DoE in the field of PDCs, Giraldo et al. developed an LC-MS method for the determination of free fasudil as a part of a stability study of a PGA conjugate using a redox-sensitive self-immolative linker (PGA-SS-FAS) [19]. The authors upgraded this method further for fasudil determination in CSF and cell medium, and partially validated the entire process according to the "Guideline on Bioanalytical Method Validation, 2008" by the European Medicines Agency (EMA) [374].

Journal Pre-proof

y and efficacy of either active moiety, the prodrug, or DDS. While techniques such as LC-MS are highly sophisticated and offer a range of scanning of analyte mass and analysis, they are often complex and lack robustness. Therefore, one must demonstrate that the developed method is fit for a specific purpose. The "Guideline on Bioanalytical Method Validation, 2008" by the EMA and "Guidance for Industry, Bioanalytical Method Validation, 2001", by the FDA provide generally accepted criteria that guide the validation of bioanalytical studies. Nevertheless, these guides are not mandatory in preclinical studies, and the parameters that must be evaluated can differ depending on the analytical method employed or the requirement of qualitative or quantitative analysis [375]. The determination of free and total combretastatin A4 from a PEG-g-PGA-CA4 conjugate present in plasma and tissue homogenate represents an excellent example of method validation for PDCs [376]. In this study, Zheng et al. developed a simple, sensitive, accurate method with an intra- and inter-day variability of less than 15% and then applied it to the study of PK and tissue distribution of PEG-g-PGA-CA4 conjugate in tumor-bearing nude mice [376].

There remains a debate regarding the analytical method validation tool that should be used in preclinical research; furthermore, whether one should invest time in this matter when clinical safety and efficacy have yet to be proven remains an open question. However, careful quality control of synthesized PDCs with fit-for-purpose analytical methodologies can improve the reproducibility of both preclinical and clinical efficacy studies.

4.4 Sample Preparation

Biological samples contain organic molecules (e.g., proteins, enzymes, hormones, and cytokines) and inorganic salts (e.g., phosphate and bicarbonate buffer, sodium chloride, potassium chloride, or ion complexes with organic molecules) [377]. One or more analytical procedures can be implemented in the preparation of these complex biological samples for one purpose – to recover the highest amount of analyte while simplifying the matrix. The complexity of

Journal Pre-proof

the p[illegible]on of the analytical chemist involved, and the inter-lab, inter-day, and intra-day repeatability and carry-over effects contribute to these errors, and they must be detected and evaluated in any type of bioanalysis [375].

Quantitative and qualitative analysis is often performed by HPLC coupled to various detectors. As LC columns cannot handle elevated matrix complexity, and detectors are incompatible with some matrix components (e.g., salts and mass spectrometer), analytes are extracted from the matrix and often concentrated [369]. Liquid-liquid extraction and solid-phase extraction in manual sample preparation before analysis can remove possible interfering compounds that coelute with the analyte under analysis and minimize matrix effects. Importantly, as current sample preparation methods can be labor-intensive and expensive, alternative approaches are much needed. Herodes et al. proposed a simple protein precipitation method in methanol for the preparation of plasma samples and the chromatographic separation of metanephrine and normetanephrine [379] that could be easily applied to PDCs. The authors established that the matrix effects derived from plasma constituents could be minimized and necessary quantitation limits achieved through the application of simple protein precipitation and dilution of the sample extract.

An alternative to the acceleration of the sample clean-up process and the elimination of human error during sample preparation is the implementation of an in-line automated sample preparation known as *column switching* where two or more columns are connected in parallel [380]. This strategy has been implemented in the determination of various drugs in biological samples and has found use in simultaneous analyte enrichment and analysis for antidepressants, anticonvulsants, anxiolytics, and antipsychotics in plasma samples from schizophrenic patients [381], antihypertensive drugs of different pharmacological classes and their metabolites in human serum [382], nucleoside drugs such as lamivudine, zidovudine, didanosine and

emtr Journal Pre-proof hinin

[385], among many others.

4.5 Sample Analysis

Chromatography methods with high selectivity, significant separation efficacy, and rapid analysis are irreplaceable and represent the most widely applied technique in bioanalysis [386]. Chromatography has undergone a century of development and is the most common and effective method for the analysis of a range of analytes in a complex mixture. The choice of column (e.g., silica purity, pore diameter, column length, and separation surface), mobile phase composition, and additives must be carefully considered to achieve successful separation [387]. Metal ion impurities in silica columns cause peak tailing and, consequently, loss of resolution, providing a reason why high purity silica columns or high concentrations of ion-pairing agents (trifluoroacetic acid – TFA, or triethanolamine) must be used. Nevertheless, elevated levels of TFA can cause a signal reduction in the negative ion mode of MS detection; therefore, a column with high purity or a lower TFA concentration (0.05% or lower) can be used. One additional concern when using TFA or other additives in the mobile phase is absorption in the low UV region and the resultant upward drift of the baseline, which is especially noticeable in the low concentration region when a gradient is used. In this case, the addition of an ion-pairing agent in the organic phase and the use of a flat baseline are recommended. The use of small pore diameter (100 angstroms) results in the inferior separation of molecules with low Mw; in contrast, wide pore silica columns can be implemented for the analysis of higher Mw (more than 3kDa) compounds. For example, the simultaneous analysis of drugs, the targeting moieties, and PDC metabolites in release studies should be performed using a column with a higher pore diameter (300 angstroms). For two or more analytes in the sample, longer columns should be used; however, since the peptides will only interact with the silica surface at the top of the column, longer columns will not lead to better retention of the polypeptides as they do for small drugs [388].

which concentration range and how are the standard solutions prepared? What type of matrix is used? Was the standard addition or internal standard method used? In articles that calculate recovery (R), many do not specify how these values are implemented in the study. A proper recovery value (70% or more) simply does not suffice; instead, one must implement the R-value in the calculation of concentration or use a matrix-matched calibration solution, which can be challenging (e.g., CSF or tissue extraction remains challenging, and provides minimal collected amount). In such cases, a surrogate matrix that mimics the composition of the real biomatrix is recommended, rather than using a simple matrix as MilliQ water [371].

The sensitivity of the method implemented may not suffice for the detection of the analytes in biological samples. For example, stability studies in plasma that determine free drug concentration require the careful consideration of the concentration range and detectors employed. Sensitivity is determined by the analyte characteristics, sample preparation, and optimization of the method. Additionally, it is critical to recover as much analyte as possible while removing matrix components efficiently, as the interference of co-eluting components from the biological matrix causes low method sensitivity. Other challenges include the inadequate response of the detector towards different compounds (like weak ionization in MS) or matrix effects. Aubry et al. suggested the optimization of three key factors to resolve these problems and develop a sensitive method: i) adequate sample preparation, ii) the choice of an adequate column for a specific molecule to obtain adequate chromatographic separation, and iii) improvement of detector signal [389].

In bioanalysis, the low concentration of an analyte exacerbates the problems mentioned above; therefore, chromatography is often coupled with MS to increase sensitivity. Additionally, the choice of detector is of great importance and should be guided by the properties of the polypeptide-conjugated drug, the purpose of the analysis, the amount of sample, and the features of the detectors (**Table 6Error! Reference source not found.**.

Journal Pre-proof

5. Conclusion and Future Perspectives

Polypeptides drug-conjugates have already reached evaluation in advanced clinical trials (mainly as cancer treatments), while their evaluation at the preclinical stage has provided evidence for enhanced therapeutic outcomes and effective disease monitoring through diverse administration vias apart from i.v. PLL, PGA, and PAsp comprise most of the reported studies, with polymeric micelles or dendrimeric systems employing PEGylation among the top candidates. Conflicting reports on PEG immunogenicity and antigenicity have promoted the development of attractive biomimetic alternatives such as N-methylated polypeptides known as polypeptoids (e.g., PSar [2,392]), which are envisioned as potential PEG replacement.

Polypeptides represent suitable components of DDSs due not only to their biodegradability and biocompatibility but also due to the myriad of opportunities deriving from their feasible synthesis, versatile architecture with tunable structural properties including size, shape, net charge, conformation, self-assembly and tailored bioresponsiveness that can provide means to fine-tune their biological output. Moreover, their multifunctionality permits the implementation of drug combinations and targeted therapies, which can provide for drug synergism and enhanced accumulation in the required site of action. Reported single or combination conjugates have underscored the importance of rational drug-linker design [91,194]. The additional optimization of the drug ratio can modulate drug release kinetics, which represents a crucial parameter to final *in vivo* efficacy and safety. To this end, the exploration of bioresponsiveness linkers in related DDS and the better understanding of the molecular conditions at the pathological site can lead to the development of improved PDCs. There remain uncharted options to explore bioresponsiveness from linkers explored in other DDS and foster a better understanding of the molecular conditions at the pathological site. The study of novel self-immolative linkers via redox and even their combination with protease-sensitive motifs

Journal Pre-proof

Journal Pre-proof

[241] ated, further studies are still needed to obtain precise information of the specific enzyme levels at the desired site and to demonstrate that *in vivo* drug release is correlated to enzymatic activity. The development of bioresponsive crosslinked and/or self-assembled systems could prompt the generation of novel architectures bearing synergistic drug combinations [96,205].

Finally, the implementation of exhaustive physico-chemical characterization procedures and the integration of innovative techniques will foster the enhanced translation of PDCs into clinical use. We require novel approaches to address the significant limitations found by regulatory agencies regarding the lack of homogeneous, pure, and well-characterized products. We also need robust methods for quality control and characterization that focus on defining the dependency of physicochemical properties with the biological activity to speed up candidate selection. LC-MS, MSI, and FFF coupled with multiple detectors can provide vast amounts of information regarding PDCs, with parameters ranging from size, Mw, shape, or protein corona analysis to degradation products in biological media. Even given the abovementioned advice, the "keep it simple" recommendation must always be considered to boost the market arrival of PDCs by reducing costs and easing upscaling.

Overall, we believe that a new generation of PDCs will provide exciting opportunities in combination and targeted therapies for a range of diseases and disorders.

Acknowledgments

The authors would like to thank Stuart P. Atkinson for English editing. The Spanish Ministry of Economy and competitiveness (grants SAF2016-80427-R and PID2019-108806RB-I00) the European Research Council (grants ERC-CoG-2014-648831 MyNano, ERC-Proof of Concept Grant-Polymmune), Fundació La Caixa

Journal Pre-proof

Healt Fund (FEDER) (PO FEDER Comunitat Valenciana 2014-2020) are acknowledged for financial support.

Figure Legends

Figure 1. Schematic representation of polypeptide-based systems discussed in this review that are present in the market and preclinical/clinical assays. Their relative placement within the nanomedicine field and the materials used for their construction are noted. Finally, any correlation between structural complexity and the degree of market transferability is also highlighted.

Figure 2. (**a**) The formation and controlled release of a PEG-PAsp-epirubicin micelle (NC-6300 EPI/m) using an acid-labile hydrazone polymer-drug linking moiety. Antitumor effects of NC-6300 and epirubicin in mice bearing subcutaneous Hep3B xenografts. NC-6300 or conventional EPI was i.v. injected on days 0, 7, and 14. The dose of NC-6300 is expressed as the dose equivalent of EPI. ○, Control; □, NC-6300 at 10 mg／kg; ■, NC-6300 at 15 mg／kg; Δ, EPI at 10 mg／kg. (**b**) The anti-tumor activity of NC-6300 or EPI evaluated by measuring changes to tumor volume. ANOVA test between NC-6300 (10 mg／kg) and EPI (10 mg／kg), P = 0.0017; NC-6300 (15 mg／kg) and EPI (10 mg／kg), P < 0.001. (**c**) Changes in relative body weight. Data derived from the same mice as those used in the previous experiment. ANOVA test between NC-6300 (10 mg／kg) and EPI (10 mg／kg), P = 0.0053; NC-6300 (15 mg／kg) and EPI (10 mg／kg), P < 0.001. Arrows, drug injections; bars, SD; points, mean. Reprinted with permission [393,394].

Figure 3. (**a**) Chemical structure of a PGA-Dox conjugate (**left**). Mechanism of action of iNPG-pDox (**right**). Sequential steps include vascular transport, tumor accumulation of iNPG-pDox in sites of interest due to innate tropism, association with diseased endothelium, in situ generation of pDox nanoparticles, cellular internalization, and transport of pDox that results in the release of Dox in the perinuclear region inside the cell. (**b**) Inhibition of tumor growth and

Journal Pre-proof

prolo wing

treatments (**left**). Kaplan-Meier plot of animal survival (**right**). Median survival time is listed in the table. Reprinted with permission [189].

Figure 4. (**a**) Synthetic scheme for pH-responsive PGA-based combination conjugates of Dox and AGM. (**b**) Kinetics of drug(s) release from PGA-(G-AGM)-(Hyd-Dox)$_L$ under hydrolytic and proteolytic (cathepsin B) conditions. (**c**) From left to right: *In vivo* antitumor and safety evaluation of combination conjugates in an orthotopic TNBC mouse model. Treatment administration routine - The treatment started at a previously determined time for maximal accumulation via the EPR effect. Tumor growth inhibition of previously selected PDCs. Kaplan-Meyer survival curves demonstrate the safety of the combination conjugates except for PGA-(G-AGM)-(EMCH-Dox)LL with only 50% survival. Relative liver weight by treatments demonstrating tumor-related hepatomegaly in the phosphate buffer saline group that was partially improved with Dox, PGA-(G-AGM)-(Hyd-Dox)$_{HL}$, PGA-(G-AGM)-(Hyd-Dox)$_{LL}$ and greater organ weight related to the treatment PGA-(G-AGM)-(EMCH-Dox)$_{LL}$. Treated mouse heart sections showing Dox-induced cardiotoxicity by Hematoxylin and Eosin (H&E) staining and Masson's immunostaining compared with the relative cardio safety displayed by the combination conjugates. (**d**) Quantification of lung metastasis following treatment. Metastasis was significantly decreased after treatment with PGA-(G-AGM)-(Hyd-Dox)$_{LL}$, *PGA-(G-AGM)-(EMCH-Dox)$_{LL}$*, and free Dox and H&E staining of representative lung lobes receiving different treatments. Red arrowheads indicate metastatic nodules. Data represent mean ± SEM. Statistical significance was determined using an ANOVA t-test, (*p < 0.05, **p < 0.01, ***p < 0.001) and comparison of tumor density with different treatments at the experimental endpoint. G = Gly, LL = Low Loading, 1% mol, Hyd = hydrazone bond, EMCH = N-ε-maleimidocaproic acid hydrazide] moiety, complex hydrazone linkage. Reprinted with permission [194].

Figure 5. The range of polypeptide-drug linkers employed in the rational design of polypeptide-drug conjugates.

Journal Pre-proof

Figur AF4 fractogram. (**c**) AF4-UV fractograms of characterized PSar nanoparticles (green), plasma (red), and plasma-incubated PSar nanoparticles (blue) [338]. Reproduced with permission from Postnova Analytics GmbH.

Tables

Table 1. Critical examples of PLL conjugates in the market or under evaluation in clinical or preclinical trials.

Product name	VivaGel® BV, Betafem® BV Gel (UK), Betadine BVTM (Europe), BetadineTM BV Gel (Asia), Fleurstat BVgel (Australia & New Zealand)	DEP® DOCETAXEL	DEP® CABAZITAXEL	DEP® IRINOTECAN	DEP-AZD0466
Technology	PLL-DNAA	$PEG_{N/A}$-$PLL_{N/A}$-Docetaxel	$PEG_{N/A}$-$PLL_{N/A}$-Cabazitaxel	$PEG_{N/A}$-$PLL_{N/A}$-Irinotecan	$PEG_{N/A}$-$PLL_{N/A}$-AZD0466
Structure	Dendrimer	Dendrimer	Dendrimer	Dendrimer	Dendrimer
Targeting moiety	-	-	-	-	-
Indication	Sexually transmitted infections (STIs)	Breast, lung, and prostate cancer	Colon and pancreatic cancer	Colon and pancreatic cancer	Solid and hematological tumors
Linker	Amide	N/A	N/A	N/A	N/A
Stage	Marketed 2019, Starpharma	Phase II	Phase II	Phase I/II	Phase I
In-vivo model, treatment regime	-	-	-	-	-
Administration	intravaginal	i.v.	i.v.	i.v.	i.v.
References	[26,395]	[118]	[118]	[118]	[118,136]

Journal Pre-proof

Produ					
Technology	Cys-PLL_{30}-PEG_{10}*CFTR	PEG_{227}-PLL_{40}-Ubenimex	Glu-PEG_{5kDa}-PLL_{71}*Fab	PEG_{114}-$PZLL_{6}$-$PAsp(DET)_{30}$-MMAE (coating PEG_{114}-PGA_{30})	$PLL_{26,5kDa}$-g-$PEG_{(1,1kDa)18}$-Dox
Structure	Linear	Linear	Linear	Linear	Dendrimer
Targeting moiety	-	-	Glucose	-	-
Indication	Cystic fibrosis	Liver cancer	Alzheimer's disease	Advanced-stage epithelial ovarian cancer	Lung cancer
Linker	Electrostatic interactions	Ester	Electrostatic interactions	Self immolative disulfide, 1,5-cyclization	Hydrazone
Stage	Phase I	Preclinical	Preclinical	Preclinical	Preclinical
In-vivo model, treatment regime	-	HuH7 hepatocarcinoma xenograft model, NOD/SCID mice, 100 µl dose of 1 mg/ml DDS; treatment every other day until day 21	Alzheimer's Disease mouse model, APP/PS1 mice, 1.8 mg/kg Fab eq., weekly x 10 treatments	LUC+ OVCAR8 tumor model or LUC+ primary HGSOC PDX tumor model; nude mice; 3 mg/kg MMAE eq., on days 0, 7, 14, and 21	Syngeneic MAT 13762 IIIB rat model of lung metastatic breast cancer; F344 rats; 3 mg/kg Dox eq., on day 0, 3, 7, and 10
Administration	intranasal	i.p.	i.p.	i.p.	intratracheal instillation
References	[38]	[43]	[107]	[42]	[44]

Product name	-		-	-
Technology	FA-PLL-DTPA-Gd	PEG_{114}-PLL_{15}-Curcumin	$PLL_{5,2kDa}$-g-PEG_{2kDA}-Gemtabicine	$PLL_{5,2kDa}$-g-PEG_{2kDA}-Dox
Structure	Branched	Linear	Dendrimer	Dendrimer
Targeting moiety	FA	-	-	-
Indication	MRI contrast agent probe	Breast cancer	Breast cancer	Ovarian cancer
Linker	Amide	Self immolative disulfide, 1,4-and 1,5 cyclization	Peptide (GFLG)	Peptide (GFLG)
Stage	Preclinical	Preclinical	Preclinical	Preclinical
In-vivo model, treatment regime	KB cells subcutaneously injected into the armpit, nude	HeLa tumor-bearing nude mouse model, 20	4T1 murine mammary adenocarcinoma model,	Subcutaneous SKOV-3 model, Balb/C mice; 5

Journal Pre-proof

	microimaging system (35 °C). MR images acquired at 1, 3, 5, 8, and 24 h after injection of contrast agents	on day 0, 4, 8, 12	eq., every five days x 5 treatments	days x 5 treatments
Administration	i.v.	i.v.	i.v.	i.v.
References	[141]	[139]	[113]	[138]

Table 2. Critical examples of PGA conjugates in the market or under evaluation in clinical or preclinical trials.

Product name	Xyotax, Opaxio, CT-2103	CT-2106	NK-012	RadProtect®	-	-
Technology	PGA_{48kDa}-PTX	PGA_{49kDa}-CPT	PEG_{12kDa}-$(PGA\text{-}SN38)_{7kDa}$	PEG_{2kDa}-PGA_{12} *Amifostine*Fe	PGA-PTX	PEG_{12kDa}-PGA_{40}-BSH
Structure	Linear	Linear	Linear	Linear	Linear	Linear
Targeting moiety	-	-	-		-	-
Indication	Ovarian cancer, non-small cell lung cancer, breast cancer	Refractory solid tumor malignancies	Refractory solid tumors (phase I), metastatic or recurrent colorectal cancer (phase I), relapsed NSCLC (phase II and advanced metastatic TNBC (phase II)	Acute radiation syndrome	Non-small-cell lung cancer	Colon cancer
Linker	Ester bond	Ester bond, Gly spacer	Ester	Complexation	β-thiopropionate ester	Self immolative disulfide, 1,5 cyclization
Stage	Phase III, Phase III, Phase II	Phase I/II	Phase I/ II	Phase I	Preclinical	Preclinical
In-vivo model, treatment regime	-	-	-	Rat (Sprague Dawley), Mice (C57BL/6 Beagle), Dog (Beagle), Rabbit (New Zealand White); 8.5 Gy irradiation for 4 hrs (long) or 10 min (short) exposure; administered 90	NCI-H460 tumor animal model, BALB/c nude mice; 125 and 200 mg/kg of PDC;	C26 colon murine adenocarcinoma sc, BALB/c mice; 100 mg/kg BSH eq.; thermal neutron irradiation (1.6–2.2 × 10^{12} neutrons/cm^2) for 1 h

Journal Pre-proof

Administration	i.v.	i.v.	i.v.	i.v.	i.v.	i.v.
References	[145,146]	[148]	[149]	[244,245]	[151]	[155]

Product name	-	-	-	-	-
Technology	$PGA_{20,7kDa}$g-$PEG_{(2kDa)16,7kDa}$*CDDP	PGA_{160}-g-$PEG_{(5kDa)8,3}$-PPT	PGA_{160}-g-$PEG_{(5kDa)8,3}$-CA4	PGA_{160}-g-$(PEG_{5kDa})_{8,3}$-CA4 + plerixafor supplement	PGA_{160}-g-$(PEG_{5kDa})_{8,3}$-CA4 + PI3Kγ inhibitor & NLG919 supplement
Structure	Polymeric brush	Polymeric brush	Polymeric brush	Polymeric brush	Polymeric brush
Targeting moiety	-	-	-	-	-
Indication	Breast cancer	Breast cancer	Colon cancer	Breast cancer	Breast cancer
Linker	Me complexation	Ester	Ester	Ester	Ester
Stage	Preclinical	Preclinical	Preclinical	Preclinical	Preclinical
In-vivo model, treatment regime	Xenograft MCF-7 human mammary adenocarcinoma, subcutaneous, Balb/C nude mice; 4 mg/kg CDDP eq.; days 0, 4, and 8	Xenograft MCF-7/ADR human multiple drug resistant breast cancer model subcutaneous; Balb/C nude mice; 15 mg/ kg for free PPT, 200 mg/kg (PPT eq.) for PLG-g-PEG-PPT; one time at day 0	Xenograft C26 colon murine adenocarcinoma, BALB/c mice; CA4 dose of 50 mg/kg CA4 eq; on days 1, 5, and 9	Orthotopic 4T1 murine breast adenocarcinoma model; BALB/c mice; 30 mg/kg or 60 mg/kg on day 1 and/or 7 CA4 eq.; PLF 2.5 mg/kg, every day	Orthotopic 4T1 murine breast adenocarcinoma model; BALB/c mice; 35 mg/kg CA4 eq.; every week x two treatments; 2.5 mg/kg PI3Kγ inhibitor (TG100-115) twice a day x 30 treatment, 10 mg/kg NLG919 once a day x 15 treatment
Administration	i.v.	i.v.	i.v.	i.v. i.p. PLF supplement	i.v. CA4 and PGA-PEG-CA4 i.p. PI3Kγ inhibitor & NLG919
References	[156]	[157]	[158]	[159]	[160]

Journal Pre-proof

Product name	-	-	-	-	-	-
Technology	PGA_{200}-ZnPc	PGA_{150}-BDMC	PGA_{10}-PEG_{20kDa}-G-CFS, PGA_{20}-PEG_{20kDa}-G-CFS, PGA_{10}-PEG_{20kDa}-hGH, PGA_{20}-PEG_{20kDa}-hGH	PGA_{100}-Fluo * HA-CP	PGA_{100}-g-$pSar_{(82)24}$-TCO	PGA_{30kDa}-P18
Structure	Linear	Branched, crosslinked	Linear	Linear conjugate in crosslinked system	Polymeric brush	Linear
Targeting moiety	-	-	-	-	-	-
Indication	Breast cancer	Acute kidney injury	Congenital and acquired neutropenia (G-CFS) and growth hormone deficiency (hGH)	Mild/moderate psoriasis	Colon cancer	Osteoarthritis
Linker	Ester	Ester	Amine	Ester	Amide	Triazole
Stage	Preclinical	Preclinical	Preclinical	Preclinical	Preclinical	Preclinical
In-vivo model, treatment regime	4T1 murine mammary tumors; BALB/c mice; 16 mg/kg PC1 eq.; carrier content at 100 mg PGA equivalent/kg) and PGA at 100 mg/kg	FA-induced acute kidney injury mouse model; C57/BL6 wild type mice; 250 mg/kg folic acid (FA)single i.p. dose induced AKI; 4 mg/kg BDMC eq. 4 h before FA administration	The effect on immune cells counts evaluated in C57BL/6 mice; 1 mg/kg G-CSF eq. single-injection; Pharmacodynamics of hGH evaluated in hypophysectomized Sprague-Dawley rats; 1.8 mg/kg hGH eq. single injection	Psoriatic mice model; BALB/c mice; psoriasis-like symptoms were induced by the daily application of 62.5 mg 5% imiquimod (IMQ) cream for seven consecutive days (3.1 mg of IMG eq. daily dose); 0.15 wt% of FLUO eq. every day x 5 treatments	CT26 colon murine adenocarcinoma subcutaneous, Balb/c mice; ^{111}In labeled compound with an apparent specific activity 10^9 MBq/mg	Osteoarthritis mice model, induced surgically by destabilizing the medial meniscus; C57BL/6 mice; 150 µL of 1 × 10−6 M P-18 eq. on week 2, 4, 6, and 8
Administration	i.v.	retro-orbital injection	s.c. (CSF) i.v. (hGH)	topical	i.v.	i.v.
References	[161,162]	[111]	[167]	[46]	[171]	[21]

Table 3. Critical examples of PAsp conjugates in the market or under evaluation in clinical or preclinical trials

Product name	NK-911	NC-6300, K-912	NC-6300 + HIFU	-	-

Journal Pre-proof

Technology	Dox	PEG-PAsp-EPI	PEG-PAsp-EPI	PEG-PAsp-EPI-antiTF1849	PEG-PAsp-EPI-antiTF1859
Structure	Linear	Linear	Linear	Linear	Linear
Targeting moiety	-	-	-	antiTF1849	antiTF1859
Indication	Metastatic pancreatic cancer	Advanced or recurrent solid tumor	Colon and pancreatic cancer	Gastric and pancreatic cancer	Pancreatic cancer
Linker	Amide, Encapsulation	Hydrazone	Hydrazone	Hydrazone (EPI), Thiosuccinimide (anti-TF)	Hydrazone (EPI), Thiosuccinimide (anti-TF)
Stage	Ph II	Ph I/II	Preclinical	Preclinical	Preclinical
In-vivo model, treatment regime	-	-	C26 colon murine adenocarcinoma subcutaneous; CD2F1 (CDF1) mice; MIA PaCa-2 pancreatic human tumor model, BALB/c nude mice; 2,5 mg/kg EPI eq. single dose; HIFU 360 or 270 W/cm2; 30s, 13 points 24 hrs after EPI administration	xenograft 44As3 gastric human adenocarcinoma; xenograft BxPC3 pancreatic human model; SUIT2 pancreatic human model; BALB /c nu /nu mice; 10 mg/kg EPI eq., on day 0,7, and 14	xenograft BxPC3 pancreatic human model; SUIT2 pancreatic human model; BALB /c nu /nu mice; 10 mg/kg EPI eq., on day 0,7, and 14
Administration	i.v.	i.v.	i.v.	i.v.	i.v.
References	[177]	[179]	[180]	[181]	[127]

Product name	-	-	-	-	-
Technology	PEG227-PAsp$_{44}$-GEM	Pasp$_{14}$-DOTA-Ga	Pasp$_{235}$-TMAPA	PEG$_{2kDa}$-PAsp$_{100}$-g-OEI-DTPA-Gd-FA	PAsp$_{33kDa}$-Dox
Structure	Linear	Linear	Linear	Linear	Linear
Targeting moiety	-	-	-	FA	-
Indication	Pancreatic cancer	PET probe (bone imaging)	Mycobacterial disease	MRI probe	Breast cancer
Linker	Cyclic acetal	Amide	Amide	Amide	Ethylene glycol-bis-succionate
Stage	Preclinical	Preclinical	Preclinical	Preclinical	Preclinical
In-vivo model, treatment regime	xenograft BxPC3 pancreatic human subcutaneous model;	ddY mice, 37 kBq/100 μL tracer solution injection	Kanamycin induces resistance mycobacterial strain (BND-443),	xenograft KB tumor model; athymic nude mice; 0,1 mmol/kg Gd eq., 1.5 T MRI	xenograft MCF-7 human breast carcinoma model, NOD-SCID mice; 5 mg/kg Dox eq.; every three days

Journal Pre-proof

	pancreatic human tumor model; 80 mg/kg GEM eq. and 10 mg/kg or 20 mg/kg for the conjugates (GEM eq.); every three days x 4 treatments		mycobacterial strain JAL-2287, virulent M. tuberculosis H37Rv strain (Mtb)		
Administration	i.v.	i.v.	-	i.v.	i.v.
References	[184]	[185]	[187]	[123]	[176]

Table 4. Examples of PDCs as part of hybrid materials in preclinical trials.

Technology	iNPG*PGA-Dox	PGA_{46kDa}-g-PEG_{5kDa}-Dox*CS_{11kDa}	$(H_3CR_5C$-g-Stearyl$)_{15kDa}$*siRNA	$(H_3CR_5C$-g-Stearyl$)_{11,5}$ $_{kDa}$*microRNA*Dox	Tf-PEG-PLL*MNP*siPLK1
Structure	Silicon-based carrier*linear PGA	Linear	Polymer brush, crosslinked	Polymer brush, crosslinked	Linear
Targeting moiety	-	-	-	-	Tf
Indication	Breast cancer	Breast cancer	Breast cancer	Prostate cancer	Glioblastoma
Linker	Hydrazone	Hydrazone	Electrostatic interactions	Electrostatic interactions (miR-34a), encapsulation (Dox)	Electrostatic interactions
Stage	Preclinical	Preclinical	Preclinical	Preclinical	Preclinical
In-vivo model, treatment regime	orthotopic murine 4T1 tumor model; BALB/c mice; MDA-MB-231/MDR; athymic nude mice were; 3 mg/kg Dox eq.(weekly) or 6 mg/kg Dox eq. (biweekly) administration, six week treatment period	Ehrlich ascites murine mammary adenocarcinoma model, Balb/C mice; 15 mg/kg Dox-eq.; on day 0, 4, 9, and 14	Luciferase gene silencing Luc-Hela xenograft tumor model, Balb/c nude mice; 1.5 mg/kg siRNA eq. everyday x 3 treatments	Xenograft DU145 human androgen-independent prostate carcinoma model, Balb/c nude mice, 5 mg/kg Dox eq., 2 mg/kg miR-34a eq., single injection	U87 bilateral striatum (1.8 mm lateral to the bregma and 4 mm of depth) in mouse model; 0.8 or 1.6 mg/kg carrier*siRNA or carrier*scrambled siRNA; every two days, x 4 treatment
Administration	i.v.	oral (6 hrs fasting before and after	i.v.	i.v.	i.v.

References	[189]	[190]	[192]	[193]	[128]

Technology	PGA_{100}-PTX-Dox	PGA_{100}-PTX-Dox	PEG_{113}-PGA_{18}-Phe_{20}-PTX-CDDP
Structure	Linear	Linear	Linear
Targeting moiety	-	-	-
Indication	Breast cancer	Breast cancer	Lung cancer
Linker	Ester (PTX), Hydrazone (Dox)	Ester (PTX), Hydrazone (Dox)	Complexation (CDDP), encapsulation (PTX)
Stage	Preclinical	Preclinical	Preclinical
In-vivo model, treatment regime	MDA-MB-231 human mammary adenocarcinoma model, Nu/nu mice; 3 times/week; 7,5 mg/kg Dox-eq. (1st dose, after 5 mg/kg); 4.5 mg/kg PTX-eq. (1^{st} dose, after 3 mg/kg) x 5 treatments	4T1 murine mammary adenocarcinoma model, Balb/C mice; 3 times/week, 5mg/kg Dox-eq.; 3 mg/kg PTX-eq. x 5 treatments	A549 human subcutaneous lung adenocarcinoma model, Balb/C nude mice; 3 mg/kg PTX eq. + 10 mg/kg CDDP eq. on day 0.7 for saline, PTX, polymer-PTX, polymer-PTX-CDDP; for free drugs combination CDDP 5 mg/kg CDDP eq. on day 1, 3, 8, and 10
Administration	i.v.	i.v.	i.v.
References	[207]	[89]	[87]

Table 5. Critical examples of combination therapy under evaluation in preclinical trials.

Technology	TREN-PEG_{112}-$gPGA_{20}$-CPT*Dox	PEG_{113}-PGA_{40}-CPT-CDDP	$PLL_{4,5kDa}$-PTX*HA_{30kDa}-GEM	FA-PEG_{114}-PGA_{90}-Phe_{25}*PTX-CDDP	PEG_{2kDa}-PLL_{18}-Asp_{30}(DIP)-Dox* siRNA
Structure	Polymer brush	Linear	Linear	Linear	Linear
Targeting moiety	-	-	-	FA	-
Indication	Lung cancer	Breast cancer	Bile duct cancer	Ovarian cancer	Liver cancer

Journal Pre-proof

Journal Pre-proof

Linker	(Dox)	(CPT), complexation (CDDP)	Ester (PTX, GEM)	encapsulation (PTX)	electrostatic interactions (siRNA)
Stage	Preclinical	Preclinical	Preclinical	Preclinical	Preclinical
In-vivo model, treatment regime	A549 human subcutaneous lung adenocarcinoma model, athymic nude mice; 5 mg/kg CPT, 5 mg/kg Dox, polymer-Dox-CPT (10 mg/kg CPT eq.); every 4-day x 5 treatments	4T1 murine breast adenocarcinoma model BALB/c mice; 5 mg/kg (CPT eq.), 2 mg/kg (CDDP eq.); every 2 days x 5 treatments	Xenograft HUCCT1 subcutaneous human Cholangiocarcinoma BALB/c nude mice, 108,8 ug GEM eq.; 54 ug PTX eq.; 2 times/week x 6 treatments	A2780/Luc human peritoneal carcinomatosis, athymic nude-nu mice; 4 mg/kg CDDP eq.; 1 mg/kg PTX eq., every four days x 4 treatments	HepG2/ADM human multidrug-resistant hepatocellular carcinoma model BALB/c nude mice
Administration	i.v. (CPT i.p.)	i.v.	i.v.	i.v. (additional group for combination i.p.)	i.v.
References	[93]	[88]	[209]	[41]	[210]

Technology	PGA_{100}-SLM-mDBF	PGA_{100}-AGM-Dox	PGA_{100}-AGM-Dox	PG_{9kDa}-PLL_{12kDa}*DTX*siRNA
Structure	Linear	Linear	Linear	Hyperbranched
Targeting moiety	-	-	-	-
Indication	Melanoma	Breast cancer	Breast cancer	Breast cancer
Linker	Ester (SLM), amide and ester (mDBF)	Amide (Dox), peptidic linker (AGM) Gly, Gly, Gly, Gly-Phe-Leu-Gly	Hydrazone (Dox), peptidic linker: Gly (AGM)	Encapsulation (DTX), electrostatic interactions (siRNA)
Stage	Preclinical	Preclinical	Preclinical	Preclinical
In-vivo model, treatment regime	subcutaneous D4M.3A murine melanoma model, C57BL/6 mice, 10 mg/kg mDBF eq.; 15 mg/kg SLM eq.; every day x 14 treatments	orthotopic 4T1 murine breast adenocarcinoma model, Balb/c mice, 10 mg/kg Dox eq., for polymer-Dox-AGM; 3 mg/kg for free Dox; every 3 days x 3 treatments	orthotopic 4T1 murine breast adenocarcinoma model, Balb/c mice, 10 mg/kg Dox eq., for polymer-Dox-AGM; 5 mg/kg for free Dox; every 3 days x 4 treatments	xenograft MCF-7 human mammary tumor model, nude mice; 0.2 mg/kg DOC eq., 5 mg/kg MMP-9 eq; everyday x 21 treatments
Administration	i.p.	i.v.	i.v.	i.v.
References	[82]	[91]	[194]	[211]

Journal Pre-proof

Journal Pre-proof

Table dichroism; ESI- electrospray ionization; FLD- fluorescence detector; ICP-OES – inductively coupled plasma optical emission spectroscopy; IR- infrared; LOD- limit of detection; LS- light scattering; MALDI- matrix-assisted laser desorption ionization; PDA- photodiode array; RI- refractive index detector).

	UV/Vis	**FLD**	**RI**	**LS**	**CD**
Sensitivity to	Concentration	Concentration	Concentration	Mass	Concentration
Selectivity	Possible (depending on the wavelength)	Selective	Universal	Universal	Universal
Additional Information Derived	Spectrum if PDA is used	Emission spectrum, excitation, and emission wavelengths	No	No	Structure, the stability of biomolecules
Response	Absorption of light in UV/Vis spectra	Fluorescence	Difference in refractive index	Scattered light	Difference in the absorption of circularly polarized light in optically active substances
Destructive	No	No	No	Yes	No
Eluent	Must not absorb at the detection wavelength	Free from fluorescence quenchers	RI from different analytes	Volatile	Must not absorb at the detection wavelength
Gradient	Yes	Yes	No	Yes	No
LOD	µg	ng	mg	5-10 nm	µg
Stability	Yes	Yes	No (temperature stabilization needed)	Yes	Yes
Robustness	Yes	No	Yes	Yes	Yes
Linearity range	4	2	4	No	2-3
Price	Cheap	Moderate	Cheap	Moderate expensive	Relatively cheap
User friendly	Yes	Yes	Yes	Yes	Yes
References	[157,276,350,396–401]	[277,286,354,400]	[286,350,396,402]	[152,194,281,286,396,402]	[157,286,287,289]

	MALDI-MS	ESI-MS/APCI-MS	IR	ICP-OE
Sensitivity to	Mass	Concentration/Mass	Concentration	Concer
Selectivity	Highly selective	Highly selective for high/low to medium polarity compounds	Selective (universal for compounds with specific bond)	Selecti interfe interfe
Additional Information Derived	Molecular mass, structure, spatial information	Molecular mass, structure	IR spectra	Simult analys possib
Response	Uniform	Uniform	No	Unifor
Destructive	No	Yes	No	Yes
Eluent	Volatile, high purity	Volatile, high purity	Should not absorb at the same wavelength	Volatil
Gradient	No	Yes	Yes	No
LOD	pg-fg	pg-fg	µg-mg	Depen ppb or
Stability	Stable	Stable	Relatively stable	Stable
Robustness	Yes	Pressure control	Yes	Yes
Linearity range	3-4	3-4	-	3-4
Price	Moderate-expensive	Moderate	Relatively cheap	Moder
User friendly	Yes	Yes	Yes	Yes
References	[339,403]	[276,287,350,398,399,404,405]	[157,347,396,399,401,406]	[332,4

Journal Pre-proof

References

[1] R. Duncan, Polymer therapeutics at a crossroads? Finding the path for improved translation in the twenty-first century, J. Drug Target. 25 (2017) 759–780. doi:10.1080/1061186X.2017.1358729.

[2] I. Ekladious, Y.L. Colson, M.W. Grinstaff, Polymer–drug conjugate therapeutics: advances, insights and prospects, Nat. Rev. Drug Discov. 18 (2019) 273–294. doi:10.1038/s41573-018-0005-0.

[3] G. Pasut, S. Zalipsky, Polymer-Protein Conjugates From Pegylation and Beyond, Elsevier, 2019.

[4] S.P. Atkinson, Z. Andreu, M.J. Vicent, Polymer therapeutics: Biomarkers and new approaches for personalized cancer treatment, J. Pers. Med. 8 (2018). doi:10.3390/jpm8010006.

[5] J. Sanchis, F. Canal, R. Lucas, M.J. Vicent, Polymer-drug conjugates for novel molecular targets, Nanomedicine. 5 (2010) 915–935. doi:10.2217/nnm.10.71.

[6] P. Thakor, V. Bhavana, R. Sharm, S. Srivastava, S.B. Singh, N.K. Mehra, Polymer–drug

conjugates: recent advances and future perspectives, Drug Discov. Today. Articles i (2020). doi:10.1016/j.drudis.2020.06.028.

[7] H. Ringsdorf, Structure and properties of pharmacologically active polymers, J. Polym. Sci. 51 (1975) 135–153.

[8] M.J. Vicent, H. Ringsdorf, R. Duncan, Polymer therapeutics: Clinical applications and challenges for development, Adv. Drug Deliv. Rev. 61 (2009) 1117–1120. doi:10.1016/j.addr.2009.08.001.

[9] A. Duro-Castano, I. Conejos-Sánchez, M.J. Vicent, Peptide-based polymer therapeutics, Polymers (Basel). 6 (2014) 515–551. doi:10.3390/polym6020515.

[10] L.I.F. Moura, A. Malfanti, C. Peres, A.I. Matos, H.F. Florindo, Functionalized branched polymers : promising immunomodulatory tools for the treatment of cancer and immune disorders, Mater. Horizons. 6 (2019) 1956–1973. doi:10.1039/c9mh00628a.

[11] R. Duncan, K. Edward, V.I.I. Avenue, The dawning era of polymer therapeutics, 2 (2003) 347–360. doi:10.1038/nrd1088.

[12] I. Conejos-Sánchez, A. Duro-Castano, A. Birke, M. Barz, M.J. Vicent, A controlled and versatile NCA polymerization method for the synthesis of polypeptides, Polym. Chem. 4 (2013) 3182–3186. doi:10.1039/c3py00347g.

[13] D.J. Walsh, M.G. Hyatt, S.A. Miller, D. Guironnet, Recent Trends in Catalytic Polymerizations, ACS Catal. 9 (2019) 11153–11188. doi:10.1021/acscatal.9b03226.

[14] M.J. Vicent, A. Duro Castaño, V.J. Nebot Cardá, Cross-linked star-shaped self-assembled polypeptides and its use as carriers in biomedical applications, WO 2017/025298 A1, 2017.

[15] J. Jiang, X. Zhang, Z. Fan, J. Du, Ring-Opening Polymerization of N -Carboxyanhydride-Induced Self- Assembly for Fabricating Biodegradable Polymer Vesicles, ACS Macro Lett. 8 (2019) 1216–1221. doi:10.1021/acsmacrolett.9b00606.

[16] A.M. Wagner, D.S. Spencer, N.A. Peppas, Recent advances in applied polymer science, J. Appl. Polym. Sci. 135 (2018) 46154. doi:10.1002/app.46279.

[17] J. Wotring, S. Countryman, F.N. Wallace, E.C. Strickland, O.T. Cummings, G.L. McIntire, Movantik™ and the Frequency of Positive Naloxone in Urine, J. Anal. Toxicol. 42 (2018) e38–e40. doi:10.1093/jat/bkx104.

[18] E. Pérez-Payá, M. Orzáez, L. Mondragón, D. Wolan, J.A. Wells, A. Messeguer, M.J. Vicent, MoleculesThat ModulateApaf-1Activity, Med Res Rev. 31 (2011) 649–675. doi:10.1002/med.20198.

[19] E. Giraldo, V. Nebot, O. Zagorodko, R. Requejo-Aguilar, A. Alastrue-Agudo, A. Armiñan, B. Martinez-Rojas, P. Bonilla-Villamil, S. Dordevic, M.J. Vicent, V. Moreno-Manzano, A Rationally Designed Self-Immolative Linker Enhances The Synergism Between A Polymer-Rock Inhibitor Conjugate And Neural Progenitor Cells In The Treatment Of Spinal Cord Injury, Adv. Funct. Mater. submitted (2020).

[20] I. Conejos-Sánchez, E. Gallon, A. Niño-Pariente, J.A. Smith, A.G. De La Fuente, L. Di Canio, S. Pluchino, R.J.M. Franklin, M.J. Vicent, Polyornithine-based polyplexes to boost effective gene silencing in CNS disorders, Nanoscale. 12 (2020) 6285–6299. doi:10.1039/c9nr06187h.

[21] A. Duro-Castano, N.H. Lim, I. Tranchant, M. Amoura, F. Beau, H. Wieland, O. Kingler, M. Herrmann, M. Nazaré, O. Plettenburg, V. Dive, M.J. Vicent, H. Nagase, In Vivo Imaging of MMP-13 Activity Using a Specific Polymer-FRET Peptide Conjugate Detects Early Osteoarthritis and Inhibitor Efficacy, Adv. Funct. Mater. 28 (2018) 1–9. doi:10.1002/adfm.201802738.

[22] H. Yang, Y. Miao, L. Chen, Z. Li, R. Yang, X. Xu, Z. Liu, L.M. Zhang, X. Jiang, Redox-responsive nanoparticles from disulfide bond-linked poly-(N-ε-carbobenzyloxy-L-lysine)-grafted hyaluronan copolymers as theranostic nanoparticles for tumor-targeted MRI and chemotherapy, Int. J. Biol. Macromol. 148 (2020) 483–492. doi:10.1016/j.ijbiomac.2020.01.071.

[23] S. Lee, T.C. Pham, C. Bae, Y. Choi, Y.K. Kim, J. Yoon, Nano theranostics platforms that utilize proteins, Coord. Chem. Rev. 412 (2020) 213258. doi:10.1016/j.ccr.2020.213258.

[24] O. Zagorodko, J.J. Arroyo-Crespo, V.J. Nebot, M.J. Vicent, Polypeptide-Based Conjugates as Therapeutics: Opportunities and Challenges, Macromol. Biosci. 17 (2017) 1–22. doi:10.1002/mabi.201600316.

[25] R. Duncan, M.J. Vicent, Polymer therapeutics-prospects for 21st century: The end of the beginning, Adv. Drug Deliv. Rev. 65 (2013) 60–70. doi:10.1016/j.addr.2012.08.012.

[26] https://starpharma.com/assets/asxannouncements/190416%20Fleurstat%20BVgel%20launched%20by%20Aspen%20in%20Australia.pdf (Accessed October 4, 2020), (n.d.).

[27] C.F. Price, D. Tyssen, S. Sonza, A. Davie, S. Evans, G.R. Lewis, S. Xia, T. Spelman, P. Hodsman, T.R. Moench, A. Humberstone, J.R.A. Paull, G. Tachedjian, SPL7013 gel (vivagel®) retains potent HIV-1 and HSV-1 inhibitory activity following vaginal administration in humans, PLoS One. 6 (2011). doi:10.1371/journal.pone.0024095.

[28] R. Duncan, Polymer therapeutics: Top 10 selling pharmaceuticals — What next?, J. Control. Release. 190 (2014) 371–380. doi:10.1016/j.jconrel.2014.05.001.

[29] B. Weinstock-Guttman, K. V. Nair, J.L. Glajch, T.C. Ganguly, D. Kantor, Two decades of glatiramer acetate: From initial discovery to the current development of generics, J. Neurol. Sci. 376 (2017) 255–259. doi:10.1016/j.jns.2017.03.030.

[30] J.Y. Song, N.R. Larson, S. Thati, I. Torres-, N. Martinez-rivera, N.J. Subelzu-aispuru, M.A. Leon, E. Rosa-molinar, C. Schöneich, R. Middaugh, C.J. Berkland, N. Martinez-rivera, N.J. Subelzu-aispuru, M.A. Leon, Glatiramer acetate persists at the injection site and draining lymph nodes via electrostatically-induced aggregation., J. Control. Release. 293 (2019) 36–47. doi:10.1016/j.jconrel.2018.11.007.

[31] A.D. Kenny, Evaluation of Sodium Poly-α, L-glutamate as a Plasma Expander, Proc. Soc. Exptl. Biol. Med. 100 (1959) 778–780.

[32] H. Sun, X. Gu, Q. Zhang, H. Xu, Z. Zhong, C. Deng, Cancer Nanomedicines Based on Synthetic Polypeptides Cancer, Biomacromolecules. 20 (2019) 4299–4311. doi:10.1021/acs.biomac.9b01291.

[33] X. Pang, X. Yang, G. Zhai, Polymer-drug conjugates: Recent progress on administration routes, Expert Opin. Drug Deliv. 11 (2014) 1075–1086. doi:10.1517/17425247.2014.912779.

[34] H. Maeda, J. Fang, T. Inutsuka, Y. Kitamoto, Vascular permeability enhancement in solid tumor: Various factors, mechanisms involved and its implications, Int. Immunopharmacol. 3 (2003) 319–328. doi:10.1016/S1567-5769(02)00271-0.

[35] M.H. Matsumura Y, Y. Matsumura, H. Maeda, A new concept for macromolecular therapeutics in cancer chemotherapy: mechanism of tumoritropic accumulation of proteins and the antitumor agent smancs, Cancer Res. 46 (1986) 6387-6392.

[36] J. Fang, W. Islam, H. Maeda, Exploiting the dynamics of the EPR effect and strategies

to improve the therapeutic effects of nanomedicines by using EPR effect enhancers, Adv. Drug Deliv. Rev. in press (2020). doi:10.1016/j.strueco.2019.07.006.

[37] T.A. Al-Hilal, F. Alam, Y. Byun, Oral drug delivery systems using chemical conjugates or physical complexes, Adv. Drug Deliv. Rev. 65 (2013) 845–864. doi:10.1016/j.addr.2012.11.002.

[38] M.W. Konstan, P.B. Davis, J.S. Wagener, K.A. Hilliard, R.C. Stern, L.J.H. Milgram, T.H. Kowalczyk, S.L. Hyatt, T.L. Fink, C.R. Gedeon, S.M. Oette, J.M. Payne, O. Muhammad, A.G. Ziady, R.C. Moen, M.J. Cooper, Compacted DNA nanoparticles administered to the nasal mucosa of cystic fibrosis subjects are safe and demonstrate partial to complete cystic fibrosis transmembrane regulator reconstitution, Hum. Gene Ther. 15 (2004) 1255–1269. doi:10.1089/hum.2004.15.1255.

[39] F. Rodriguez-Otormin, A. Duro-Castano, I. Conejos-Sánchez, M.J. Vicent, Envisioning the future of polymer therapeutics for brain disorders, WIREs Nanomed Nanobiotechnol. 11 (2019) e1532. doi:10.1002/wnan.1532.

[40] L.B. Vong, Y. Ibayashi, Y. Lee, D.N. Ngo, Y. Nishikawa, Y. Nagasaki, Poly(ornithine)-based self-assembling drug for recovery of hyperammonemia and damage in acute liver injury, J. Control. Release. 310 (2019) 74–81. doi:10.1016/j.jconrel.2019.08.011.

[41] S.S. Desale, K.S. Soni, S. Romanova, S.M. Cohen, T.K. Bronich, Targeted delivery of platinum-taxane combination therapy in ovarian cancer, J. Control. Release. 220 (2015) 651–659. doi:10.1016/j.jconrel.2015.09.007.

[42] R. Qi, Y. Wang, P.M. Bruno, H. Xiao, Y. Yingjie, T. Li, S. Lauffer, W. Wei, Q. Chen, X. Kang, H. Song, X. Yang, X. Huang, A. Devappe, U. Matulonis, D. Pepin, M.T. Hemann, M.J. Birrer, P.P. Ghoroghchian, Nanoparticle conjugates of a highly potent toxin enhance safety and circumvent platinum resistance in ovarian cancer, Nat. Commun. 8 (2017). doi:10.1038/s41467-017-02390-7.

[43] R. Toshiyama, M. Konno, H. Eguchi, H. Takemoto, T. Noda, A. Asai, J. Koseki, N. Haraguchi, Y. Ueda, K. Matsushita, K. Asukai, T. Ohashi, Y. Iwagami, D. Yamada, D. Sakai, T. Asaoka, T. Kudo, K. Kawamoto, K. Gotoh, S. Kobayashi, T. Satoh, Y. Doki, N. Nishiyama, M. Mori, H. Ishii, Poly(ethylene glycol)–poly(lysine) block copolymer–ubenimex conjugate targets aminopeptidase N and exerts an antitumor effect in hepatocellular carcinoma stem cells, Oncogene. 38 (2019) 244–260. doi:10.1038/s41388-018-0406-x.

[44] L.M. Kaminskas, V.M. Mcleod, G.M. Ryan, B.D. Kelly, J.M. Haynes, M. Williamson, N. Thienthong, D.J. Owen, C.J.H. Porter, Pulmonary administration of a doxorubicin-conjugated dendrimer enhances drug exposure to lung metastases and improves cancer therapy, J. Control. Release. 183 (2014) 18–26. doi:10.1016/j.jconrel.2014.03.012.

[45] N. Marasini, S. Haque, L.M. Kaminskas, Polymer-drug conjugates as inhalable drug delivery systems: A review, Curr. Opin. Colloid Interface Sci. 31 (2017) 18–29. doi:10.1016/j.cocis.2017.06.003.

[46] I. Dolz-Pérez, M.A. Sallam, E. Masiá, D. Morelló-Bolumar, M.D. Pérez del Caz, P. Graff, D. Abdelmonsif, S. Hedtrich, V.J. Nebot, M.J. Vicent, Polypeptide-corticosteroid conjugates as a topical treatment approach to psoriasis, J. Control. Release. 318 (2020) 210–222. doi:10.1016/j.jconrel.2019.12.016.

[47] A. Mandal, R. Bisht, I.D. Rupenthal, A.K. Mitra, Polymeric micelles for ocular drug delivery: From structural frameworks to recent preclinical studies, J. Control. Release. 248 (2017) 96–116. doi:10.1016/j.jconrel.2017.01.012.

[48] R. Duncan, R. Gaspar, Nanomedicine (s) under the Microscope, Mol. Pharm. 8 (2011) 2101–2141. doi:10.1021/mp200394t.
[49] I. Wagner, H. Musso, New Naturally Occurring Amino Acids, Angew. Chemie Int. Ed. English. 22 (1983) 816–828. doi:10.1002/anie.198308161.
[50] M. Barz, R. Luxenhofer, R. Zentel, M.J. Vicent, Overcoming the PEG-addiction: Well-defined alternatives to PEG, from structure-property relationships to better defined therapeutics, Polym. Chem. 2 (2011) 1900–1918. doi:10.1039/c0py00406e.
[51] I. Cohen-Erez, H. Rapaport, Negatively charged polypeptide-peptide nanoparticles showing efficient drug delivery to the mitochondria, Colloids Surfaces B Biointerfaces. 162 (2018) 186–192. doi:10.1016/j.colsurfb.2017.11.048.
[52] H. Kirschke, A.J. Barrett, N.D. Rawlings, Lysosomal Cysteine Proteinases, 2nd ed., Oxford University Press, 1998.
[53] B. Chen, W. Dai, B. He, H. Zhang, X. Wang, Y. Wang, Current Multistage Drug Delivery Systems Based on the Tumor Microenvironment, Theranostics. 7 (2017) 538–558. doi:10.7150/thno.16684.
[54] W. Chen, G. Luo, Q. Lei, H. Jia, S. Hong, Q. Wang, R. Zhang, X. Zhang, MMP-2 responsive polymeric micelles for cancer-targeted intracellular drug delivery, Chem. Commun. 51 (2015) 465–468. doi:10.1039/C4CC07563C.
[55] Y. Tu, L. Zhu, Matrix Metalloproteinase-Sensitive, in: Smart Pharm. Nanocarriers, 2016: pp. 83–116.
[56] Z. Song, H. Fu, R. Wang, L.A. Pacheco, X. Wang, Y. Lin, J. Cheng, Secondary structures in synthetic polypeptides from N-carboxyanhydrides: design, modulation, association, and material applications, Chem. Soc. Rev. 47 (2018) 7401–7425. doi:10.1039/c8cs00095f.
[57] I. Saiki, J. Murata, J. Iida, T. Sakurai, N. Nishi, K. Matsuno, I. Azuma, Antimetastatic effects of synthetic polypeptides containing repeated structures of the cell adhesive arg-gly-asp (RGD) and tyr-ile-gly-ser-arg (YIGSR) sequences, Br. J. Cancer. 60 (1989) 722–728. doi:10.1038/bjc.1989.347.
[58] I. Saiki, J. Murata, K. Matsuno, R. Ogawa, N. Nishi, S. Tokura, I. Azuma, Anti-metastatic and Anti-Invasive Effects of Polymeric Arg-Gly-Asp (RGD) Peptide, poly(RGD), and Its Analogues, Jpn. J. Cancer Res. 81 (1990) 660–667.
[59] S. Banskota, P. Yousefpour, N. Kirmani, X. Li, A. Chilkoti, Long circulating genetically encoded intrinsically disordered zwitterionic polypeptides for drug delivery, Biomaterials. 192 (2019) 475–485. doi:10.1016/j.biomaterials.2018.11.012.
[60] H. Yin, R.L. Kanasty, A.A. Eltoukhy, A.J. Vegas, J.R. Dorkin, D.G. Anderson, Non-viral vectors for gene-based therapy, Nat. Rev. Genet. 15 (2014) 541–555. doi:10.1038/nrg3763.
[61] S.E. Barrett, R.S. Burke, M.T. Abrams, C. Bason, M. Busuek, E. Carlini, B.A. Carr, L.S. Crocker, H. Fan, R.M. Garbaccio, E.N. Guidry, J.H. Heo, B.J. Howell, E.A. Kemp, R.A. Kowtoniuk, A.H. Latham, A.M. Leone, M. Lyman, R.G. Parmar, M. Patel, S.Y. Pechenov, T. Pei, N.T. Pudvah, C. Raab, S. Riley, L. Sepp-Lorenzino, S. Smith, E.D. Soli, S. Staskiewicz, M. Stern, Q. Truong, M. Vavrek, J.H. Waldman, E.S. Walsh, J.M. Williams, S. Young, S.L. Colletti, Development of a liver-targeted siRNA delivery platform with a broad therapeutic window utilizing biodegradable polypeptide-based polymer conjugates, J. Control. Release. 183 (2014) 124–137. doi:10.1016/j.jconrel.2014.03.028.
[62] D.M.M. Jaradat, Thirteen decades of peptide synthesis: key developments in solid

phase peptide synthesis and amide bond formation utilized in peptide ligation, Amino Acids. 50 (2018) 39–68. doi:10.1007/s00726-017-2516-0.

[63] A.K. Varanko, J.C. Su, A. Chilkoti, Elastin-Like Polypeptides for Biomedical Applications, Annu. Rev. Biomed. Eng. 22 (2020) 343–369. doi:10.1146/annurev-bioeng-092419-061127.

[64] T.J. Deming, Synthetic polypeptides for biomedical applications, Prog. Polym. Sci. 32 (2007) 858–875. doi:10.1016/j.progpolymsci.2007.05.010.

[65] T.J. Deming, Synthesis of Side-Chain Modified Polypeptides, Chem. Rev. 116 (2016) 786–808. doi:10.1021/acs.chemrev.5b00292.

[66] Y. Zhang, R. Liu, H. Jin, W. Song, R. Augustine, I. Kim, Straightforward access to linear and cyclic polypeptides, Commun. Chem. 1 (2018) 1–7. doi:10.1038/s42004-018-0040-0.

[67] R. Holm, D. Schwiertz, B. Weber, J. Schultze, J. Kuhn, K. Koynov, U. Lächelt, M. Barz, Multifunctional Cationic PeptoStars as siRNA Carrier : Influence of Architecture and Histidine Modification on Knockdown Potential, Macromol. Biosci. 20 (2020) 1900152. doi:10.1002/mabi.201900152.

[68] A. Duro-Castano, J. Movellan, M.J. Vicent, Smart branched polymer drug conjugates as nano-sized drug delivery systems, Biomater. Sci. 3 (2015) 1321–1334. doi:10.1039/c5bm00166h.

[69] R. Holm, M. Douverne, B. Weber, T. Bauer, A. Best, P. Ahlers, K. Koynov, P. Besenius, M. Barz, Impact of Branching on the Solution Behavior and Serum Stability of Starlike Block Copolymers, Biomacromolecules. 20 (2019) 375–388. doi:10.1021/acs.biomac.8b01545.

[70] D. Schwiertz, R. Holm, M. Barz, Facile synthesis of amphiphilic AB 3 and A 3 B miktoarm PeptoMiktoStars, Polym. J. 52 (2020) 119–132. doi:10.1038/s41428-019-0269-1.

[71] D. Tyssen, S.A. Henderson, A. Johnson, J. Sterjovski, K. Moore, J. La, M. Zanin, S. Sonza, P. Karellas, M.P. Giannis, G. Krippner, S. Wesselingh, T. McCarthy, P.R. Gorry, P.A. Ramsland, R. Cone, J.R.A. Paull, G.R. Lewis, G. Tachedjian, Structure activity relationship of dendrimer microbicides with dual action antiviral activity, PLoS One. 5 (2010) e12309. doi:10.1371/journal.pone.0012309.

[72] H. Cabral, K. Miyata, K. Osada, K. Kataoka, Block Copolymer Micelles in Nanomedicine Applications, Chem. Rev. 118 (2018) 6844–6892. doi:10.1021/acs.chemrev.8b00199.

[73] H. Kang, S. Rho, W.R. Stiles, S. Hu, Y. Baek, Size-Dependent EPR Effect of Polymeric Nanoparticles on Tumor Targeting, Adv. Healthc. Mater. 9 (2020) 1901223. doi:10.1002/adhm.201901223.

[74] D.E. Owens, N.A. Peppas, Opsonization, biodistribution, and pharmacokinetics of polymeric nanoparticles, Int. J. Pharm. 307 (2006) 93–102. doi:10.1016/j.ijpharm.2005.10.010.

[75] T.T.H. Thi, E.H. Pilkington, D.H. Nguyen, J.S. Lee, K.D. Park, N.P. Truong, The importance of Poly(ethylene glycol) alternatives for overcoming PEG immunogenicity in drug delivery and bioconjugation, Polymers (Basel). 12 (2020) 298. doi:10.3390/polym12020298.

[76] L. Xu, J. Yang, B. Xue, C. Zhang, L. Shi, C. Wu, Y. Su, X. Jin, Y. Liu, X. Zhu, Molecular Insights for the Biological Interactions Between Polyethylene Glycol and Cells, Biomaterials. 147 (2017) 1–13. doi:10.1016/j.biomaterials.2017.09.002.

[77] R. Webster, E. Didier, P. Harris, N. Siegel, J. Stadler, L. Tilbury, D. Smith, PEGylated

proteins: Evaluation of their safety in the absence of definitive metabolism studies, Drug Metab. Dispos. 35 (2007) 9–16. doi:10.1124/dmd.106.012419.

[78] Q. Shen, Y. Lin, T. Handa, M. Doi, M. Sugie, K. Wakayama, N. Okada, T. Fujita, A. Yamamoto, Modulation of intestinal P-glycoprotein function by polyethylene glycols and their derivatives by in vitro transport and in situ absorption studies, Int. J. Pharm. 313 (2006) 49–56. doi:10.1016/j.ijpharm.2006.01.020.

[79] A. Birke, J. Ling, M. Barz, Polysarcosine-containing copolymers: Synthesis, characterization, self-assembly, and applications, Prog. Polym. Sci. 81 (2018) 163–208. doi:10.1016/j.progpolymsci.2018.01.002.

[80] H. Cabral, Y. Matsumoto, K. Mizuno, Q. Chen, M. Murakami, M. Kimura, Y. Terada, M.R. Kano, K. Miyazono, M. Uesaka, N. Nishiyama, K. Kataoka, Accumulation of sub-100 nm polymeric micelles in poorly permeable tumours depends on size, Nat. Nanotechnol. (2011). doi:10.1038/nnano.2011.166.

[81] S.K. Golombek, J.N. May, B. Theek, L. Appold, N. Drude, F. Kiessling, T. Lammers, Tumor targeting via EPR: Strategies to enhance patient responses, Adv. Drug Deliv. Rev. 130 (2018) 17–38. doi:10.1016/j.addr.2018.07.007.

[82] E. Pisarevsky, R. Blau, Y. Epshtein, D. Ben-shushan, A. Eldar-boock, G. Tiram, S. Koshrovski-michael, A. Scomparin, S. Pozzi, A. Krivitsky, G. Shenbach-koltin, E. Yeini, L. Fridrich, R. White, R. Satchi-fainaro, Rational Design of Polyglutamic Acid Delivering an Optimized Combination of Drugs Targeting Mutated BRAF and MEK in Melanoma, Adv. Ther. 2000028 (2020) 1–17. doi:10.1002/adtp.202000028.

[83] H.S. El-sawy, A. Al-abd, T. Ahmed, K.M. El-say, V.P. Torchilin, Stimuli-Responsive Nano-Architectures Drug Delivery Systems to Solid Tumor Micromilieu : Past , Present and Future Perspectives Stimuli-Responsive Nano-Architectures Drug Delivery Systems to Solid Tumor Department of Pharmaceutics and Pharmaceutical Techn, ACS Nano. 12 (2018) 10636–10664. doi:10.1021/acsnano.8b06104.

[84] Y. Gaoa, C.-M. Dong, Reduction- and thermo-sensitive core-cross-linked polypeptide hybrid micelles for triggered and intracellular drug release, Polym. Chem. 8 (2017) 1223–1232. doi:10.1039/C6PY01929C.

[85] J. Qu, Q. Wang, K. Chen, J. Luo, Q. Zhou, J. Lin, Reduction / temperature / pH multi-stimuli responsive core cross-linked polypeptide hybrid micelles for triggered and intracellular drug release, Colloids Surfaces B Biointerfaces. 170 (2018) 373–381. doi:10.1016/j.colsurfb.2018.06.015.

[86] B. Li, M. Shan, X. Di, C. Gong, L. Zhang, Y. Wang, G. Wu, A dual pH- and reduction-responsive anticancer drug delivery system based on PEG–SS–poly(amino acid) block copolymer, RSC Adv. 7 (2017) 30242–30249. doi:10.1039/C7RA04254J.

[87] W. Song, Z. Tang, M. Li, S. Lv, H. Sun, M. Deng, H. Liu, X. Chen, Polypeptide-based combination of paclitaxel and cisplatin for enhanced chemotherapy efficacy and reduced side-effects, Acta Biomater. 10 (2014) 1392–1402. doi:10.1016/j.actbio.2013.11.026.

[88] Y. Li, H. Lu, S. Liang, S. Xu, Dual Stable Nanomedicines Prepared by Cisplatin-Crosslinked Camptothecin Prodrug Micelles for Effective Drug Delivery, ACS Appl. Mater. Interfaces. 11 (2019) 20649–20659. doi:10.1021/acsami.9b03960.

[89] H. Baabur-Cohen, L. Isabel, H. Rune, A. Eldar-boock, E. Yeini, N. Landa-rouben, G. Tiram, S. Wedepohl, E. Markovsky, J. Leor, M. Calderón, R. Satchi-fainaro, In vivo comparative study of distinct polymeric architectures bearing a combination of paclitaxel and doxorubicin at a synergistic ratio, J. Control. Release. 257 (2017) 118–

131. doi:10.1016/j.jconrel.2016.06.037.
[90] J. Qian, M. Xu, A. Suo, W. Xu, T. Liu, X. Liu, Y. Yao, H. Wang, Folate-decorated hydrophilic three-arm star-block terpolymer as a novel nanovehicle for targeted co-delivery of doxorubicin and Bcl-2 siRNA in breast cancer therapy, ACTA Biomater. 15 (2015) 102–116. doi:10.1016/j.actbio.2014.12.018.
[91] J.J. Arroyo-Crespo, C. Deladriere, V.J. Nebot, D. Charbonnier, E. Masiá, A. Paul, C. James, A. Armiñán, M.J. Vicent, Anticancer Activity Driven by Drug Linker Modification in a Polyglutamic Acid-Based Combination-Drug Conjugate, Adv. Funct. Mater. 28 (2018) 1800931. doi:10.1002/adfm.201800931.
[92] B. Sui, H. Xu, J. Jin, J. Gou, J. Liu, X. Tang, Y. Zhang, J. Xu, H. Zhang, X. Jin, Self-Assembled Micelles Composed of Doxorubicin Conjugated Y-Shaped PEG-Poly(glutamic acid)2 Copolymers via Hydrazone Linkers, Molecules. 19 (2014) 11915–11932. doi:10.3390/molecules190811915.
[93] W. Tai, R. Mo, Y. Lu, T. Jiang, Z. Gu, Folding graft copolymer with pendant drug segments for co-delivery of anticancer drugs, Biomaterials. 35 (2014) 7194–7203. doi:10.1016/j.biomaterials.2014.05.004.
[94] Z. Zhou, J. Tang, Q. Sun, W.J. Murdochc, Y. Shen, A multifunctional PEG–PLL drug conjugate forming redox-responsive nanoparticles for intracellular drug delivery, Mater. Chem. B. 3 (2015) 7594–7603. doi:10.1039/C5TB01027F.
[95] H.C. Kolb, M.G. Finn, K.B. Sharpless, Click Chemistry: Diverse Chemical Function from a Few Good Reactions, Angew. Chemie - Int. Ed. 40 (2001) 2004–2021. doi:10.1002/1521-3773(20010601)40:11<2004::AID-ANIE2004>3.0.CO;2-5.
[96] A. Duro-Castano, V.J.J. Nebot, A. Niño Parente, A. Armiñán, J.J.J. Arroyo-Crespo, A. Paul, N. Feiner-Gracia, L. Albertazzi, M.J.J. Vicent, Capturing “Extraordinary” Soft-Assembled Charge-Like Polypeptides as a Strategy for Nanocarrier Design, Adv. Mater. 29 (2017) 1702888. doi:10.1002/adma.201702888.
[97] C.A. Deforest, B.D. Polizzotti, K.S. Anseth, Sequential click reactions for synthesizing and patterning three-dimensional cell microenvironments, Nat. Mater. 8 (2009) 659–664. doi:10.1038/nmat2473.
[98] Z. Zhang, C. He, X. Chen, Injectable click polypeptide hydrogels via tetrazine-norbornene chemistry for localized cisplatin release, Polymers (Basel). 12 (2020) 1–15. doi:10.3390/POLYM12040884.
[99] S. Florinas, M. Liu, R. Fleming, L. Van Vlerken-Ysla, J. Ayriss, R. Gilbreth, N. Dimasi, C. Gao, H. Wu, Z.Q. Xu, S. Chen, A. Dirisala, K. Kataoka, H. Cabral, R.J. Christie, A Nanoparticle Platform to Evaluate Bioconjugation and Receptor-Mediated Cell Uptake Using Cross-Linked Polyion Complex Micelles Bearing Antibody Fragments, Biomacromolecules. 17 (2016) 1818–1833. doi:10.1021/acs.biomac.6b00239.
[100] A.B. Lowe, Thiol-ene “click” reactions and recent applications in polymer and materials synthesis: A first update, Polym. Chem. 5 (2014) 4820–4870. doi:10.1039/c4py00339j.
[101] Y. Jiang, J. Chen, C. Deng, E.J. Suuronen, Z. Zhong, Click hydrogels, microgels and nanogels: Emerging platforms for drug delivery and tissue engineering, Biomaterials. 35 (2014) 4969–4985. doi:10.1016/j.biomaterials.2014.03.001.
[102] M. Gao, J. Deng, H. Chu, Y. Tang, Z. Wang, Y. Zhao, G. Li, Stereoselective Stabilization of Polymeric Vitamin E Conjugate Micelles, Biomacromolecules. 18 (2017) 4349–4356. doi:10.1021/acs.biomac.7b01409.
[103] J.S. Jan, P.S. Chen, P.L. Hsieh, B.Y. Chen, Silicification of genipin-cross-linked

polypeptide hydrogels toward biohybrid materials and mesoporous oxides, ACS Appl. Mater. Interfaces. 4 (2012) 6865–6874. doi:10.1021/am302016c.

[104] G. Horvát, B. Gyarmati, S. Berkó, P. Szabó-Révész, B.Á. Szilágyi, A. Szilágyi, J. Soós, G. Sandri, M.C. Bonferoni, S. Rossi, F. Ferrari, C. Caramella, E. Csányi, M. Budai-Szucs, Thiolated poly(aspartic acid) as potential in situ gelling, ocular mucoadhesive drug delivery system, Eur. J. Pharm. Sci. 67 (2015) 1–11. doi:10.1016/j.ejps.2014.10.013.

[105] H.B. Ruttala, N. Chitrapriya, K. Kaliraj, T. Ramasamy, W.H. Shin, J.H. Jeong, J.O.J.R. Kim, S.K. Ku, H.G. Choi, C.S. Yong, J.O.J.R. Kim, Facile construction of bioreducible crosslinked polypeptide micelles for enhanced cancer combination therapy, Acta Biomater. 63 (2017) 135–149. doi:10.1016/j.actbio.2017.09.002.

[106] Q. Liu, L. Song, S. Chen, J. Gao, P. Zhao, J. Du, A superparamagnetic polymersome with extremely high T2 relaxivity for MRI and cancer-targeted drug delivery, Biomaterials. 114 (2017) 23–33. doi:10.1016/j.biomaterials.2016.10.027.

[107] J. Xie, D. Gonzalez-Carter, T.A. Tockary, N. Nakamura, Y. Xue, M. Nakakido, H. Akiba, A. Dirisala, X. Liu, K. Toh, T. Yang, Z. Wang, S. Fukushima, J. Li, S. Quader, K. Tsumoto, T. Yokota, Y. Anraku, K. Kataoka, Dual-Sensitive Nanomicelles Enhancing Systemic Delivery of Therapeutically Active Antibodies Specifically into the Brain, ACS Nano. (2020). doi:10.1021/acsnano.9b09991.

[108] J. Ren, Y. Zhang, J. Zhang, H. Gao, G. Liu, R. Ma, Y. An, D. Kong, L. Shi, PH/sugar dual responsive core-cross-linked PIC micelles for enhanced intracellular protein delivery, Biomacromolecules. 14 (2013) 3434–3443. doi:10.1021/bm4007387.

[109] H. Yang, C. Zhang, C. Li, Y. Liu, Y. An, R. Ma, L. Shi, Glucose-Responsive Polymer Vesicles Templated by α-CD/PEG Inclusion Complex, Biomacromolecules. 16 (2015) 1372–1381. doi:10.1021/acs.biomac.5b00155.

[110] Y. Li, Q.N. Bui, L.T.M. Duy, H.Y. Yang, D.S. Lee, One-Step Preparation of pH-Responsive Polymeric Nanogels as Intelligent Drug Delivery Systems for Tumor Therapy, Biomacromolecules. 19 (2018) 2062–2070. doi:10.1021/acs.biomac.8b00195.

[111] G. Córdoba-David, A. Duro-Castano, R.C. Castelo-Branco, C. González-Guerrero, P. Cannata, A.B. Sanz, M.J. Vicent, A. Ortiz, A.M. Ramos, Effective Nephroprotection Against Acute Kidney Injury with a Star-Shaped Polyglutamate-Curcuminoid Conjugate, Sci. Rep. 10 (2020) 1–15. doi:10.1038/s41598-020-58974-9.

[112] A.C. Hunter, Molecular hurdles in polyfectin design and mechanistic background to polycation induced cytotoxicity, Adv. Drug Deliv. Rev. 58 (2006) 1523–1531. doi:10.1016/j.addr.2006.09.008.

[113] C. Zhang, D. Pan, J. Li, J. Hu, A. Bains, N. Guys, H. Zhu, X. Li, K. Luo, Q. Gong, Z. Gu, Z. Guc, Enzyme-responsive peptide dendrimer-gemcitabine conjugate as a controlled-release drug delivery vehicle with enhanced antitumor efficacy, Acta Biomater. 55 (2017) 153–162. doi:10.1016/j.actbio.2017.02.047.

[114] D. Ma, Q.M. Lin, L.M. Zhang, Y.Y. Liang, W. Xue, A star-shaped porphyrin-arginine functionalized poly(l-lysine) copolymer for photo-enhanced drug and gene co-delivery, Biomaterials. 35 (2014) 4357–4367. doi:10.1016/j.biomaterials.2014.01.070.

[115] S.S. Han, Z.Y. Li, J.Y. Zhu, K. Han, Z.Y. Zeng, W. Hong, W.X. Li, H.Z. Jia, Y. Liu, R.X. Zhuo, X.Z. Zhang, Dual-pH sensitive charge-reversal polypeptide micelles for tumor-triggered targeting uptake and nuclear drug delivery, Small. 11 (2015) 2543–2554. doi:10.1002/smll.201402865.

[116] K.M. Takeda, Y. Yamasaki, A. Dirisala, S. Ikeda, T.A. Tockary, K. Toh, K. Osada, K. Kataoka, Effect of shear stress on structure and function of polyplex micelles from

poly(ethylene glycol)-poly(L-lysine) block copolymers as systemic gene delivery carrier, Biomaterials. 126 (2017) 31–38. doi:10.1016/j.biomaterials.2017.02.012.
[117] D. Owen, B.D. Kelly, P. Karellas, US10265409B2, 2019.
[118] https://starpharma.com/drug_delivery (Accessed October 4, 2020), (n.d.).
[119] A. Duro-Castano, R.M. England, D. Razola, E. Romero, M. Oteo-Vives, M.A. Morcillo, M.J. Vicent, Well-defined star-shaped polyglutamates with improved pharmacokinetic profiles as excellent candidates for biomedical applications, Mol. Pharm. 12 (2015) 3639–3649. doi:10.1021/acs.molpharmaceut.5b00358.
[120] P. Mi, H. Cabral, K. Kataoka, Ligand-Installed Nanocarriers toward Precision Therapy, Adv. Mater. 32 (2020) 1–29. doi:10.1002/adma.201902604.
[121] M.A. Quadir, S.W. Morton, L.B. Mensah, K. Shopsowitz, J. Dobbelaar, N. Effenberger, P.T. Hammond, Ligand-decorated click polypeptide derived nanoparticles for targeted drug delivery applications, Nanomedicine Nanotechnology, Biol. Med. 13 (2017) 1797–1808. doi:10.1016/j.nano.2017.02.010.
[122] H. Yi, P. Liu, N. Sheng, P. Gong, Y. Ma, L. Cai, In situ crosslinked smart polypeptide nanoparticles for multistage responsive tumor-targeted drug delivery, Nanoscale. 8 (2016) 5985–5995. doi:10.1039/c5nr07348k.
[123] B. Jiang, M. Liu, K. Zhang, G. Zu, J. Dong, Y. Cao, L. Zhang, R. Pei, Oligoethylenimine grafted PEGylated poly(aspartic acid) as a macromolecular contrast agent: Properties and: In vivo studies, J. Mater. Chem. B. 4 (2016) 3324–3330. doi:10.1039/c6tb00278a.
[124] G. Hou, J. Qian, W. Xu, T. Sun, J. Wang, Y. Wang, A. Suo, Multifunctional PEG-b-polypeptide-decorated gold nanorod for targeted combined chemo-photothermal therapy of breast cancer, Colloids Surfaces B Biointerfaces. 181 (2019) 602–611. doi:10.1016/j.colsurfb.2019.05.025.
[125] S. Misra, P. Heldin, V.C. Hascall, N.K. Karamanos, S.S. Skandalis, R.R. Markwald, S. Ghatak, Hyaluronan-CD44 interactions as potential targets for cancer therapy, FEBS J. 278 (2011) 1429–1443. doi:10.1111/j.1742-4658.2011.08071.x.
[126] M. Lee, J. Jeong, D. Kim, Intracellular uptake and pH-dependent release of doxorubicin from the self-assembled micelles based on amphiphilic polyaspartamide graft copolymers, Biomacromolecules. 16 (2015) 136–144. doi:10.1021/bm501272c.
[127] A. Sugaya, I. Hyodo, Y. Koga, Y. Yamamoto, H. Takashima, R. Sato, R. Tsumura, F. Furuya, M. Yasunaga, M. Harada, R. Tanaka, Y. Matsumura, Utility of epirubicin-incorporating micelles tagged with anti-tissue factor antibody clone with no anticoagulant effect, Cancer Sci. 107 (2016) 335–340. doi:10.1111/cas.12863.
[128] D. zhou Liu, C. Ying, R. qiao Cai, W. Wang, H. Cui, M. Liu, B. le Zhang, Q. bing Mei, S. yuan Zhou, Y. Cheng, R. qiao Cai, W. wen Wang, BD, H. Cui, M. Liu, B. le Zhang, Q. bing Mei, S. yuan Zhou, The enhancement of siPLK1 penetration across BBB and its anti glioblastoma activity in vivo by magnet and transferrin co-modified nanoparticle, Nanomedicine Nanotechnology, Biol. Med. 14 (2018) 991–1003. doi:10.1016/j.nano.2018.01.004.
[129] M. Alipour, M. Baneshi, S. Hosseinkhani, R. Mahmoudi, A. Jabari Arabzadeh, M. Akrami, J. Mehrzad, H. Bardania, Recent progress in biomedical applications of RGD-based ligand: From precise cancer theranostics to biomaterial engineering: A systematic review, J. Biomed. Mater. Res. - Part A. 108 (2020) 839–850. doi:10.1002/jbm.a.36862.
[130] Y. Liu, J. Li, K. Shao, R. Huang, L. Ye, J. Lou, C. Jiang, A leptin derived 30-amino-acid peptide modified pegylated poly-l-lysine dendrigraft for brain targeted gene delivery,

Biomaterials. 31 (2010) 5246–5257. doi:10.1016/j.biomaterials.2010.03.011.
[131] S. Hua, M.B.C. de Matos, J.M. Metselaar, G. Storm, Current trends and challenges in the clinical translation of nanoparticulate nanomedicines: Pathways for translational development and commercialization, Front. Pharmacol. 9 (2018) 1–14. doi:10.3389/fphar.2018.00790.
[132] R. van der Meel, L.J.C. Vehmeijer, R.J. Kok, G. Storm, E.V.B. van Gaal, Ligand-targeted particulate nanomedicines undergoing clinical evaluation: Current status, Adv. Drug Deliv. Rev. 65 (2013) 1284–1298. doi:10.1016/j.addr.2013.08.012.
[133] K. Maso, A. Grigoletto, M.J. Vicent, G. Pasut, Molecular platforms for targeted drug delivery, 1st ed., Elsevier Inc., 2019. doi:10.1016/bs.ircmb.2019.03.001.
[134] S. Guan, J. Rosenecker, Nanotechnologies in delivery of mRNA therapeutics using nonviral vector-based delivery systems, Gene Ther. 24 (2017) 133–143. doi:10.1038/gt.2017.5.
[135] C. Shi, Y. He, X. Feng, D. Fu, ε-Polylysine and next-generation dendrigraft poly-L-lysine: Chemistry, activity, and applications in biopharmaceuticals, J. Biomater. Sci. Polym. Ed. 26 (2015) 1343–1356. doi:10.1080/09205063.2015.1095023.
[136] https://starpharma.com/news/385 (Accessed October 4, 2020), (n.d.).
[137] C.M. Patterson, K.J. Hill, I. Grant, J. Parker, S. Gales, A. Harmer, S. Redmond, S. Balachander, Srividya Wen, A. Adam, A. Schuller, J. Cidado, M. Wild, F.D. Gibbons, E. Gangl, D. Owen, M.B. Ashford1, Design and optimization of a dendrimer-conjugated Bcl-2/xL inhibitor, AZD0466, with improved developability and therapeutic index, in: AACR Virtual Annu. Meet. II, 2020: p. P-1718.
[138] C. Zhang, D. Pan, K. Luo, N. Li, C. Guo, X. Zheng, Z. Gu, Dendrimer-doxorubicin conjugate as enzyme-sensitive and polymeric nanoscale drug delivery vehicle for ovarian cancer therapy, Polym. Chem. 5 (2014) 5227–5235. doi:10.1039/c4py00601a.
[139] X. Meng, M. Gao, J. Deng, D. Liu, A. Fan, D. Ding, D. Kong, Z. Wang, Y. Zhao, Self-immolative micellar drug delivery: The linker matters, Nano Res. 11 (2018) 6177–6189. doi:10.1007/s12274-018-2134-5.
[140] J. Liu, X. Ai, H. Zhang, W. Zhuo, P. Mi, Polymeric micelles with endosome escape and redox-responsive functions for enhanced intracellular drug delivery, J. Biomed. Nanotechnol. 15 (2019) 373–381. doi:10.1166/jbn.2019.2693.
[141] G. Zu, M. Liu, K. Zhang, S. Hong, J. Dong, Y. Cao, B. Jiang, L. Luo, R. Pei, Functional Hyperbranched Polylysine as Potential Contrast Agent Probes for Magnetic Resonance Imaging, Biomacromolecules. 17 (2016) 2302–2308. doi:10.1021/acs.biomac.6b00605.
[142] J.S. Mort, D.J. Buttle, Molecules in focus Cathepsin B, Int. J. Biochem. Cell Biol. 29 (1997) 715–720. doi:10.1016/S1357-2725(96)00152-5.
[143] https://clinicaltrials.gov (Accessed October 4, 2020), (n.d.).
[144] R. Duncan, Development of HPMA copolymer-anticancer conjugates: Clinical experience and lessons learnt, Adv. Drug Deliv. Rev. 61 (2009) 1131–1148. doi:10.1016/j.addr.2009.05.007.
[145] J.W. Singer, Paclitaxel poliglumex (XYOTAX^{TM}, CT-2103): A macromolecular taxane, J. Control. Release. 109 (2005) 120–126. doi:10.1016/j.jconrel.2005.09.033.
[146] P. Chou, Y. Huang, M. Cheng, K. Rau, Y. Fang, Improvement of Paclitaxel-Associated Adverse Reactions (ADRs) via the Use of Nano-Based Drug Delivery Systems : A Systematic Review and Network Meta-Analysis, Int J Nanomedicine. 15 (2020) 1731–1743.

[147] J. Zhao, E.J. Koay, T. Li, X. Wen, C. Li, A hindsight reflection on the clinical studies of poly(l-glutamic acid)-paclitaxel, Wiley Interdiscip. Rev. Nanomedicine Nanobiotechnology. 10 (2018) 1–18. doi:10.1002/wnan.1497.

[148] J. Homsi, G.R. Simon, C.R. Garrett, G. Springett, R. De Conti, A.A. Chiappori, P.N. Munster, M.K. Burton, S. Stromatt, C. Allievi, P. Angiuli, A. Eisenfeld, D.M. Sullivan, A.I. Daud, Phase I trial of poly-L-glutamate camptothecin (CT-2106) administered weekly in patients with advanced solid malignancies, Clin. Cancer Res. 13 (2007) 5855–5861. doi:10.1158/1078-0432.CCR-06-2821.

[149] Y. Wen, Y. Wang, X. Liu, W. Zhang, X. Xiong, Z. Han, X. Liang, Camptothecin-based nanodrug delivery systems, Cancer Biol. Med. 14 (2017) 363–370. doi:10.20892/j.issn.2095-3941.2017.0099.

[150] T.M. Beer, C. Ryan, J. Alumkal, C.W. Ryan, J. Sun, K.M. Eilers, A phase II study of paclitaxel poliglumex in combination with transdermal estradiol for the treatment of metastatic castration-resistant prostate cancer after docetaxel chemotherapy, Anticancer. Drugs. 21 (2010) 433–438. doi:10.1097/CAD.0b013e3283355211.

[151] L. Han, Y. Xiao, M. Fan, J. Wang, Z. Yan, Y. Wang, L. Yu, H. Peng, J. Zhu, Synthesis and biological evaluation of an anticancer drug delivery system: Poly(L-γ-glutamyl-L-carbocisteine)-paclitaxel nanoconjugate, Mater. Sci. Eng. C. 81 (2017) 113–119. doi:10.1016/j.msec.2017.07.032.

[152] A. Eldar-Boock, K. Miller, J. Sanchis, R. Lupu, M.J. Vicent, R. Satchi-Fainaro, Integrin-assisted drug delivery of nano-scaled polymer therapeutics bearing paclitaxel, Biomaterials. 32 (2011) 3862–3874. doi:10.1016/j.biomaterials.2011.01.073.

[153] T. Hamaguchi, A. Tsuji, K. Yamaguchi, K. Takeda, H. Uetake, T. Esaki, A phase II study of NK012 , a polymeric micelle formulation of SN-38 , in unresectable , metastatic or recurrent colorectal cancer patients, Cancer Chemother. Pharmacol. 82 (2018) 1021–1029. doi:10.1007/s00280-018-3693-6.

[154] Y. Mochida, H. Cabral, K. Kataoka, Polymeric Micelles for Targeted Tumor Therapy of Platinum Anticancer Drugs, Polymeric Micelles for Targeted Tumor Therapy of Platinum Anticancer Drugs, Expert Opin. Drug Deliv. 14 (2017) 1423–1438. doi:10.1080/17425247.2017.1307338.

[155] P. Mi, H. Yanagie, N. Dewi, H.C. Yen, X. Liu, M. Suzuki, Y. Sakurai, K. Ono, H. Takahashi, H. Cabral, K. Kataoka, N. Nishiyama, Block copolymer-boron cluster conjugate for effective boron neutron capture therapy of solid tumors, J. Control. Release. 254 (2017) 1–9. doi:10.1016/j.jconrel.2017.03.036.

[156] H. Yu, Z. Tang, M. Li, W. Song, D. Zhang, Y. Zhang, Y. Yang, H. Sun, M. Deng, X. Chen, Cisplatin Loaded Poly(L-glutamic acid)-g-Methoxy Poly(ethylene glycol) Complex Nanoparticles for Potential Cancer Therapy: Preparation, In Vitro and In Vivo Evaluation, J. Biomed. Nanotechnol. 12 (2016) 69–78. doi:10.1166/jbn.2016.2152.

[157] H. Zhou, S. Lv, D. Zhang, M. Deng, X. Zhang, Z. Tang, X. Chen, A polypeptide based podophyllotoxin conjugate for the treatment of multi drug resistant breast cancer with enhanced efficiency and minimal toxicity, Acta Biomater. 73 (2018) 388–399. doi:10.1016/j.actbio.2018.04.016.

[158] T. Liu, D. Zhang, W. Song, Z. Tang, J. Zhu, Z. Ma, X. Wang, X. Chen, T. Tong, A poly (L - glutamic acid) -combretastatin A4 conjugate for solid tumor therapy : Markedly improved therapeutic efficiency through its low tissue penetration in solid tumor, Acta Biomater. 53 (2017) 179–189. doi:10.1016/j.actbio.2017.02.001.

[159] J. Jiang, N. Shen, W. Song, H. Yu, K. Sakurai, Z. Tang, G. Li, Combretastatin A4

nanodrug combined plerixafor for inhibiting tumor growth and metastasis simultaneously, Biomater. Sci. 7 (2019) 5283–5291. doi:10.1039/c9bm01418g.

[160] H. Qin, H. Yu, J. Sheng, D. Zhang, N. Shen, L. Liu, Z. Tang, X. Chen, PI3Kgamma Inhibitor Attenuates Immunosuppressive Effect of Poly (l -Glutamic Acid) - Combretastatin A4 Conjugate in Metastatic Breast Cancer, Adv. Sci. 6 (2019) 1900327. doi:10.1002/advs.201900327.

[161] L.V. Kiew, H.Y. Cheah, S.H. Voon, E. Gallon, J. Movellan, K.H. Ng, S. Alpugan, H.B. Lee, F. Dumoulin, M.J. Vicent, L.Y. Chung, Near-infrared activatable phthalocyanine-poly-L-glutamic acid conjugate: increased cellular uptake and light–dark toxicity ratio toward an effective photodynamic cancer therapy, Nanomedicine Nanotechnology, Biol. Med. 13 (2017) 1447–1458. doi:10.1016/j.nano.2017.02.002.

[162] H.Y. Cheah, E. Gallon, F. Dumoulin, S.Z. Hoe, N. Japundžić-Žigon, S. Glumac, H.B. Lee, P. Anand, L.Y. Chung, M.J. Vicent, L.V. Kiew, Near-Infrared Activatable Phthalocyanine-Poly-L-Glutamic Acid Conjugate: Enhanced in Vivo Safety and Antitumor Efficacy toward an Effective Photodynamic Cancer Therapy, Mol. Pharm. 15 (2018) 2594–2605. doi:10.1021/acs.molpharmaceut.8b00132.

[163] B. Santamaría, A.C. Ucero, A. Benito-Martin, M.J. Vicent, M. Orzáez, A. Celdrán, R. Selgas, M. Ruíz-Ortega, A. Ortiz, Biocompatibility reduces inflammation-induced apoptosis in mesothelial cells exposed to peritoneal dialysis Fluid, Blood Purif. 39 (2015) 200–209. doi:10.1159/000374103.

[164] E. Pérez-Payá, M. Orzáez, L. Mondragón, D. Wolan, J.A. Wells, A. Messeguer, M.J. Vicent, MoleculesThat ModulateApaf-1Activity, Harv. Bus. Rev. 86 (2008) 84–92. doi:10.1002/med.

[165] L. Mondragón, M. Orzáez, G. Sanchis-Perens, A. Moure, A. Armiñán, P. Sepúlveda, A. Messeguer, M.J. Vicent, E. Pérez-Payá, Modulation of cellular apoptosis with Apoptotic protease-activating factor 1 (Apaf-1) inhibitors, J. Med. Chem. 51 (2008) 521–529. doi:10.1021/jm701145i.

[166] A. Roncador, E. Oppici, M. Talelli, A.N. Pariente, M. Donini, S. Dusi, C.B. Voltattorni, M.J. Vicent, B. Cellini, Use of polymer conjugates for the intraperoxisomal delivery of engineered human alanine:glyoxylate aminotransferase as a protein therapy for primary hyperoxaluria type I, Nanomedicine Nanotechnology, Biol. Med. 13 (2017) 897–907. doi:10.1016/j.nano.2016.12.011.

[167] K. Maso, A. Grigoletto, L. Raccagni, M. Bellini, I. Marigo, V. Ingangi, A. Suzuki, M. Hirai, M. Kamiya, H. Yoshioka, G. Pasut, Poly(L-glutamic acid)-co-poly(ethylene glycol) block copolymers for protein conjugation, J. Control. Release. 324 (2020) 228–237. doi:10.1016/j.meegid.2020.104265.

[168] X. Wen, E.F. Jackson, R.E. Price, E.E. Kim, Q. Wu, S. Wallace, C. Charnsangavej, J.G. Gelovani, C. Li, Synthesis and characterization of poly(L-glutamic acid) gadolinium chelate: A new biodegradable MRI contrast agent, Bioconjug. Chem. 15 (2004) 1408–1415. doi:10.1021/bc049910m.

[169] G. Zhang, R. Zhang, X. Wen, L. Li, C. Li, Micelles based on biodegradable poly(L-glutamic acid)-b-polylactide with paramagnetic Gd ions chelated to the shell layer as a potential nanoscale MRI-Visible delivery system, Biomacromolecules. 9 (2008) 36–42. doi:10.1021/bm700713p.

[170] G. Zhang, R. Zhang, M.P. Melancon, K. Wong, J. You, Q. Huang, J. Bankson, D. Liang, C. Li, The degradation and clearance of Poly(N-hydroxypropyl-l-glutamine)-DTPA-Gd as a blood pool MRI contrast agent, Biomaterials. 33 (2012) 5376–5383.

doi:10.1016/j.biomaterials.2012.03.081.
[171] E.J.L. Stéen, J.T. Jørgensen, K. Johann, K. Nørregaard, B. Sohr, D. Svatunek, A. Birke, V. Shalgunov, P.E. Edem, R. Rossin, C. Seidl, F. Schmid, M.S. Robillard, J.L. Kristensen, H. Mikula, M. Barz, A. Kjær, M.M. Herth, Trans-Cyclooctene-Functionalized PeptoBrushes with Improved Reaction Kinetics of the Tetrazine Ligation for Pretargeted Nuclear Imaging, ACS Nano. 14 (2020) 568–584. doi:10.1021/acsnano.9b06905.
[172] K. Johann, D. Svatunek, C. Seidl, S. Rizzelli, T.A. Bauer, L. Braun, K. Koynov, H. Mikula, M. Barz, Tetrazine- and trans-cyclooctene-functionalised polypept(o)ides for fast bioorthogonal tetrazine ligation, Polym. Chem. 11 (2020) 4396–4407. doi:10.1039/c000660m.
[173] L. Gao, J. Zhou, J. Yu, Q. Li, X. Liu, L. Sun, T. Peng, J. Wang, J. Zhu, J. Sun, W. Lu, L. Yu, Z. Yan, Y. Wang, A Novel Gd-DTPA-conjugated Poly(L-Y-glutamyl-glutamine)-paclitaxel Polymeric Delivery System for Tumor Theranostics, Sci. Rep. 7 (2017) 1–13. doi:10.1038/s41598-017-03633-9.
[174] S. Correa, N. Boehnke, A.E. Barberio, E. Deiss-Yehiely, A. Shi, B. Oberlton, S.G. Smith, I. Zervantonakis, E.C. Dreaden, P.T. Hammond, Tuning Nanoparticle Interactions with Ovarian Cancer through Layer-by-Layer Modification of Surface Chemistry, ACS Nano. 14 (2020) 2224–2237. doi:10.1021/acsnano.9b09213.
[175] S.M. Thombre, B.D. Sarwade, Synthesis and biodegradability of polyaspartic acid: A critical review, J. Macromol. Sci. - Pure Appl. Chem. 42 A (2005) 1299–1315. doi:10.1080/10601320500189604.
[176] C. Di Meo, F. Cilurzo, M. Licciardi, G. Sciallabba, R. Sabia, D. Paolino, D. Capitani, M. Fresta, G. Giammona, C. Villani, P. Matricardi, Polyaspartamide-Doxorubicin Conjugate as Potential Prodrug for Anticancer Therapy, Pharm. Res. 32 (2015) 1557–1569. doi:10.1007/s11095-014-1557-2.
[177] Y. Matsumura, T. Hamaguchi, T. Ura, K. Muro, Y. Yamada, Y. Shimada, K. Shirao, T. Okusaka, H. Ueno, M. Ikeda, N. Watanabe, Phase I clinical trial and pharmacokinetic evaluation of NK911, a micelle-encapsulated doxorubicin, Br. J. Cancer. 91 (2004) 1775–1781. doi:10.1038/sj.bjc.6602204.
[178] H. Cabral, K. Kataoka, Progress of drug-loaded polymeric micelles into clinical studies, J. Control. Release. 190 (2014) 465–476. doi:10.1016/j.jconrel.2014.06.042.
[179] H. Mukai, T. Kogawa, N. Matsubara, Y. Naito, A first-in-human Phase 1 study of epirubicin-conjugated polymer micelles (K-912 / NC-6300) in patients with advanced or recurrent solid tumors, Invest. New Drugs. 35 (2017) 307–314. doi:10.1007/s10637-016-0422-z.
[180] M. Maeda, Y. Muragaki, J. Okamoto, S. Yoshizawa, N. Abe, H. Nakamoto, H. Ishii, K. Kawabata, S. Umemura, N. Nishiyama, K. Kataoka, H. Iseki, Sonodynamic therapy based on combined use of low dose administration of epirubicin-incorporating drug delivery system and focused ultrasound, Ultrasound Med. Biol. 43 (2017) 2295–2301. doi:10.1016/j.ultrasmedbio.2017.06.003.
[181] Y. Yamamoto, I. Hyodo, Y. Koga, R. Tsumura, R. Sato, T. Obonai, H. Fuchigami, F. Furuya, M. Yasunaga, M. Harada, Y. Kato, A. Ohtsu, Y. Matsumura, Enhanced antitumor effect of anti-tissue factor antibody-conjugated epirubicin-incorporating micelles in xenograft models, Cancer Sci. 106 (2015) 627–634. doi:10.1111/cas.12645.
[182] L.L. Tayo, Stimuli-responsive nanocarriers for intracellular delivery, Biophys. Rev. 9 (2017) 931–940.

[183] P. Mi, Stimuli-responsive nanocarriers for drug delivery, tumor imaging, therapy and theranostics, Theranostics. 10 (2020) 4557–4588. doi:10.7150/thno.38069.
[184] H. Takemoto, T. Inaba, T. Nomoto, M. Matsui, X. Liu, M. Toyoda, Y. Honda, K. Taniwaki, N. Yamada, J. Kim, K. Tomoda, N. Nishiyama, Polymeric modification of gemcitabine via cyclic acetal linkage for enhanced anticancer potency with negligible side effects, Biomaterials. 235 (2020) 119804. doi:10.1016/j.biomaterials.2020.119804.
[185] K. Ogawa, A. Ishizaki, K. Takai, Y. Kitamura, T. Kiwada, K. Shiba, A. Odani, Development of novel radiogallium-labeled bone imaging agents using oligo-aspartic acid peptides as carriers, PLoS One. 8 (2013) 1–9. doi:10.1371/journal.pone.0084335.
[186] P. Yuan, Z. Ruan, T. Li, Y. Tian, Q. Cheng, L. Yan, Sharp pH-sensitive amphiphilic polypeptide macrophotosensitizer for near infrared imaging-guided photodynamic therapy, Nanomedicine Nanotechnology, Biol. Med. 15 (2019) 198–207. doi:10.1016/j.nano.2018.09.017.
[187] P.S. Yavvari, S. Gupta, D. Arora, V.K. Nandicoori, A. Srivastava, A. Bajaj, Clathrin-Independent Killing of Intracellular Mycobacteria and Biofilm Disruptions Using Synthetic Antimicrobial Polymers, Biomacromolecules. 18 (2017) 2024–2033. doi:10.1021/acs.biomac.7b00106.
[188] M.S. Saveleva, K. Eftekhari, A. Abalymov, T.E.L. Douglas, D. Volodkin, B. V. Parakhonskiy, A.G. Skirtach, Hierarchy of hybrid materials-the place of inorganics-in-organics in it, their composition and applications, Front. Chem. 7 (2019) 1–21. doi:10.3389/fchem.2019.00179.
[189] R. Xu, G. Zhang, J. Mai, X. Deng, V. Segura-Ibarra, S. Wu, J. Shen, H. Liu, Z. Hu, L. Chen, Y. Huang, E. Koay, Y. Huang, J. Liu, J.F. Ensor, E. Blanco, X. Liu, M. Ferrari, H. Shen, An injectable nanoparticle generator enhances delivery of cancer therapeutics, Nat. Biotechnol. 34 (2016) 414–418. doi:10.1038/nbt.3506.
[190] L. Deng, H. Dong, A. Dong, J. Zhang, A strategy for oral chemotherapy via dual pH-sensitive polyelectrolyte complex nanoparticles to achieve gastric survivability, intestinal permeability, hemodynamic stability and intracellular activity, Eur. J. Pharm. Biopharm. 97 (2015) 107–117. doi:10.1016/j.ejpb.2015.10.010.
[191] M.C. Chen, F.L. Mi, Z.X. Liao, C.W. Hsiao, K. Sonaje, M.F. Chung, L.W. Hsu, H.W. Sung, Recent advances in chitosan-based nanoparticles for oral delivery of macromolecules, Adv. Drug Deliv. Rev. 65 (2013) 865–879. doi:10.1016/j.addr.2012.10.010.
[192] Z. Tai, X. Wang, J. Tian, Y. Gao, L. Zhang, C. Yao, X. Wu, W. Zhang, Q. Zhu, S. Gao, A biodegradable stearylated peptide with internal disulfide bonds for efficient delivery of siRNA in vitro and in vivo, Biomacromolecules. 16 (2015) 1119–1130. doi:10.1021/bm501777a.
[193] C. Yao, J. Liu, X. Wu, Z. Tai, Y. Gao, Q. Zhu, J. Li, L. Zhang, C. Hu, F. Gu, J. Gao, S. Gao, Reducible self-assembling cationic polypeptide-based micelles mediate co-delivery of doxorubicin and microRNA-34a for androgen-independent prostate cancer therapy, J. Control. Release. 232 (2016) 203–214. doi:10.1016/j.jconrel.2016.04.034.
[194] J.J. Arroyo-Crespo, A. Armiñán, D. Charbonnier, L. Balzano-Nogueira, F. Huertas-López, C. Martí, S. Tarazona, J. Forteza, A. Conesa, M.J. Vicent, Tumor microenvironment-targeted poly-L-glutamic acid-based combination conjugate for enhanced triple negative breast cancer treatment, Biomaterials. 186 (2018) 8–21. doi:10.1016/j.biomaterials.2018.09.023.
[195] W. Huang, L. Chen, L. Kang, M. Jin, P. Sun, X. Xin, Z. Gao, Y.H. Bae, Nanomedicine-

based combination anticancer therapy between nucleic acids and small-molecular drugs, Adv. Drug Deliv. Rev. 115 (2017) 82–97. doi:10.1016/j.addr.2017.06.004.
[196] M. Hasan, R.K. Leak, R.E. Stratford, D.P. Zlotos, P.A. Witt-Enderby, Drug conjugates-an emerging approach to treat breast cancer, Pharmacol. Res. Perspect. 6 (2018) e00417. doi:10.1002/prp2.417.
[197] A. Ianevski, A.K. Giri, P. Gautam, A. Kononov, S. Potdar, J. Saarela, K. Wennerberg, T. Aittokallio, Prediction of drug combination effects with a minimal set of experiments, Nat. Mach. Intell. 1 (2019) 568–577. doi:10.1038/s42256-019-0122-4.
[198] T. Pemovska, J.W. Bigenzahn, G. Superti-Furga, Recent advances in combinatorial drug screening and synergy scoring, Curr. Opin. Pharmacol. 42 (2018) 102–110. doi:10.1016/j.coph.2018.07.008.
[199] L. Miao, S. Guo, C.M. Lin, Q. Liu, L. Huang, Nanoformulations for combination or cascade anticancer therapy, Adv. Drug Deliv. Rev. 115 (2017) 3–22. doi:10.1016/j.addr.2017.06.003.
[200] F. Greco, M.J. Vicent, Polymer-drug conjugates: current status and future trends, Front. Biosci. 13 (2008) 2744–2756.
[201] F. Greco, M.J. Vicent, Combination therapy : Opportunities and challenges for polymer – drug conjugates as anticancer nanomedicines, Adv. Drug Deliv. Rev. 61 (2009) 1203–1213. doi:10.1016/j.addr.2009.07.006.
[202] X. Xu, W. Ho, X. Zhang, N. Bertrand, O. Farokhzad, Cancer nanomedicine: From targeted delivery to combination therapy, Trends Mol. Med. 21 (2015) 223–232. doi:10.1016/j.molmed.2015.01.001.
[203] M. Zhang, E. Liu, Y. Cui, Y. Huang, Nanotechnology-based combination therapy for overcoming multidrug-resistant cancer, Cancer Biol. Med. 14 (2017) 212–227. doi:10.20892/j.issn.2095-3941.2017.0054.
[204] T. Lammers, V. Subr, K. Ulbrich, W.E. Hennink, G. Storm, F. Kiessling, Polymeric nanomedicines for image-guided drug delivery and tumor-targeted combination therapy, Nano Today. 5 (2010) 197–212. doi:10.1016/j.nantod.2010.05.001.
[205] L.B. Vong, N.-T. Trinh, Y. Nagasaki, Design of amino acid-based self-assembled nano-drugs for therapeutic applications, J. Control. Release. 326 (2020) 140–149. doi:10.1016/j.jconrel.2020.06.009.
[206] M.J. Vicent, F. Greco, R.I. Nicholson, A. Paul, P.C. Griffiths, R. Duncan, Polymer therapeutics designed for a combination therapy of hormone-dependent cancer, Angew. Chemie - Int. Ed. 44 (2005) 4061–4066. doi:10.1002/anie.200462960.
[207] E. Markovsky, H. Baabur-Cohen, R. Satchi-Fainaro, Anticancer polymeric nanomedicine bearing synergistic drug combination is superior to a mixture of individually-conjugated drugs, J. Control. Release. 187 (2014) 145–157. doi:10.1016/j.jconrel.2014.05.025.
[208] Z. Eroglu, A. Ribas, Combination therapy with BRAF and MEK inhibitors for melanoma: Latest evidence and place in therapy, Ther. Adv. Med. Oncol. 8 (2016) 48–56. doi:10.1177/1758834015616934.
[209] I. Noh, H.O. Kim, J. Choi, Y. Choi, D.K. Lee, Y.M. Huh, S. Haam, Co-delivery of paclitaxel and gemcitabine via CD44-targeting nanocarriers as a prodrug with synergistic antitumor activity against human biliary cancer, Biomaterials. 53 (2015) 763–774. doi:10.1016/j.biomaterials.2015.03.006.
[210] W. Sun, X. Chen, C. Xie, Y. Wang, L. Lin, K. Zhu, X. Shuai, Co-Delivery of Doxorubicin and Anti-BCL-2 siRNA by pH-Responsive Polymeric Vector to Overcome Drug

Resistance in In Vitro and in Vivo HepG2 Hepatoma Model, Biomacromolecules. 19 (2018) 2248–2256. doi:10.1021/acs.biomac.8b00272.
[211] X. Zhou, Q. Zheng, C. Wang, J. Xu, J.P. Wu, T.B. Kirk, D. Ma, W. Xue, Star-Shaped Amphiphilic Hyperbranched Polyglycerol Conjugated with Dendritic Poly(l -lysine) for the Codelivery of Docetaxel and MMP-9 siRNA in Cancer Therapy, ACS Appl. Mater. Interfaces. 8 (2016) 12609–12619. doi:10.1021/acsami.6b01611.
[212] A. Kavand, N. Anton, T. Vandamme, A. Serra, D. Chan-seng, Synthesis and functionalization of hyperbranched polymers for targeted drug delivery, J. Control. Release. 321 (2020) 285–311. doi:10.1016/j.jconrel.2020.02.019.
[213] X. Liu, W. Gao, Precision Conjugation: An Emerging Tool for Generating Protein-Polymer Conjugates, Angew. Chemie Int. Ed. in press (2020). doi:10.1002/anie.202003708.
[214] L. Milane, S. Ganesh, S. Shah, Z.F. Duan, M. Amiji, Multi modal strategies for overcoming tumor drug resistance: Hypoxia, the Warburg effect, stem cells, and multifunctional nanotechnology, J. Control. Release. 155 (2011) 237–247. doi:10.1016/j.jconrel.2011.03.032.
[215] K. Praveen, S. Das, V. Dhaware, B. Pandey, B. Mondal, S. Sen Gupta, pH-Responsive "Supra-Amphiphilic" Nanoparticles Based on Homoarginine Polypeptides, ACS Appl. Bio Mater. 2 (2019) 4162–4172. doi:10.1021/acsabm.9b00432.
[216] N. Deirram, C. Zhang, S.S. Kermaniyan, A.P.R. Johnston, G.K. Such, pH-Responsive Polymer Nanoparticles for Drug Delivery, Macromol. Rapid Commun. 40 (2019) 1800917. doi:10.1002/marc.201800917.
[217] J. Kalia, R.T. Raines, Hydrolytic stability of hydrazones and oximes, Angew. Chemie - Int. Ed. 47 (2008) 7523–7526. doi:10.1002/anie.200802651.
[218] F. Seidi, R. Jenjob, D. Crespy, Designing Smart Polymer Conjugates for Controlled Release of Payloads, Chem. Rev. 118 (2018) 3965–4036. doi:10.1021/acs.chemrev.8b00006.
[219] F.A. Carey, R.J. Sundberg, Advanced Organic Chemistry Part A: Structure and Mechanisms, 2007. doi:10.1021/ed065pA139.2.
[220] P.T. Wong, S.K. Choi, Mechanisms of Drug Release in Nanotherapeutic Delivery Systems, Chem. Rev. 115 (2015) 3388–3432. doi:10.1021/cr5004634.
[221] S. Ma, W. Song, Y. Xu, X. Si, D. Zhang, S. Lv, C. Yang, L. Ma, Z. Tang, X. Chen, Neutralizing tumor-promoting inflammation with polypeptide-dexamethasone conjugate for microenvironment modulation and colorectal cancer therapy, Biomaterials. 232 (2020) 119676. doi:10.1016/j.biomaterials.2019.119676.
[222] C.M. Overall, O. Kleifeld, Validating matrix metalloproteinases as drug targets and anti-targets for cancer therapy, Nat. Rev. Cancer. 6 (2006) 227–239. doi:10.1038/nrc1821.
[223] G. Murphy, H. Nagase, Reappraising metalloproteinases in rheumatoid arthritis and osteoarthritis: Destruction or repair?, Nat. Clin. Pract. Rheumatol. 4 (2008) 128–135. doi:10.1038/ncprheum0727.
[224] R. de la Rica, D. Aili, M.M. Stevens, Enzyme-responsive nanoparticles for drug release and diagnostics, Adv. Drug Deliv. Rev. 64 (2012) 967–978. doi:10.1016/j.addr.2012.01.002.
[225] Q. Hu, P.S. Katti, Z. Gu, Enzyme-responsive nanomaterials for controlled drug delivery, Nanoscale. 6 (2014) 12273–12286. doi:10.1039/c4nr04249b.
[226] Y. Ding, Y. Kang, X. Zhang, Enzyme-responsive polymer assemblies constructed

through covalent synthesis and supramolecular strategy, Chem. Commun. 51 (2015) 996–1003. doi:10.1039/c4cc05878j.

[227] W.A.R. Van Heeswijk, C.J.T. Hoes, T. Stoffer, M.J.D. Eenink, W. Potman, J. Feijen, The synthesis and characterization of polypeptide-adriamycin conjugates and its complexes with adriamycin. Part I, J. Control. Release. 1 (1985) 301–315. doi:10.1016/0168-3659(85)90006-9.

[228] N. Aggarwal, B.F. Sloane, Cathepsin B: Multiple roles in cancer, Proteomics - Clin. Appl. 8 (2014) 427–437. doi:10.1002/prca.201300105.

[229] A. Benchoua, J. Braudeau, A. Reis, C. Couriaud, B. Onténiente, Activation of proinflammatory caspases by cathepsin B in focal cerebral ischemia, J. Cereb. Blood Flow Metab. 24 (2004) 1272–1279. doi:10.1097/01.WCB.0000140272.54583.FB.

[230] N.J. Leong, D. Mehta, V.M. McLeod, B.D. Kelly, R. Pathak, D.J. Owen, C.J.H. Porter, L.M. Kaminskas, Doxorubicin Conjugation and Drug Linker Chemistry Alter the Intravenous and Pulmonary Pharmacokinetics of a PEGylated Generation 4 Polylysine Dendrimer in Rats, J. Pharm. Sci. 107 (2018) 2509–2513. doi:10.1016/j.xphs.2018.05.013.

[231] H. Pan, P. Kopečková, D. Wang, J. Yang, S. Miller, J. Kopeček, Water-soluble HPMA copolymer - Prostaglandin E1 conjugates containing a cathepsin K sensitive spacer, J. Drug Target. 14 (2006) 425–435. doi:10.1080/10611860600834219.

[232] G. Bonzi, S. Salmaso, A. Scomparin, A. Eldar-Boock, R. Satchi-Fainaro, P. Caliceti, Novel Pullulan Bioconjugate for Selective Breast Cancer Bone Metastases Treatment, Bioconjug. Chem. 26 (2015) 489–501. doi:10.1021/bc500614b.

[233] E. Segal, H. Pan, P. Ofek, T. Udagawa, P. Kopečková, J. Kopeček, R. Satchi-Fainaro, Targeting angiogenesis-dependent calcified neoplasms using combined polymer therapeutics, PLoS One. 4 (2009). doi:10.1371/journal.pone.0005233.

[234] S.O. Yoon, S.J. Park, C.H. Yun, A.S. Chung, Roles of matrix metalloproteinases in tumor metastasis and angiogenesis, J. Biochem. Mol. Biol. 36 (2003) 128–137. doi:10.5483/bmbrep.2003.36.1.128.

[235] U. Mahmood, C.H. Tung, A. Bogdanov, R. Weissleder, Near-infrared optical imaging of protease activity for tumor detection, Radiology. 213 (1999) 866–870. doi:10.1148/radiology.213.3.r99dc14866.

[236] R. Weissleder, C.H. Tung, U. Mahmood, A. Bogdanov, In vivo imaging of tumors with protease-activated near-infrared fluorescent probes, Nat. Biotechnol. 17 (1999) 375–378. doi:10.1038/7933.

[237] C.H. Tung, U. Mahmood, S. Bredow, R. Weissleder, In vivo imaging of proteolytic enzyme activity using a novel molecular reporter, Cancer Res. 60 (2000) 4953–4958.

[238] K. Tsuchikama, Z. An, Antibody-drug conjugates: recent advances in conjugation and linker chemistries, Protein Cell. 9 (2018) 33–46. doi:10.1007/s13238-016-0323-0.

[239] V. Taresco, C. Alexander, N. Singh, A.K. Pearce, Stimuli-Responsive Prodrug Chemistries for Drug Delivery, Adv. Ther. 1 (2018) 1800030. doi:10.1002/adtp.201800030.

[240] B. Klahan, F. Seidi, D. Crespy, Oligo(thioether-ester)s Blocks in Polyurethanes for Slowly Releasing Active Payloads, Macromol. Chem. Phys. 219 (2018) 1–9. doi:10.1002/macp.201800392.

[241] H.J. Jin, J. Lu, X. Wu, Development of a new enzyme-responsive self-immolative spacer conjugate applicable to the controlled drug release, Bioorganic Med. Chem. 20 (2012) 3465–3469. doi:10.1016/j.bmc.2012.04.012.

[242] L. Zhang, Y. Liu, K. Zhang, Y. Chen, X. Luo, Redox-responsive comparison of diselenide micelles with disulfide micelles, Colloid Polym. Sci. 297 (2019) 225–238. doi:10.1007/s00396-018-4457-x.
[243] J.H. Ha, D.Y. Lee, S.H. Lee, C.O. Yun, Y.C. Kim, Development of apoptosis-inducing polypeptide via simultaneous mitochondrial membrane disruption and Ca2+ delivery, Biomaterials. 197 (2019) 51–59. doi:10.1016/j.biomaterials.2019.01.006.
[244] C.H. Chen, M.L. Kuo, J.L. Wang, W.C. Liao, L.C. Chang, L.P. Chan, J. Lin, CCM-AMI, a polyethylene glycol micelle with amifostine, as an acute radiation syndrome protectant in C57BL/6 mice, Health Phys. 109 (2015) 242–248. doi:10.1097/HP.0000000000000326.
[245] C. Hui Wang, C. Yi Cheng, C.H. Chen, W. Chuan Liao, J. Lin, Chelating Complex Micelles for Delivering Cytoprotectant Amifostine and its Application in Radiation Protection, J. Pharmacovigil. 06 (2018) 3–8. doi:10.4172/2329-6887.1000263.
[246] C.A. Weeks, B. Aden, S.M. Kilbey, A. V. Janorkar, Synthesis and Characterization of an Array of Elastin-like Polypeptide-Polyelectrolyte Conjugates with Varying Chemistries and Amine Content for Biomedical Applications, ACS Biomater. Sci. Eng. 2 (2016) 2196–2206. doi:10.1021/acsbiomaterials.6b00393.
[247] P.A. Hassan, G. Verma, R. Ganguly, Soft materials-properties and applications, in: Funct. Mater., 2012. doi:10.1016/B978-0-12-385142-0.00001-5.
[248] S. Sinha, D. Vohora, Pharmaceutical Medici, Elsevier Inc., 2018. doi:10.1016/B978-0-12-802103-3.00002-X.
[249] S.C. Gad, S.C. Gad, Introduction: Drug Discovery in the 21 st Century , Pharm. Sci. Encycl. (2010). doi:10.1002/9780470571224.pse001.
[250] R.Y.C. Huang, G. Chen, Characterization of antibody-drug conjugates by mass spectrometry: Advances and future trends, Drug Discov. Today. 21 (2016) 850–855. doi:10.1016/j.drudis.2016.04.004.
[251] B. Gorovits, R. Pillutla, Emerging Bioanalytical Methods for the Bioanalysis of Biotherapeutics, Third Edit, Elsevier, 2017. doi:10.1016/b978-0-12-409547-2.12418-7.
[252] I. van den Broek, W.M.A. Niessen, W.D. van Dongen, Bioanalytical LC-MS/MS of protein-based biopharmaceuticals, J. Chromatogr. B Anal. Technol. Biomed. Life Sci. 929 (2013) 161–179. doi:10.1016/j.jchromb.2013.04.030.
[253] and T.G.H. Stig Pedersen-Bjergaard , Bente Gammelgaard, Introduction to pharmaceutical analytical chemistry, Wiley, 2019.
[254] A. Niño-pariente, V.J. Nebot, M.J. Vicent, M.J. Vicent, Relevant Physicochemical Descriptors of “Soft Nanomedicines” to Bypass Biological Barriers, Curr. Pharm. Des. 22 (2016) 1274–1291. doi:10.2174/1381612822666151216152143.
[255] J. Kopeček, Polymer-drug conjugates: Origins, progress to date and future directions, Adv. Drug Deliv. Rev. 65 (2013) 49–59. doi:10.1016/j.addr.2012.10.014.
[256] F. Greco, M.J. Vicent, Combination therapy: Opportunities and challenges for polymer-drug conjugates as anticancer nanomedicines, Adv. Drug Deliv. Rev. 61 (2009) 1203–1213. doi:10.1016/j.addr.2009.05.006.
[257] B.S.P. Bentham Science Publisher, Investigation of Drug Delivery Behaviors by NMR Spectroscopy, Struct. Relatsh. Stud. Drug Dev. by NMR Spectrosc. (2012) 36–66. doi:10.2174/978160805164911101010036.
[258] K. Saalwächter, H.W. Spiess, Solid-State NMR of Polymers, in: Polym. Sci. A Compr. Ref. 10 Vol. Set, 2012. doi:10.1016/B978-0-444-53349-4.00025-X.
[259] J.H. Ardenkjaer-Larsen, G.S. Boebinger, A. Comment, S. Duckett, A.S. Edison, F.

Engelke, C. Griesinger, R.G. Griffin, C. Hilty, H. Maeda, G. Parigi, T. Prisner, E. Ravera, J. Van Bentum, S. Vega, A. Webb, C. Luchinat, H. Schwalbe, L. Frydman, Facing and Overcoming Sensitivity Challenges in Biomolecular NMR Spectroscopy, Angew. Chemie - Int. Ed. 54 (2015) 9162–9185. doi:10.1002/anie.201410653.

[260] U. Holzgrabe, B. Diehl, I. Wawer, NMR Spectroscopy in Pharmaceutical Analysis, 2008. doi:10.1016/B978-0-444-53173-5.X0001-7.

[261] S. Cai, C. Seu, Z. Kovacs, A.D. Sherry, Y. Chen, Sensitivity enhancement of multidimensional NMR experiments by paramagnetic relaxation effects, J. Am. Chem. Soc. (2006). doi:10.1021/ja0634526.

[262] S. Hiller, G. Wider, T. Etezady-Esfarjani, R. Horst, K. Wüthrich, Managing the solvent water polarization to obtain improved NMR spectra of large molecular structures, J. Biomol. NMR. (2005). doi:10.1007/s10858-005-3070-8.

[263] G. Otting, Prospects for lanthanides in structural biology by NMR, J. Biomol. NMR. (2008). doi:10.1007/s10858-008-9256-0.

[264] D. Marion, Combining methods for speeding up multi-dimensional acquisition. Sparse sampling and fast pulsing methods for unfolded proteins, J. Magn. Reson. (2010). doi:10.1016/j.jmr.2010.06.007.

[265] P. Schanda, H. Van Melckebeke, B. Brutscher, Speeding up three-dimensional protein NMR experiments to a few minutes, J. Am. Chem. Soc. (2006). doi:10.1021/ja062025p.

[266] T. Fujiwara, A. Ramamoorthy, How Far Can the Sensitivity of NMR Be Increased?, Annu. Reports NMR Spectrosc. (2006). doi:10.1016/S0066-4103(05)58003-7.

[267] J.M. Franck, S. Han, Overhauser Dynamic Nuclear Polarization for the Study of Hydration Dynamics, Explained, in: Methods Enzymol., 2019. doi:10.1016/bs.mie.2018.09.024.

[268] M. Ragavan, H.Y. Chen, G. Sekar, C. Hilty, Solution NMR of polypeptides hyperpolarized by dynamic nuclear polarization, Anal. Chem. 83 (2011) 6054–6059. doi:10.1021/ac201122k.

[269] Z. Pang, H. Guan, L. Gao, W. Cao, J. Yin, X. Kong, Fundamentals and applications of NMR hyperpolarization techniques, Wuli Huaxue Xuebao/ Acta Phys. - Chim. Sin. (2019). doi:10.3866/PKU.WHXB201906018.

[270] R.A. Green, R.W. Adams, S.B. Duckett, R.E. Mewis, D.C. Williamson, G.G.R. Green, The theory and practice of hyperpolarization in magnetic resonance using parahydrogen, Prog. Nucl. Magn. Reson. Spectrosc. (2012). doi:10.1016/j.pnmrs.2012.03.001.

[271] B.J. Albert, C. Gao, E.L. Sesti, E.P. Saliba, N. Alaniva, F.J. Scott, S.T. Sigurdsson, A.B. Barnes, Dynamic Nuclear Polarization Nuclear Magnetic Resonance in Human Cells Using Fluorescent Polarizing Agents, Biochemistry. (2018). doi:10.1021/acs.biochem.8b00257.

[272] D.I. Hoult, R.E. Richards, The signal-to-noise ratio of the nuclear magnetic resonance experiment, J. Magn. Reson. (1976). doi:10.1016/0022-2364(76)90233-X.

[273] T.M. De Swiet, Optimal electric fields for different sample shapes in high resolution NMR spectroscopy, J. Magn. Reson. (2005). doi:10.1016/j.jmr.2005.02.007.

[274] J.D. Martin, M. Panagi, C. Wang, T.T. Khan, M.R. Martin, C. Voutouri, K. Toh, P. Papageorgis, F. Mpekris, C. Polydorou, G. Ishii, S. Takahashi, N. Gotohda, T. Suzuki, M.E. Wilhelm, V.A. Melo, S. Quader, J. Norimatsu, R.M. Lanning, M. Kojima, M.D. Stuber, T. Stylianopoulos, K. Kataoka, H. Cabral, Dexamethasone Increases Cisplatin-Loaded Nanocarrier Delivery and Efficacy in Metastatic Breast Cancer by Normalizing

the Tumor Microenvironment, ACS Nano. (2019). doi:10.1021/acsnano.8b07865.
[275] Z. Song, Z. Han, S. Lv, C. Chen, L. Chen, L. Yin, J. Cheng, Synthetic polypeptides: From polymer design to supramolecular assembly and biomedical application, Chem. Soc. Rev. (2017). doi:10.1039/c7cs00460e.
[276] C. Yang, W. Song, D. Zhang, H. Yu, L. Yin, N. Shen, M. Deng, Z. Tang, J. Gu, X. Chen, Poly (L-glutamic acid)-g-methoxy poly (ethylene glycol)-gemcitabine conjugate improves the anticancer efficacy of gemcitabine, Int. J. Pharm. (2018). doi:10.1016/j.ijpharm.2018.08.037.
[277] M. Wang, C. Zhou, J. Chen, Y. Xiao, J. Du, Multifunctional biocompatible and biodegradable folic acid conjugated poly(ε-caprolactone)-polypeptide copolymer vesicles with excellent antibacterial activities, Bioconjug. Chem. (2015). doi:10.1021/acs.bioconjchem.5b00061.
[278] Z. Wang, Q. He, W. Zhao, J. Luo, W. Gao, Tumor-homing, pH- and ultrasound-responsive polypeptide-doxorubicin nanoconjugates overcome doxorubicin resistance in cancer therapy, J. Control. Release. (2017). doi:10.1016/j.jconrel.2017.08.017.
[279] I. Conejos-Sánchez, I. Cardoso, M. Oteo-Vives, E. Romero-Sanz, A. Paul, A.R. Sauri, M.A. Morcillo, M.J. Saraiva, M.J. Vicent, Polymer-doxycycline conjugates as fibril disrupters: An approach towards the treatment of a rare amyloidotic disease, J. Control. Release. 198 (2015) 80–90. doi:10.1016/j.jconrel.2014.12.003.
[280] ICH Harmonised Tripartite Guideline, Stability testing of new drug substances and products Q1A(R2), (2003). https://database.ich.org/sites/default/files/Q1A%28R2%29 Guideline.pdf.
[281] O. Zagorodko, V.J. Nebot, M.J. Vicent, The generation of stabilized supramolecular nanorods from star-shaped polyglutamates, Polym. Chem. 11 (2020) 1220–1229. doi:10.1039/c9py01442j.
[282] A. Niño-Pariente, A. Armiñán, S. Reinhard, C. Scholz, E. Wagner, M.J. Vicent, Design of Poly-l-Glutamate-Based Complexes for pDNA Delivery, Macromol. Biosci. 17 (2017) 1–15. doi:10.1002/mabi.201700029.
[283] J.B. Guilbaud, A. Saiani, Using small angle scattering (SAS) to structurally characterise peptide and protein self-assembled materials, Chem. Soc. Rev. (2011). doi:10.1039/c0cs00105h.
[284] A. Saiani, A. Mohammed, H. Frielinghaus, R. Collins, N. Hodson, C.M. Kielty, M.J. Sherratt, A.F. Miller, Self-assembly and gelation properties of α-helix versus β-sheet forming peptides, Soft Matter. (2009). doi:10.1039/b811288f.
[285] H. Yu, Y. Huang, Q. Huang, Synthesis and characterization of novel antimicrobial emulsifiers from ε-Polylysine, J. Agric. Food Chem. (2010). doi:10.1021/jf903300m.
[286] J. Lai, Y. Huang, Fibril aggregates of the poly(glutamic acid)-drug conjugate, RSC Adv. (2015). doi:10.1039/c5ra06755c.
[287] R.J. Nevagi, W. Dai, Z.G. Khalil, W.M. Hussein, R.J. Capon, M. Skwarczynski, I. Toth, Self-assembly of trimethyl chitosan and poly(anionic amino acid)-peptide antigen conjugate to produce a potent self-adjuvanting nanovaccine delivery system, Bioorganic Med. Chem. (2019). doi:10.1016/j.bmc.2019.05.033.
[288] M.N. Zhou, C.S. Delaveris, J.R. Kramer, J.A. Kenkel, E.G. Engleman, C.R. Bertozzi, N-Carboxyanhydride Polymerization of Glycopolypeptides That Activate Antigen-Presenting Cells through Dectin-1 and Dectin-2, Angew. Chemie - Int. Ed. 57 (2018) 3137–3142. doi:10.1002/anie.201713075.

[289] B. Tian, X. Tao, T. Ren, Y. Weng, X. Lin, Y. Zhang, X. Tang, Polypeptide-based vesicles: Formation, properties and application for drug delivery, J. Mater. Chem. (2012). doi:10.1039/c2jm31806g.
[290] S. Bleher, J. Buck, C. Muhl, S. Sieber, S. Barnert, D. Witzigmann, J. Huwyler, M. Barz, R. Süss, Poly(Sarcosine) Surface Modification Imparts Stealth-Like Properties to Liposomes, Small. 15 (2019) 1904716. doi:10.1002/smll.201904716.
[291] C. Muhl, M. Conrad, D. Unthan, M. Barz, Synthesis and characterization of bisalkylated polysarcosine-based lipopolymers, Eur. Polym. J. (2019). doi:10.1016/j.eurpolymj.2019.109223.
[292] C.J. Fee, J.M. Van Alstine, Prediction of the viscosity radius and the size exclusion chromatography behavior of PEGylated proteins, in: Bioconjug. Chem., 2004. doi:10.1021/bc049843w.
[293] D. Schwiertz, R. Holm, M. Barz, Facile synthesis of amphiphilic AB3 and A3B miktoarm PeptoMiktoStars, Polym. J. (2020). doi:10.1038/s41428-019-0269-1.
[294] J. Yao, P. He, Y. Zhang, H. Zhang, P. Zhang, M. Deng, C. Xiao, PEGylated polylysine derived copolymers with reduction-responsive side chains for anticancer drug delivery, Polym. Int. 68 (2019) 1817–1825. doi:10.1002/pi.5892.
[295] X. Gu, M. Qiu, H. Sun, J. Zhang, L. Cheng, C. Deng, Z. Zhong, Polytyrosine nanoparticles enable ultra-high loading of doxorubicin and rapid enzyme-responsive drug release, Biomater. Sci. 6 (2018) 1526–1534. doi:10.1039/c8bm00243f.
[296] H. Cölfen, M. Antonietti, Field-flow fractionation techniques for polymer and colloid analysis, Adv. Polym. Sci. (2000). doi:10.1007/3-540-48764-6_2.
[297] F. Caputo, J. Clogston, L. Calzolai, M. Rösslein, A. Prina-Mello, Measuring particle size distribution of nanoparticle enabled medicinal products, the joint view of EUNCL and NCI-NCL. A step by step approach combining orthogonal measurements with increasing complexity, J. Control. Release. (2019). doi:10.1016/j.jconrel.2019.02.030.
[298] K. Rebolj, D. Pahovnik, E. Žagar, Characterization of a protein conjugate using an asymmetrical-flow field-flow fractionation and a size-exclusion chromatography with multi-detection system, Anal. Chem. 84 (2012) 7374–7383. doi:10.1021/ac3010378.
[299] P.S. Williams, F. Carpino, M. Zborowski, Characterization of magnetic nanoparticles using programmed quadrupole magnetic field-flow fractionation, in: Philos. Trans. R. Soc. A Math. Phys. Eng. Sci., 2010. doi:10.1098/rsta.2010.0133.
[300] T. Orita, L.R. Moore, P. Joshi, M. Tomita, T. Horiuchi, M. Zborowski, A quantitative determination of magnetic nanoparticle separation using on-off field operation of quadrupole magnetic field-flow fractionation (QMgFFF), Anal. Sci. (2013). doi:10.2116/analsci.29.761.
[301] F. Carpino, L.R. Moore, M. Zborowski, J.J. Chalmers, P.S. Williams, Analysis of magnetic nanoparticles using quadrupole magnetic field-flow fractionation, in: J. Magn. Magn. Mater., 2005. doi:10.1016/j.jmmm.2005.01.071.
[302] P.S. Williams, F. Carpino, M. Zborowski, Magnetic nanoparticle drug carriers and their study by quadrupole magnetic field-flow fractionation, in: Mol. Pharm., 2009. doi:10.1021/mp900018v.
[303] N. Faisant, S. Battu, F. Senftleber, J.P. Benoit, P.J.P. Cardot, Sedimentation field-flow fractionation and granulometric analysis of PLGA microspheres, J. Sep. Sci. (2003). doi:10.1002/jssc.200301516.
[304] C. Contado, E. Vighi, A. Dalpiaz, E. Leo, Influence of secondary preparative parameters and aging effects on PLGA particle size distribution: A sedimentation field flow

fractionation investigation, Anal. Bioanal. Chem. (2013). doi:10.1007/s00216-012-6113-5.
[305] S.K. Ratanathanawongs Williams, D. Lee, Field-flow fractionation of proteins polysaccharides, synthetic polymers, and supramolecular assemblies, J. Sep. Sci. (2006). doi:10.1002/jssc.200600151.
[306] M. Wagner, S. Holzschuh, A. Traeger, A. Fahr, U.S. Schubert, Asymmetric flow field-flow fractionation in the field of nanomedicine, Anal. Chem. 86 (2014) 5201–5210. doi:10.1021/ac501664t.
[307] S. Boye, D. Appelhans, V. Boyko, S. Zschoche, H. Komber, P. Friedel, P. Formanek, A. Janke, B.I. Voit, A. Lederer, PH-triggered aggregate shape of different generations lysine-dendronized maleimide copolymers with maltose shell, Biomacromolecules. (2012). doi:10.1021/bm301489s.
[308] Z. Kuklenyik, M.S. Gardner, B.A. Parks, D.M. Schieltz, J.C. Rees, L.G. Mcwilliams, Y.M. Williamson, J.L. Pirkle, J.R. Barr, Multivariate DoE Optimization of Asymmetric Flow Field Flow of Lipoprotein Subclasses, (2015) 96–117. doi:10.3390/chromatography2010096.
[309] A. Zattoni, D. Melucci, G. Torsi, P. Reschiglian, Quantitative analysis in field-flow fractionation using ultraviolet-visible detectors: An experimental design for absolute measurements, J. Chromatogr. Sci. 38 (2000) 122–128. doi:10.1093/chromsci/38.3.122.
[310] A.A. Galyean, J.J. Filliben, R.D. Holbrook, M.N. Vreeland, H.S. Weinberg, Asymmetric flow field flow fractionation with light scattering detection – an orthogonal sensitivity analysis, J. Chromatogr. A. 1473 (2016) 122–132. doi:10.1016/j.chroma.2016.10.063.
[311] A. Lederer, S. Boye, Asymmetrical flow field flow fractionation for investigating intermolecular interactions of multifunctional polymers, LC GC Eur. (2011).
[312] S. López-Sanz, N.R. Fariñas, R. del C.R. Martín-Doimeadios, Á. Ríos, Analytical strategy based on asymmetric flow field flow fractionation hyphenated to ICP-MS and complementary techniques to study gold nanoparticles transformations in cell culture medium, Anal. Chim. Acta. (2019). doi:10.1016/j.aca.2018.11.053.
[313] A. Engel, M. Plöger, D. Mulac, K. Langer, Asymmetric flow field-flow fractionation (AF4) for the quantification of nanoparticle release from tablets during dissolution testing, Int. J. Pharm. (2014). doi:10.1016/j.ijpharm.2013.11.044.
[314] L. Diaz, C. Peyrot, K.J. Wilkinson, Characterization of Polymeric Nanomaterials Using Analytical Ultracentrifugation, Environ. Sci. Technol. (2015). doi:10.1021/acs.est.5b00243.
[315] D. Mehn, P. Iavicoli, N. Cabaleiro, S.E. Borgos, F. Caputo, O. Geiss, L. Calzolai, F. Rossi, D. Gilliland, Analytical ultracentrifugation for analysis of doxorubicin loaded liposomes, Int. J. Pharm. (2017). doi:10.1016/j.ijpharm.2017.03.046.
[316] S. Gioria, F. Caputo, P. Urbán, C.M. Maguire, S. Bremer-Hoffmann, A. Prina-Mello, L. Calzolai, D. Mehn, Are existing standard methods suitable for the evaluation of nanomedicines: Some case studies, Nanomedicine. (2018). doi:10.2217/nnm-2017-0338.
[317] F. Groell, O. Jordan, G. Borchard, In vitro models for immunogenicity prediction of therapeutic proteins, Eur. J. Pharm. Biopharm. 130 (2018) 128–142. doi:10.1016/j.ejpb.2018.06.008.
[318] A.S. Rosenberg, Z.E. Sauna, Immunogenicity assessment during the development of protein therapeutics, J. Pharm. Pharmacol. 70 (2018) 584–594.

doi:10.1111/jphp.12810.
[319] B.C. Evans, C.E. Nelson, S.S. Yu, K.R. Beavers, A.J. Kim, H. Li, H.M. Nelson, T.D. Giorgio, C.L. Duvall, Ex vivo red blood cell hemolysis assay for the evaluation of pH-responsive endosomolytic agents for cytosolic delivery of biomacromolecular drugs., J. Vis. Exp. (2013) 6–10. doi:10.3791/50166.
[320] S. Chen, L. Rong, Q. Lei, P.X. Cao, S.Y. Qin, D.W. Zheng, H.Z. Jia, J.Y. Zhu, S.X. Cheng, R.X. Zhuo, X.Z. Zhang, A surface charge-switchable and folate modified system for co-delivery of proapoptosis peptide and p53 plasmid in cancer therapy, Biomaterials. 77 (2016) 149–163. doi:10.1016/j.biomaterials.2015.11.013.
[321] G. Becker, S. Winzen, T. Steinbach, K. Mohr, F.R. Wurm, Protein adsorption is required for stealth effect of stealth effect of nanocarriers, Nat. Nanotechnol. (2015). doi:10.1038/NNANO.2015.330.
[322] B. Weber, C. Seidl, D. Schwiertz, M. Scherer, S. Bleher, F. Süss, M. Barz, Polysarcosine-based lipids: From lipopolypeptoid micelles to stealth-like lipids in Langmuir Blodgett monolayers, Polymers (Basel). (2016). doi:10.3390/polym8120427.
[323] V. Torrisi, A. Graillot, L. Vitorazi, Q. Crouzet, G. Marletta, C. Loubat, J.F. Berret, Preventing corona effects: Multiphosphonic acid poly(ethylene glycol) copolymers for stable stealth iron oxide nanoparticles, Biomacromolecules. (2014). doi:10.1021/bm500832q.
[324] J.R. Wingard, M.H. White, E. Anaissie, J. Raffalli, J. Goodman, A. Arrieta, A Randomized, Double-Blind Comparative Trial Evaluating the Safety of Liposomal Amphotericin B versus Amphotericin B Lipid Complex in the Empirical Treatment of Febrile Neutropenia, Clin. Infect. Dis. (2000). doi:10.1086/317451.
[325] L. Papafilippou, A. Claxton, P. Dark, K. Kostarelos, M. Hadjidemetriou, Protein corona fingerprinting to differentiate sepsis from non-infectious systemic inflammation, Nanoscale. (2020). doi:10.1039/d0nr02788j.
[326] N. Bertrand, P. Grenier, M. Mahmoudi, E.M. Lima, E.A. Appel, F. Dormont, J.M. Lim, R. Karnik, R. Langer, O.C. Farokhzad, Mechanistic understanding of in vivo protein corona formation on polymeric nanoparticles and impact on pharmacokinetics, Nat. Commun. (2017). doi:10.1038/s41467-017-00600-w.
[327] E. Casals, T. Pfaller, A. Duschl, G.J. Oostingh, V. Puntes, Time evolution of the nanoparticle protein corona, ACS Nano. (2010). doi:10.1021/nn901372t.
[328] D. Wang, S.S. El-Amouri, M. Dai, C.Y. Kuan, D.Y. Hui, R.O. Brady, D. Pan, Engineering a lysosomal enzyme with a derivative of receptor-binding domain of apoE enables delivery across the blood-brain barrier, Proc. Natl. Acad. Sci. U. S. A. (2013). doi:10.1073/pnas.1222742110.
[329] V. Mirshafiee, R. Kim, S. Park, M. Mahmoudi, M.L. Kraft, Impact of protein pre-coating on the protein corona composition and nanoparticle cellular uptake, Biomaterials. (2016). doi:10.1016/j.biomaterials.2015.10.019.
[330] Z. Zhang, J. Guan, Z. Jiang, Y. Yang, J. Liu, W. Hua, Y. Mao, C. Li, W. Lu, J. Qian, C. Zhan, Brain-targeted drug delivery by manipulating protein corona functions, Nat. Commun. (2019). doi:10.1038/s41467-019-11593-z.
[331] F. Greco, M.J. Vicent, N.A. Penning, R.I. Nicholson, R. Duncan, HPMA copolymer-aminoglutethimide conjugates inhibit aromatase in MCF-7 cell lines, J. Drug Target. 13 (2005) 459–470. doi:10.1080/10611860500383788.
[332] W. Song, Z. Tang, N. Shen, H. Yu, Y. Jia, D. Zhang, J. Jiang, C. He, H. Tian, X. Chen, Combining disulfiram and poly(l-glutamic acid)-cisplatin conjugates for combating

cisplatin resistance, J. Control. Release. (2016). doi:10.1016/j.jconrel.2016.02.039.
[333] S.A. Shaffer, C. Baker-Lee, J. Kennedy, M.S. Lai, P. De Vries, K. Buhler, J.W. Singer, In vitro and in vivo metabolism of paclitaxel poliglumex: Identification of metabolites and active proteases, Cancer Chemother. Pharmacol. (2007). doi:10.1007/s00280-006-0296-4.
[334] M.A. Dobrovolskaia, Pre-clinical immunotoxicity studies of nanotechnology-formulated drugs: Challenges, considerations and strategy, J. Control. Release. (2015). doi:10.1016/j.jconrel.2015.08.056.
[335] E. Markovsky, H. Baabur-Cohen, A. Eldar-Boock, L. Omer, G. Tiram, S. Ferber, P. Ofek, D. Polyak, A. Scomparin, R. Satchi-Fainaro, Administration, distribution, metabolism and elimination of polymer therapeutics, J. Control. Release. (2012). doi:10.1016/j.jconrel.2011.12.021.
[336] Y.Y. Yuan, C.Q. Mao, X.J. Du, J.Z. Du, F. Wang, J. Wang, Surface charge switchable nanoparticles based on zwitterionic polymer for enhanced drug delivery to tumor, Adv. Mater. (2012). doi:10.1002/adma.201202296.
[337] Q. Huo, J. Zhu, Y. Niu, H. Shi, Y. Gong, Y. Li, H. Song, Y. Liu, PH-triggered surface charge-switchable polymer micelles for the co-delivery of paclitaxel/disulfiram and overcoming multidrug resistance in cancer, Int. J. Nanomedicine. 12 (2017) 8631–8647. doi:10.2147/IJN.S144452.
[338] I. Alberg, S. Kramer, M. Schinnerer, Q. Hu, C. Seidl, C. Leps, N. Drude, D. Möckel, C. Rijcken, T. Lammers, M. Diken, M. Maskos, S. Morsbach, K. Landfester, S. Tenzer, M. Barz, R. Zentel, Polymeric Nanoparticles with Neglectable Protein Corona, Small. (2020). doi:10.1002/smll.201907574.
[339] A. Balliu, L. Baltzer, Conjugation of Dipicolyl Chelate to Polypeptide Conjugates Increases Binding Affinities for Human Serum Albumin and Survival Times in Human Serum, ChemBioChem. (2017). doi:10.1002/cbic.201700049.
[340] T. Schafer, C. Muhl, M. Barz, F. Schmid, G. Settanni, Interactions Between Blood Proteins and Nanoparticles Investigated Using Molecular Dynamics Simulations, in: W.E. Nagel, D.H. Kröner, M.M. Resch (Eds.), High Perform. Comput. Sci. Eng. ' 18, Springer International Publishing, Cham, 2019: pp. 63–74. doi:10.1007/978-3-030-13325-2_4.
[341] D. Frenkel, B. Smit, J. Tobochnik, S.R. McKay, W. Christian, Understanding Molecular Simulation, Comput. Phys. (1997). doi:10.1063/1.4822570.
[342] A.D. MacKerell, D. Bashford, M. Bellott, R.L. Dunbrack, J.D. Evanseck, M.J. Field, S. Fischer, J. Gao, H. Guo, S. Ha, D. Joseph-McCarthy, L. Kuchnir, K. Kuczera, F.T.K. Lau, C. Mattos, S. Michnick, T. Ngo, D.T. Nguyen, B. Prodhom, W.E. Reiher, B. Roux, M. Schlenkrich, J.C. Smith, R. Stote, J. Straub, M. Watanabe, J. Wiórkiewicz-Kuczera, D. Yin, M. Karplus, All-atom empirical potential for molecular modeling and dynamics studies of proteins, J. Phys. Chem. B. (1998). doi:10.1021/jp973084f.
[343] L.I.F. Moura, N. Martinho, L.C. Silva, T.S. Barata, S. Brocchini, H.F. Florindo, M. Zloh, Poly-glutamic dendrimer-based conjugates for cancer vaccination–a computational design for targeted delivery of antigens, J. Drug Target. (2017). doi:10.1080/1061186X.2017.1363213.
[344] G. Settanni, J. Zhou, T. Suo, S. Schöttler, K. Landfester, F. Schmid, V. Mailänder, Protein corona composition of poly(ethylene glycol)-and poly (phosphoester)-coated nanoparticles correlates strongly with the amino acid composition of the protein surface, Nanoscale. (2017). doi:10.1039/c6nr07022a.

Journal Pre-proof

[345] G. Settanni, T. Schäfer, C. Muhl, M. Barz, F. Schmid, Poly-sarcosine and Poly(Ethylene-Glycol) Interactions with Proteins Investigated Using Molecular Dynamics Simulations, Comput. Struct. Biotechnol. J. (2018). doi:10.1016/j.csbj.2018.10.012.
[346] J.C. Dabrowiak, J. Goodisman, A.K. Souid, Kinetic study of the reaction of cisplatin with thiols, Drug Metab. Dispos. (2002). doi:10.1124/dmd.30.12.1378.
[347] H. Wang, Y. Xiong, R. Wang, Y. Yu, J. Wang, Z. Hu, C. Sun, J. Tu, D. He, Cisplatin-stitched α-poly(glutamatic acid) nanoconjugate for enhanced safety and effective tumor inhibition, Eur. J. Pharm. Sci. 119 (2018) 189–199. doi:10.1016/j.ejps.2018.04.022.
[348] S. Mukherjee, V.P. Reddy B., I. Mitra, R. Saha, C.B.K. Jagadeesh, S. Reddy Dodda, W. Linert, S.C. Moi, In vitro model reaction of sulfur containing bio-relevant ligands with Pt(II) complex: Kinetics, mechanism, bioactivity and computational studies, RSC Adv. (2015). doi:10.1039/c5ra15740d.
[349] M. Hashida, Role of Pharmacokinetic Consideration for the Development of Drug Delivery Systems: A historical overview, Adv. Drug Deliv. Rev. (2020). https://doi.org/doi:10.1016/j.addr.2020.06.015.
[350] A. Eldar-Boock, R. Blau, C. Ryppa, H. Baabur-Cohen, A. Many, M.J. Vicent, F. Kratz, J. Sanchis, R. Satchi-Fainaro, Integrin-targeted nano-sized polymeric systems for paclitaxel conjugation: a comparative study, J. Drug Target. (2017). doi:10.1080/1061186X.2017.1358727.
[351] A. Armiñán, M. Palomino-Schätzlein, C. Deladriere, J.J. Arroyo-Crespo, S. Vicente-Ruiz, M.J. Vicent, A. Pineda-Lucena, Metabolomics facilitates the discrimination of the specific anti-cancer effects of free and polymer-conjugated doxorubicin in breast cancer models, Biomaterials. (2018). doi:10.1016/j.biomaterials.2018.02.015.
[352] K. Segers, S. Declerck, D. Mangelings, Y. Vander Heyden, A. Van Eeckhaut, Analytical techniques for metabolomic studies: A review, Bioanalysis. (2019). doi:10.4155/bio-2019-0014.
[353] F. Zheng, W. Xiong, S. Sun, P. Zhang, J.J. Zhu, Recent advances in drug release monitoring, Nanophotonics. (2019). doi:10.1515/nanoph-2018-0219.
[354] T. Li, C. Li, Z. Ruan, P. Xu, X. Yang, P. Yuan, Q. Wang, L. Yan, Polypeptide-Conjugated Second Near-Infrared Organic Fluorophore for Image-Guided Photothermal Therapy, ACS Nano. 13 (2019) 3691–3702. doi:10.1021/acsnano.9b00452.
[355] I. Negwer, A. Best, M. Schinnerer, O. Schäfer, L. Capeloa, M. Wagner, M. Schmidt, V. Mailänder, M. Helm, M. Barz, H.J. Butt, K. Koynov, Monitoring drug nanocarriers in human blood by near-infrared fluorescence correlation spectroscopy, Nat. Commun. (2018). doi:10.1038/s41467-018-07755-0.
[356] J.G. Swales, G. Hamm, M.R. Clench, R.J.A. Goodwin, Mass spectrometry imaging and its application in pharmaceutical research and development: A concise review, Int. J. Mass Spectrom. (2019). doi:10.1016/j.ijms.2018.02.007.
[357] S. Torok, A. Vegvari, M. Rezeli, T.E. Fehniger, J. Tovari, S. Paku, V. Laszlo, B. Hegedus, A. Rozsas, B. Dome, G. Marko-Varga, Localization of sunitinib, its metabolites and its target receptors in tumour-bearing mice: A MALDI-MS imaging study, Br. J. Pharmacol. (2015). doi:10.1111/bph.12990.
[358] A. Buck, S. Halbritter, C. Späth, A. Feuchtinger, M. Aichler, H. Zitzelsberger, K.P. Janssen, A. Walch, Distribution and quantification of irinotecan and its active metabolite SN-38 in colon cancer murine model systems using MALDI MSI, Anal. Bioanal. Chem. (2015). doi:10.1007/s00216-014-8237-2.

[359] X. Liu, C. Flinders, S.M. Mumenthaler, A.B. Hummon, MALDI Mass Spectrometry Imaging for Evaluation of Therapeutics in Colorectal Tumor Organoids, J. Am. Soc. Mass Spectrom. (2018). doi:10.1007/s13361-017-1851-4.

[360] K. Huber, A. Feuchtinger, D.M. Borgmann, Z. Li, M. Aichler, S.M. Hauck, H. Zitzelsberger, M. Schwaiger, U. Keller, A. Walch, Novel approach of MALDI drug imaging, immunohistochemistry, and digital image analysis for drug distribution studies in tissues, Anal. Chem. (2014). doi:10.1021/ac502177y.

[361] X. Liu, J.K. Lukowski, C. Flinders, S. Kim, R.A. Georgiadis, S.M. Mumenthaler, A.B. Hummon, MALDI-MSI of Immunotherapy: Mapping the EGFR-Targeting Antibody Cetuximab in 3D Colon-Cancer Cell Cultures, Anal. Chem. (2018). doi:10.1021/acs.analchem.8b02151.

[362] L. Morosi, P. Spinelli, M. Zucchetti, F. Pretto, A. Carrà, M. D'Incalci, R. Giavazzi, E. Davoli, Determination of Paclitaxel Distribution in Solid Tumors by Nano-Particle Assisted Laser Desorption Ionization Mass Spectrometry Imaging, PLoS One. (2013). doi:10.1371/journal.pone.0072532.

[363] M. Cesca, L. Morosi, A. Berndt, I.F. Nerini, R. Frapolli, F. Richter, A. Decio, O. Dirsch, E. Micotti, S. Giordano, M. D'Incalci, E. Davoli, M. Zucchetti, R. Giavazzi, Bevacizumab-induced inhibition of angiogenesis promotes a more homogeneous intratumoral distribution of paclitaxel, improving the antitumor response, Mol. Cancer Ther. (2016). doi:10.1158/1535-7163.MCT-15-0063.

[364] F.P.Y. Barré, B.S.R. Claes, F. Dewez, C. Peutz-Kootstra, H.F. Munch-Petersen, K. Grønbæk, A.H. Lund, R.M.A. Heeren, C. Côme, B. Cillero-Pastor, Specific Lipid and Metabolic Profiles of R-CHOP-Resistant Diffuse Large B-Cell Lymphoma Elucidated by Matrix-Assisted Laser Desorption Ionization Mass Spectrometry Imaging and in Vivo Imaging, Anal. Chem. (2018). doi:10.1021/acs.analchem.8b02910.

[365] M.R.L. Paine, J. Liu, D. Huang, C.R. Ellis, D. Trede, J.H. Kobarg, R.M.A. Heeren, F.M. Fernández, T.J. MacDonald, Three-Dimensional Mass Spectrometry Imaging Identifies Lipid Markers of Medulloblastoma Metastasis, Sci. Rep. (2019). doi:10.1038/s41598-018-38257-0.

[366] S. Giordano, L. Morosi, P. Veglianese, S.A. Licandro, R. Frapolli, M. Zucchetti, G. Cappelletti, L. Falciola, V. Pifferi, S. Visentin, M. D'Incalci, E. Davoli, 3D Mass Spectrometry Imaging Reveals a Very Heterogeneous Drug Distribution in Tumors, Sci. Rep. (2016). doi:10.1038/srep37027.

[367] M. Yasunaga, M. Furuta, K. Ogata, Y. Koga, Y. Yamamoto, M. Takigahira, Y. Matsumura, The significance of microscopic mass spectrometry with high resolution in the visualisation of drug distribution, Sci. Rep. (2013). doi:10.1038/srep03050.

[368] S. Ashton, Y.H. Song, J. Nolan, E. Cadogan, J. Murray, R. Odedra, J. Foster, P.A. Hall, S. Low, P. Taylor, R. Ellston, U.M. Polanska, J. Wilson, C. Howes, A. Smith, R.J.A. Goodwin, J.G. Swales, N. Strittmatter, Z. Takáts, A. Nilsson, P. Andren, D. Trueman, M. Walker, C.L. Reimer, G. Troiano, D. Parsons, D. De Witt, M. Ashford, J. Hrkach, S. Zale, P.J. Jewsbury, S.T. Barry, Aurora kinase inhibitor nanoparticles target tumors with favorable therapeutic index in vivo, Sci. Transl. Med. (2016). doi:10.1126/scitranslmed.aad2355.

[369] H. Kataoka, New trends in sample preparation for clinical and pharmaceutical analysis, TrAC - Trends Anal. Chem. (2003). doi:10.1016/S0165-9936(03)00402-3.

[370] R. Leardi, Experimental design in chemistry: A tutorial, Anal. Chim. Acta. 652 (2009) 161–172. doi:10.1016/j.aca.2009.06.015.

Journal Pre-proof

[371] J.N. Miller, J.C. Miller, Chemometrics for Analytical Chemistry, 2005.
[372] E.S. Hecht, A.L. Oberg, D.C. Muddiman, Optimizing Mass Spectrometry Analyses: A Tailored Review on the Utility of Design of Experiments, J. Am. Soc. Mass Spectrom. 27 (2016) 767–785. doi:10.1007/s13361-016-1344-x.
[373] A. Kruve, K. Herodes, I. Leito, Optimization of electrospray interface and quadrupole ion trap mass spectrometer parameters in pesticide liquid chromatography/electrospray ionization mass spectrometry analysis, Rapid Commun. Mass Spectrom. 24 (2010) 919–926. doi:10.1002/rcm.4470.
[374] Moreno-Manzano, V., Giraldo-Reboloso, E., Requejo Aguilar, R.,Alastrue Agudo, A., Vicent Docon, M.J., Armiñan de Benito, A., Arroyo-Crespo, J.J., Nebot Carda, V.J., Zagorodko, O., Dordevic, S., Polymeric conjugates and uses thereof, PCT/EP2020/058940, n.d.
[375] S. Hooshfar, M.G. Bartlett, Hazards in chromatographic bioanalysis method development and applications, Biomed. Chromatogr. (2017). doi:10.1002/bmc.3859.
[376] Q. Zeng, Y. Liu, Y. Song, B. Feng, P. Xu, B. Shan, Z. Liao, K. Liu, Y. Zhong, L. Chen, D. Su, A UHPLC–MS/MS method coupled with simple and efficient alkaline hydrolysis for free and total determination of conjugate nanomedicine: Pharmacokinetic and biodistribution study of poly (L-glutamic acid)-graft-methoxy poly (ethylene glycol)/combretastatin , J. Pharm. Biomed. Anal. 169 (2019) 215–224. doi:10.1016/j.jpba.2019.03.001.
[377] W.B. Dunn, D. Broadhurst, P. Begley, E. Zelena, S. Francis-Mcintyre, N. Anderson, M. Brown, J.D. Knowles, A. Halsall, J.N. Haselden, A.W. Nicholls, I.D. Wilson, D.B. Kell, R. Goodacre, Procedures for large-scale metabolic profiling of serum and plasma using gas chromatography and liquid chromatography coupled to mass spectrometry, Nat. Protoc. (2011). doi:10.1038/nprot.2011.335.
[378] G. Tiwari, R. Tiwari, Bioanalytical method validation: An updated review, Pharm. Methods. (2010). doi:10.4103/2229-4708.72226.
[379] R. Rebane, K. Herodes, Matrix interference in LC-ESI-MS/MS analysis of metanephrines in protein precipitated plasma samples, Eur. J. Mass Spectrom. (2020). doi:10.1177/1469066719862423.
[380] L. Chen, H. Wang, O. Zang, Y. Xu, L. Sun, H. Xu, L. Ding, On-line coupling of solid-phase extraction to liquid chromatography-A review, J. Chromatogr. Sci. (2009). doi:10.1093/chromsci/47.8.614.
[381] D.S. Domingues, L.D. de Souza, M.E.C. Queiroz, Analysis of drugs in plasma samples from schizophrenic patients by column-switching liquid chromatography-tandem mass spectrometry with organic-inorganic hybrid cyanopropyl monolithic column, J. Chromatogr. B Anal. Technol. Biomed. Life Sci. (2015). doi:10.1016/j.jchromb.2015.04.040.
[382] H.D. de Faria, C.T. Bueno, J.E. Krieger, E.M. Krieger, A.C. Pereira, P.C.J.L. Santos, E.C. Figueiredo, Online extraction of antihypertensive drugs and their metabolites from untreated human serum samples using restricted access carbon nanotubes in a column switching liquid chromatography system, J. Chromatogr. A. (2017). doi:10.1016/j.chroma.2017.10.072.
[383] M. Wang, P. Ma, X. Xi, L. Liu, Y. Wen, K. Liu, L. Sun, Y. Lu, Z. Yin, Online solid phase extraction and liquid chromatography-mass spectrometric determination of nucleoside drugs in plasma, Talanta. (2016). doi:10.1016/j.talanta.2016.08.050.
[384] V.R. Acquaro, D.S. Domingues, M.E. Costa Queiroz, Column switching UHPLC-MS/MS

with restricted access material for the determination of CNS drugs in plasma samples, Bioanalysis. (2017). doi:10.4155/bio-2016-0301.

[385] L. Liu, K.N. Liu, Y. Bin Wen, H.W. Zhang, Y.X. Lu, Z. Yin, Development of a fully automated on-line solid phase extraction and high-performance liquid chromatography with diode array detection method for the pharmacokinetic evaluation of bavachinin: A study on absolute bioavailability and dose proportionality, J. Chromatogr. B Anal. Technol. Biomed. Life Sci. (2012). doi:10.1016/j.jchromb.2012.02.020.

[386] J.M.W. Van den Ouweland, I.P. Kema, The role of liquid chromatography-tandem mass spectrometry in the clinical laboratory, J. Chromatogr. B Anal. Technol. Biomed. Life Sci. (2012). doi:10.1016/j.jchromb.2011.11.044.

[387] J. Miller, Chromatography: Concepts and Contrasts, 2nd Edition, 2005.

[388] C.T. Mant, Y. Chen, Z. Yan, T. V. Popa, J.M. Kovacs, J.B. Mills, B.P. Tripet, R.S. Hodges, HPLC analysis and purification of peptides., Methods Mol. Biol. (2007). doi:10.1007/1-59745-430-3_1.

[389] A.F. Aubry, LC-MS/MS bioanalytical challenge: Ultra-high sensitivity assays, Bioanalysis. (2011). doi:10.4155/bio.11.166.

[390] M. Swartz, HPLC detectors: A brief review, J. Liq. Chromatogr. Relat. Technol. (2010). doi:10.1080/10826076.2010.484356.

[391] S.R.C. D.Skoog, D. West, F.J.Holler, Analytical Chemistry 9th Edition, 2014.

[392] Y. Hu, Y. Hou, H. Wang, H. Lu, Polysarcosine as an Alternative to PEG for Therapeutic Protein Conjugation, Bioconjug. Chem. (2018). doi:10.1021/acs.bioconjchem.8b00237.

[393] T. Chida, Y. Miura, H. Cabral, T. Nomoto, K. Kataoka, N. Nishiyama, Epirubicin-loaded polymeric micelles effectively treat axillary lymph nodes metastasis of breast cancer through selective accumulation and pH-triggered drug release, J. Control. Release. 292 (2018) 130–140. doi:10.1016/j.jconrel.2018.10.035.

[394] A. Takahashi, Y. Yamamoto, M. Yasunaga, Y. Koga, J.I. Kuroda, M. Takigahira, M. Harada, H. Saito, T. Hayashi, Y. Kato, T. Kinoshita, N. Ohkohchi, I. Hyodo, Y. Matsumura, NC-6300, an epirubicin-incorporating micelle, extends the antitumor effect and reduces the cardiotoxicity of epirubicin, Cancer Sci. 104 (2013) 920–925. doi:10.1111/cas.12151.

[395] N. Hegde, V. Vemkar, B. Prabhakar, An Update on Design and Pharmacology of Dendritic Poly (l -lysine), Int. J. Pept. Res. Ther. 25 (2019) 1539–1562. doi:10.1007/s10989-018-9798-2.

[396] Y. Zhang, J. Zhang, W. Xu, G. Xiao, J. Ding, X. Chen, Tumor microenvironment-labile polymer–doxorubicin conjugate thermogel combined with docetaxel for in situ synergistic chemotherapy of hepatoma, Acta Biomater. (2018). doi:10.1016/j.actbio.2018.07.021.

[397] Á. Orosz, S. Bősze, G. Mező, I. Szabó, L. Herényi, G. Csík, Oligo- and polypeptide conjugates of cationic porphyrins: binding, cellular uptake, and cellular localization, Amino Acids. (2017). doi:10.1007/s00726-017-2428-z.

[398] K. Uray, M. V. Pimm, F. Hudecz, The effect of the branched chain polypeptide carrier on biodistribution of covalently attached B-cell epitope peptide (APDTRPAPG) derived from mucin 1 glycoprotein, Arch. Biochem. Biophys. (2019). doi:10.1016/j.abb.2019.02.003.

[399] S. Pillarisetti, S. Maya, S. Sathianarayanan, R. Jayakumar, Tunable pH and redox-

responsive drug release from curcumin conjugated γ-polyglutamic acid nanoparticles in cancer microenvironment, Colloids Surfaces B Biointerfaces. 159 (2017) 809–819. doi:10.1016/j.colsurfb.2017.08.057.

[400] S. Saxena, M. Jayakannan, π-Conjugate Fluorophore-Tagged and Enzyme-Responsive l -Amino Acid Polymer Nanocarrier and Their Color-Tunable Intracellular FRET Probe in Cancer Cells, Biomacromolecules. (2017). doi:10.1021/acs.biomac.7b00710.

[401] B.A. Aderibigbe, Z. Mhlwatika, M. Nwamadi, M.O. Balogun, W.M.R. Matshe, Synthesis, characterization and in vitro analysis of polymer-based conjugates containing dihydrofolate reductase inhibitors, J. Drug Deliv. Sci. Technol. (2019). doi:10.1016/j.jddst.2019.01.038.

[402] W. Teng, F. Jia, H. Han, Z. Qin, Q. Jin, J. Ji, Polyamino acid-based gemcitabine nanocarriers for targeted intracellular drug delivery, Polym. Chem. (2017). doi:10.1039/c7py00443e.

[403] J. Bhattacharyya, X.R. Ren, R.A. Mook, J. Wang, I. Spasojevic, R.T. Premont, X. Li, A. Chilkoti, W. Chen, Niclosamide-conjugated polypeptide nanoparticles inhibit Wnt signaling and colon cancer growth, Nanoscale. (2017). doi:10.1039/c7nr01973d.

[404] R. Chen, J. Wang, C. Qian, Y. Ji, C. Zhu, L. Wu, W. Li, X. Pi, Y. Wang, G. Cao, Z. Chen, From Nanofibers to Nanorods: Nanostructure of Peptide-Drug Conjugates Regulated by Polypeptide-PEG Derivative and Enhanced Antitumor Effect, Adv. Funct. Mater. 29 (2019) 1–9. doi:10.1002/adfm.201806058.

[405] Z. Wang, J. Guo, J. Sun, P. Liang, Y. Wei, X. Deng, W. Gao, Thermoresponsive and Protease-Cleavable Interferon-Polypeptide Conjugates with Spatiotemporally Programmed Two-Step Release Kinetics for Tumor Therapy, Adv. Sci. (2019). doi:10.1002/advs.201900586.

[406] H.E. Mukaya, R.L. van Zyl, N.J. van Vuuren, X.Y. Mbianda, Synthesis and characterization of water-soluble polyaspartamides containing platinum(II) complex and bisphosphonate as potential antimalarial drug, Polym. Bull. (2017). doi:10.1007/s00289-016-1880-x.

Journal Pre-proof

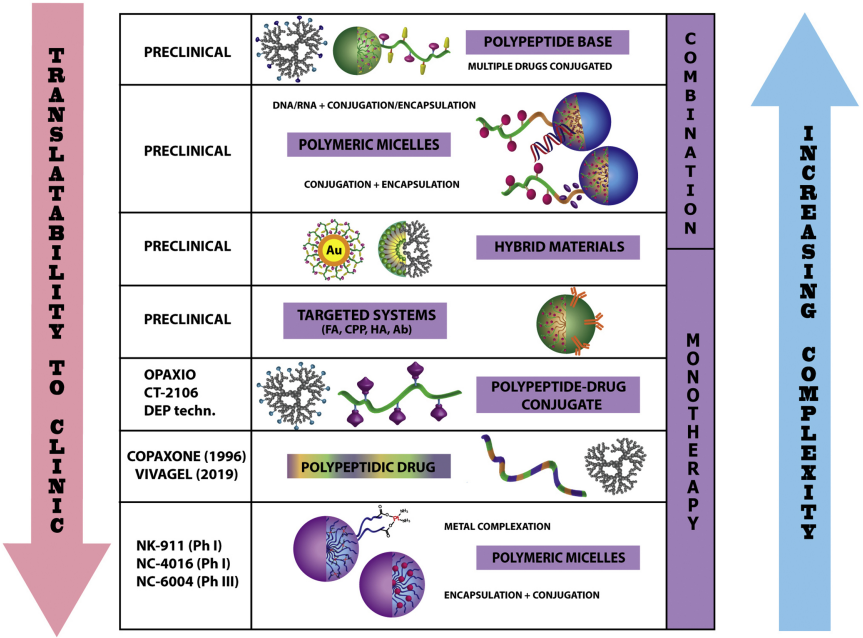

POLYPEPTIDES: POSITION IN THE NANOMEDICINE WORLD

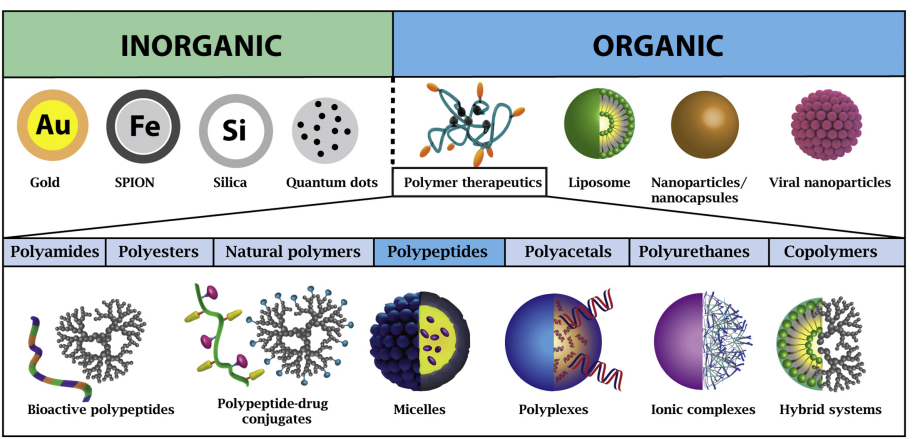

Figure 1

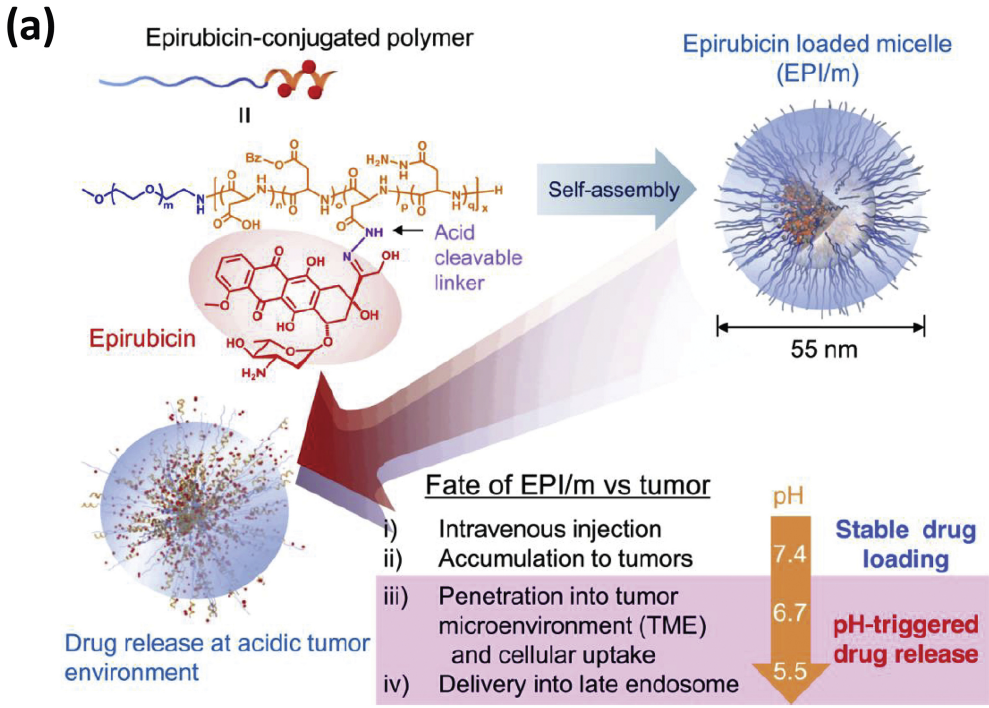
(a)
Epirubicin-conjugated polymer
Epirubicin loaded micelle (EPI/m)
Self-assembly
Acid cleavable linker
Epirubicin
55 nm
Fate of EPI/m vs tumor
i) Intravenous injection
ii) Accumulation to tumors
iii) Penetration into tumor microenvironment (TME) and cellular uptake
iv) Delivery into late endosome
pH
7.4
6.7
5.5
Stable drug loading
pH-triggered drug release
Drug release at acidic tumor environment

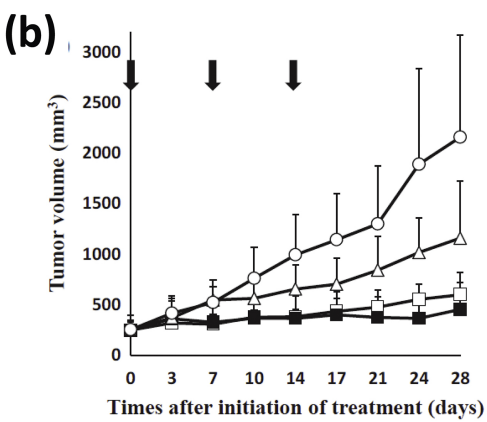
(b)
Tumor volume (mm³)
3000
2500
2000
1500
1000
500
0
0 3 7 10 14 17 21 24 28
Times after initiation of treatment (days)

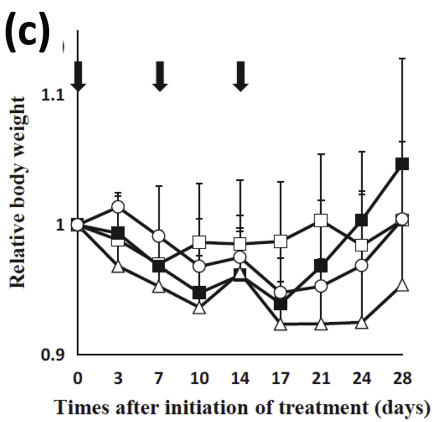
(c)
Relative body weight
1.1
1
0.9
0 3 7 10 14 17 21 24 28
Times after initiation of treatment (days)

Figure 2

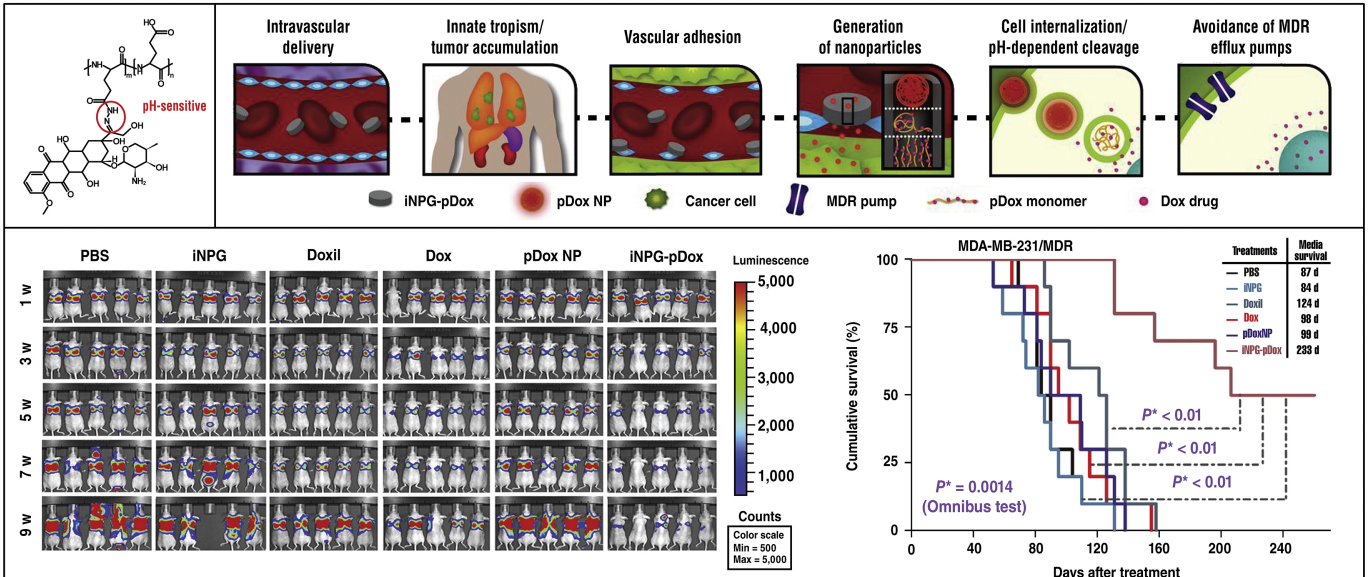
pH-sensitive
Intravascular delivery
Innate tropism/ tumor accumulation
Vascular adhesion
Generation of nanoparticles
Cell internalization/ pH-dependent cleavage
Avoidance of MDR efflux pumps
iNPG-pDox
pDox NP
Cancer cell
MDR pump
pDox monomer
Dox drug
PBS
iNPG
Doxil
Dox
pDox NP
iNPG-pDox
1 w
3 w
5 w
7 w
9 w
Luminescence
5,000
4,000
3,000
2,000
1,000
Counts
Color scale
Min = 500
Max = 5,000
MDA-MB-231/MDR
Cumulative survival (%)
Days after treatment
P* < 0.01
P* < 0.01
P* < 0.01
P* = 0.0014
(Omnibus test)
Treatments
Media survival
PBS 87 d
iNPG 84 d
Doxil 124 d
Dox 98 d
pDoxNP 99 d
iNPG-pDox 233 d

Figure 3

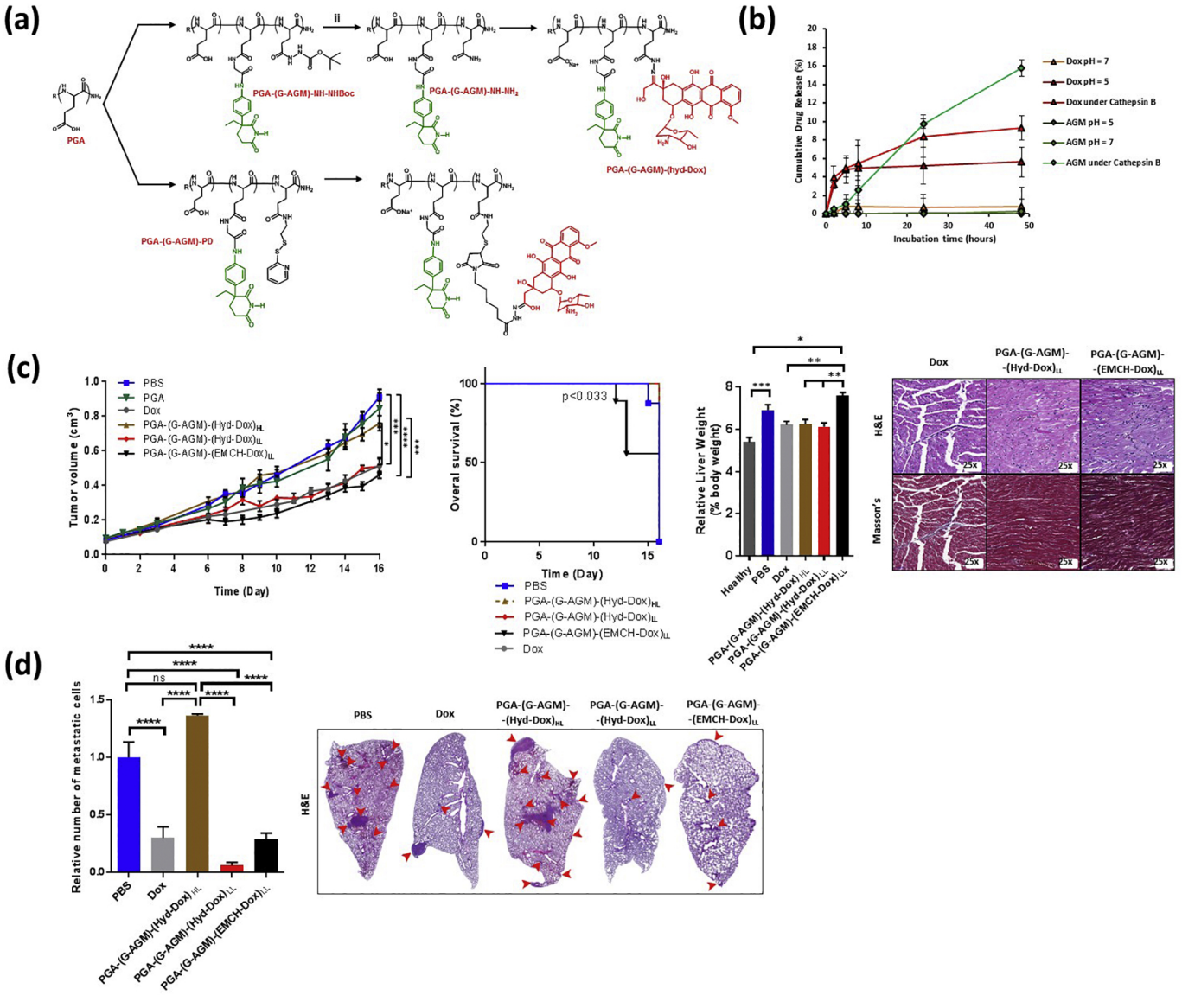
(a)
PGA
ii
PGA-(G-AGM)-NH-NHBoc
PGA-(G-AGM)-NH-NH2
PGA-(G-AGM)-(hyd-Dox)
PGA-(G-AGM)-PD
(b)
Cumulative Drug Release (%)
Incubation time (hours)
Dox pH = 7
Dox pH = 5
Dox under Cathepsin B
AGM pH = 5
AGM pH = 7
AGM under Cathepsin B
(c)
PBS
PGA
Dox
PGA-(G-AGM)-(Hyd-Dox)HL
PGA-(G-AGM)-(Hyd-Dox)IL
PGA-(G-AGM)-(EMCH-Dox)IL
Tumor volume (cm3)
Time (Day)
Overal survival (%)
p<0.033
Relative Liver Weight (% body weight)
Healthy
PBS
Dox
PGA-(G-AGM)-(Hyd-Dox)IL
PGA-(G-AGM)-(Hyd-Dox)LL
PGA-(G-AGM)-(EMCH-Dox)LL
Dox
PGA-(G-AGM)-(Hyd-Dox)LL
PGA-(G-AGM)-(EMCH-Dox)LL
H&E
Masson's
25x
(d)
ns
Relative number of metastatic cells
PBS
Dox
PGA-(G-AGM)-(Hyd-Dox)HL
PGA-(G-AGM)-(Hyd-Dox)LL
PGA-(G-AGM)-(EMCH-Dox)LL
H&E

Figure 4

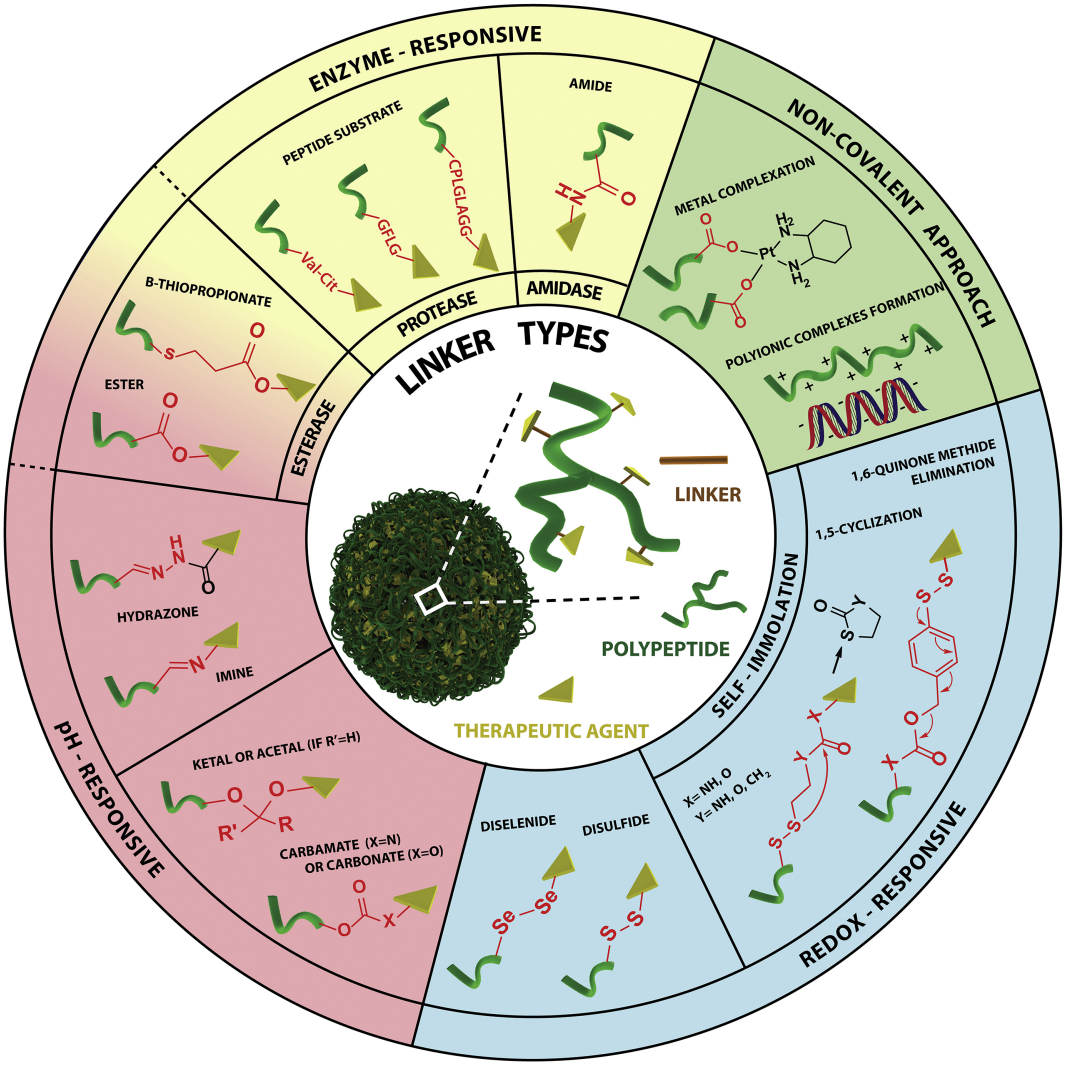
ENZYME - RESPONSIVE
PEPTIDE SUBSTRATE
GFLG
CPLGLAGG
Val-Cit
AMIDE
PROTEASE
AMIDASE
B-THIOPROPIONATE
ESTER
ESTERASE
NON-COVALENT APPROACH
METAL COMPLEXATION
POLYIONIC COMPLEXES FORMATION
LINKER TYPES
LINKER
POLYPEPTIDE
THERAPEUTIC AGENT
SELF - IMMOLATION
1,6-QUINONE METHIDE ELIMINATION
1,5-CYCLIZATION
pH - RESPONSIVE
HYDRAZONE
IMINE
KETAL OR ACETAL (IF R'=H)
CARBAMATE (X=N)
OR CARBONATE (X=O)
REDOX - RESPONSIVE
DISELENIDE
DISULFIDE
X= NH, O
Y= NH, O, CH2

Figure 5

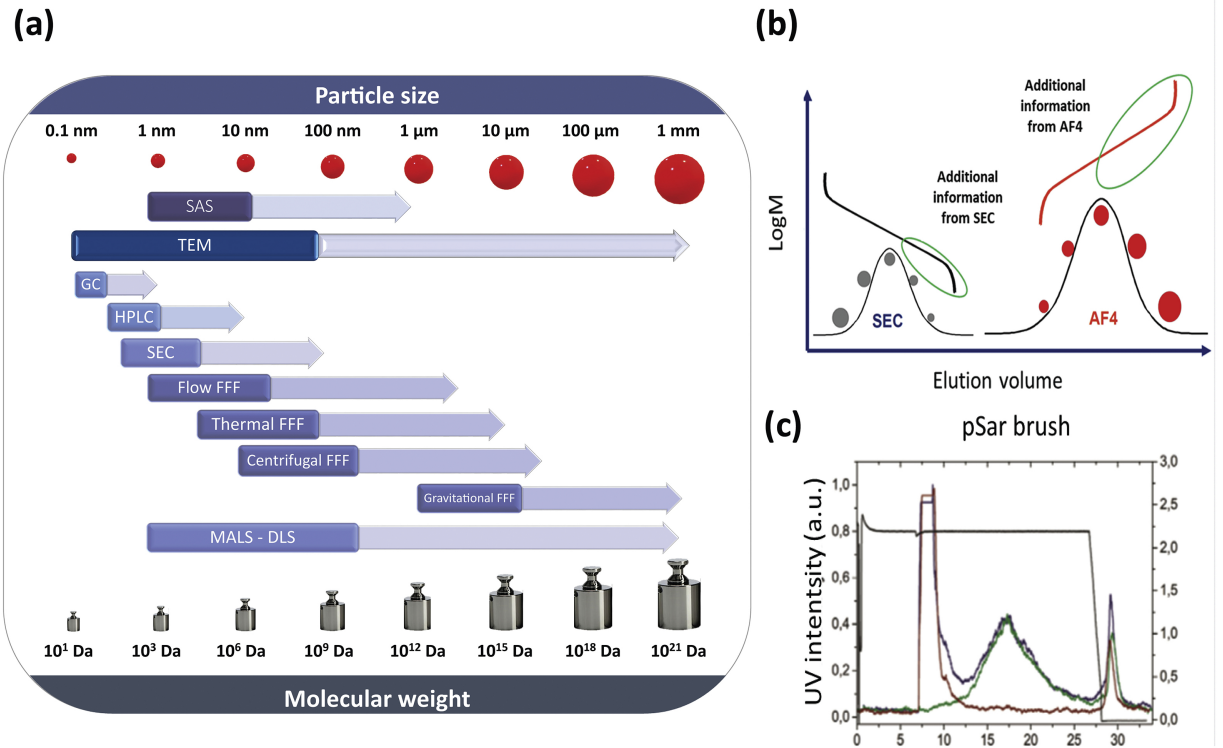
(a)
Particle size
0.1 nm
1 nm
10 nm
100 nm
1 µm
10 µm
100 µm
1 mm
SAS
TEM
GC
HPLC
SEC
Flow FFF
Thermal FFF
Centrifugal FFF
Gravitational FFF
MALS - DLS
10^1 Da
10^3 Da
10^6 Da
10^9 Da
10^12 Da
10^15 Da
10^18 Da
10^21 Da
Molecular weight
(b)
LogM
Additional information from AF4
Additional information from SEC
SEC
AF4
Elution volume
(c)
pSar brush
UV intentsity (a.u.)
1,0
0,8
0,6
0,4
0,2
0,0
3,0
2,5
2,0
1,5
1,0
0,5
0,0
0
5
10
15
20
25
30

Figure 6